Supplementary Information

Ligand-field transition-induced C–S bond formation from nickelacycles

Jeongcheol Shin†, Jiseon Lee†, Jong-Min Suh, and Kiyoung Park*

Department of Chemistry, Korea Advanced Institute of Science and Technology (KAIST), Daejeon 34141, Republic of Korea

† These authors contributed equally to this work.

*Correspondence to: kiyoung.park@kaist.ac.kr

Methods and Materials

Material Synthesis. Reagents were purchased from commercial suppliers (Alfa Aesar, Sigma-Aldrich, and Acros Organics), stored under N_2 conditions, and used as it is. All reactions were performed under anaerobic and dry conditions by using N_2-filled glove boxes and Schlenk lines, as following previously reported synthetic protocols for Py_3CH in refs [1], Ni(bpy)Cl_2 in ref [2], Ni(dmpe)Cl_2 in ref [3], [Ni(PMe_3)(SC)]$_2$, Ni(bpy)(SC) (**1**$_{\mathbf{bpy}}$), and Ni(dmpe)(SC) (**1**$_{\mathbf{dmpe}}$) in ref [4], [Ni(PMe_3)(OC)]$_2$, Ni(bpy)(OC) (**2**$_{\mathbf{bpy}}$), and Ni(dmpe)(OC) (**2**$_{\mathbf{dmpe}}$) in ref [5], Ni$(Py)_2$(CC) in ref [6], Ni$(PMe_3)_2$(CC) in ref [7], Ni(bpy)(CC) (**3**$_{\mathbf{bpy}}$) in ref [8], Ni(Py_3CH)(CC) (**3**$_{\mathbf{Py_3CH}}$) in ref [9], Ni(dmpe)(CC) (**3**$_{\mathbf{dmpe}}$) in ref [10], Ni(bpy)($CH_2CH_2CH_2CH_2$) (**7**$_{\mathbf{bpy}}$) in ref [11], and Ni(bpy)($OCH_2CH_2CH_2CH_2$) (**8**$_{\mathbf{bpy}}$) in ref [12].

Ni(dmpe)(Me)(Cl). Trimethylammonium chloride (17 mg, 0.18 mmol) dissolved in acetonitrile was added to the acetonitrile solution of **6**$_{\mathbf{dmpe}}$ (44 mg, 0.18 mmol). The dark yellow solution mixture was stirred for 1 hour. The solvent was evaporated under vacuo, and the resulting solid was washed with *n*-pentane (2 mL, 2 times). Yield: 44 mg (92 %). ^{1}H NMR (400 MHz, CD_3CN, 25 °C): δ = 1.84-1.70 (m, 2H, PCH_2), 1.61-1.46 (m, 2H, PCH_2), 1.39 (dd, *J* = 10.5, 0.7 Hz, 6H, PCH_3), 1.32 (d, *J* = 8.9 Hz, 6H, PCH_3), –0.26 ppm (dd, *J* = 6.0, 5.2 Hz, 3H, $NiCH_3$). ^{31}P NMR (162 MHz, CD_3CN, 25 °C): 42.9 (d, *J* = 17.6 Hz), 32.1 ppm (d, *J* = 17.5 Hz).

Ni(Py_3CH)(SC) (**1**$_{\mathbf{Py_3CH}}$). [Ni(PMe_3)(SC)]$_2$ (43 mg, 0.07 mmol) dissolved in 10 mL benzene was mixed with the 5 mL benzene solution of Py_3CH (35 mg, 0.14 mmol). The mixture was stirred for 30 min at room temperature. After removing the solvent, the solid obtained was washed with *n*-pentane and diethyl ether. Yield: 26 mg (40 %). Elemental analysis for this complex was unsuccessful due to O_2 sensitivity. UV-Vis (CH_3CN, 25 °C): λ_{max}, nm (ε, M^{-1} cm^{-1}) = 401 (2900), 320 (7760). ^{1}H NMR (400 MHz, CD_3CN, 25 °C): δ = 8.73 (d, *J* = 4.7 Hz, 3H, Py_3CH), 7.83 (td, *J* = 7.7, 1.8 Hz, 3H, Py_3CH), 7.50 (d, *J* = 7.6 Hz, 3H, Py_3CH), 7.30 (ddd, *J* = 7.6, 5.3, 1.4 Hz, 3H, Py_3CH), 7.28-7.24 (m, 1H, C_6H_4), 7.00-6.93 (m, 1H, C_6H_4), 6.78-6.69 (m, 2H, C_6H_4), 5.99 (s, 1H, Py_3CH), 0.99 (s, 6H, CMe_2), 0.66 ppm (s, 2H, $NiCH_2$). MS (*m/z*): Calcd. for $C_{18}H_{16}N_4Ni$ $[M - SC + CH_3CN]^{2+}$: 173.04; found: 173.04; Calcd. for $C_{28}H_{27}F_3N_3NiO_2S$ $[M + CF_3COOH + H]^{2+}$: 292.06; found: 292.07; Calcd. for $C_{28}H_{26}F_3N_3NiO_2S$ $[M + CF_3COOH]^+$: 583.10; found: 583.13. Resonance Raman (powder, 25 °C, λ_{ext} = 514 nm): ν(Ni–S) = 414, ν(Ni–C) = 620, ν(C–S) = 691 cm^{-1}.

Ni(Py_3CH)(OC) (**2**$_{\mathbf{Py_3CH}}$). The 10 mL benzene solution of [Ni(PMe_3)(OC)]$_2$ (41 mg, 0.07 mmol) was mixed with Py_3CH (52 mg, 0.2 mmol) dissolved in 5 mL benzene. The mixture was stirred for 20 min at room temperature and the solvent was removed under reduced pressure. The solid obtained was washed with diethyl ether and dried in vacuo. Yield: 48 mg (73 %). Elemental analysis for this complex was unsuccessful due to O_2 sensitivity. UV-Vis (CH_3CN, 25 °C): λ_{max}, nm (ε, M^{-1} cm^{-1}) = 426 (5400), 340 (9280), 303 (11500). ^{1}H NMR (400 MHz, CD_3CN, 25 °C): δ = 8.72 (d, *J* = 5.0 Hz, 3H, Py_3CH), 7.84 (td, *J* = 7.6, 1.8 Hz, 3H, Py_3CH), 7.48 (d, *J* = 8.1 Hz, 3H, Py_3CH), 7.31 (ddd, *J* = 7.6, 5.5, 1.4 Hz, 3H, Py_3CH), 6.82 (dd, *J* = 7.5, 1.8 Hz, 1H, C_6H_4), 6.70 (ddd, *J* = 7.9, 7.0, 1.8, Hz, 1H, C_6H_4), 6.48 (dd, *J* = 7.9, 1.4 Hz, 1H, C_6H_4), 6.26 (td, *J* = 7.3, 1.4 Hz, 1H, C_6H_4), 5.94 (s, 1H, Py_3CH), 0.88 (s, 6H, CMe_2), 0.82 ppm (s, 2H, $NiCH_2$). MS (*m/z*): Calcd. for $C_{26}H_{25}N_3NiO$ $[M]^+$: 453.13; found: 453.13.

Resonance Raman (powder, 25 °C, λ_{ext} = 514 nm): ν(Ni–O) = 584, ν(Ni–C) = 625 cm^{-1}.

Ni(dppe)(SC) (**1$_{dppe}$**). $[Ni(PMe_3)(SC)]_2$ (43 mg, 0.072 mmol) dissolved in 5 mL ether was mixed with the 3 mL ether solution of dppe (57 mg, 0.144 mmol). The mixture was stirred for 30 min at room temperature. After removing the solvent, the solid obtained was washed with *n*-pentane and diethyl ether. Yield: 57 mg (64 %). Elemental analysis for this complex was unsuccessful due to O_2 sensitivity. UV-Vis (C_6H_6, 25 °C): λ_{max}, nm (ε, M^{-1} cm^{-1}) = 373 (4910), 283 (25900). ^{1}H NMR (400 MHz, C_6D_6, 25 °C): δ = 8.12-8.06 (m, 1H, C_6H_4), 7.95 (ddd, *J* = 9.9, 7.9, 1.7 Hz, 4H, dppe), 7.53 (ddd, *J* = 9.8, 7.5, 1.8 Hz, 4H, dppe), 7.42-7.37 (m, 1H, C_6H_4), 7.13-6.97 (m, 14H, dppe+C_6H_4), 1.94-1.60 (m, 4H, PCH_2), 1.90 (dd, *J* = 13.2, 3.6 Hz, 2H, $NiCH_2$), 1.50 ppm (s, 6H, CMe_2). ^{31}P NMR (162 MHz, C_6D_6, 25 °C): δ = 58.4 (d, *J* = 3.7 Hz), 43.7 ppm (d, *J* = 3.4 Hz). MS (*m/z*): Calcd. for $C_{36}H_{37}NiP_2S$ $[M + H]^+$: 621.14; found: 621.14. Raman (powder, 25 °C, λ_{ext} = 514 nm): ν(Ni–S) = 404, ν(Ni–C) = 603, ν(C–S) = 738 cm^{-1}.

Ni(dppe)(OC) (**2$_{dppe}$**). The 5 mL ether solution of $[Ni(PMe_3)(OC)]_2$ (68.4 mg, 0.121 mmol) was mixed with dppe (96 mg, 0.241 mmol) dispersed in 3 mL ether. The mixture was stirred for 30 min at room temperature and the solvent was removed under reduced pressure. The solid obtained was washed with diethyl ether and dried in vacuo. Yield: 145 mg (99 %). Found: C, 71.93; H, 6.46. Calcd. for $C_{36}H_{36}NiOP_2$: 71.43; H, 5.99 %. UV-Vis (C_6H_6, 25 °C): λ_{max}, nm (ε, M^{-1} cm^{-1}) = 364 (3400), 287 (10400). ^{1}H NMR (400 MHz, C_6D_6, 25 °C): δ = 8.16 (ddd, *J* = 9.6, 8.2, 1.4 Hz, 4H, dppe), 7.53 (ddd, *J* = 10.4, 8.0, 1.7 Hz, 4H, dppe), 7.47 (d, *J* = 6.8 Hz, 1H, C_6H_4), 7.39-7.36 (m, 2H, C_6H_4), 7.13-6.90 (m, 13H, dppe+C_6H_4), 1.90-1.75 (m, 2H, PCH_2), 1.59 (s, 6H, CMe_2), 1.62-1.47 ppm (m, 4H, PCH_2+$NiCH_2$). ^{31}P NMR (162 MHz, C_6D_6, 25 °C): δ = 59.9 (d, *J* = 8.9 Hz), 23.4 ppm (d, *J* = 8.9 Hz). ESI-MS (m/z): $[M]^+$ calcd. for $C_{36}H_{36}NiOP_2$, 604.16; found, 604.09. MS (*m/z*): Calcd. for $C_{36}H_{36}NiOP_2$ $[M]^+$: 604.16; found: 604.09. Raman (powder, 25 °C, λ_{ext} = 514 nm): ν(Ni–O) = 562, ν(Ni–C) = 602 cm^{-1}.

Ni(dppe)(CC) (**3$_{dppe}$**). The 7 mL ether solution of $Ni(PMe_3)_2(CC)$ (208.3 mg, 0.607 mmol) was mixed with dppe (241.9 mg, 0.607 mmol) dispersed in 5 mL ether. The mixture was stirred for 30 min at room temperature and the solvent was removed under reduced pressure. The solid obtained was washed with diethyl ether and dried in vacuo. Yield: 312 mg (87 %). Elemental analysis for this complex was unsuccessful due to O_2 sensitivity. UV-Vis (C_6H_6, 25 °C): λ_{max}, nm (ε, M^{-1} cm^{-1}) = 358 (6300). ^{1}H NMR (400 MHz, C_6D_6, 25 °C): δ = 7.87 (ddd, *J* = 9.6, 7.3, 2.2 Hz, 4H, C_6H_4), 7.68-7.57 (m, 4H, dppe), 7.28 (d, *J* = 7.2 Hz, 1H, C_6H_4), 7.08-6.97 (m, 12H, dppe+C_6H_4), 6.92 (tt, *J* = 7.3, 1.5 Hz, 1H, C_6H_4), 2.39 (dd, *J* = 10.8, 3.7 Hz, 2H, $NiCH_2$), 1.89-1.75 (m, 4H, PCH_2), 1.66 ppm (s, 6H, CMe_2). ^{31}P NMR (162 MHz, C_6D_6, 25 °C): δ = 56.3 (d, *J* = 14.6 Hz), 49.2 ppm (d, *J* = 14.4 Hz). MS (*m/z*): Calcd. for $C_{36}H_{37}NiP_2$ $[M + H]^+$: 589.17; found: 589.17. Raman (powder, 25 °C, λ_{ext} = 514 nm): ν(Ni–C_{sp2}) = 344, ν(Ni–C_{sp3}) = 598 cm^{-1}.

Ni(tmeda)(SC) (**1$_{tmeda}$**). **3$_{tmeda}$** (116.5 mg, 0.38 mmol) dissolved in 20 mL diethyl ether was mixed with molecular sulfur (24 mg, 0.76 mmol) at −70 °C, stirred for 1 hour, and then filtered through Celite 545. The solid obtained after removing the solvent was washed with cold *n*-pentane. Yield: 12.5 mg (9.7 %). Elemental analysis for this complex was unsuccessful due to O_2 sensitivity. UV-Vis (C_6H_6, 25 °C): λ_{max}, nm (ε, M^{-1} cm^{-1}) = 447 (420), 330

(7250). ^{1}H NMR (400 MHz, C_6D_6, 25 °C): δ = 8.13 (dd, *J* = 7.4, 1.8 Hz, 1H, C_6H_4), 7.43 (dd, *J* = 7.5, 1.8 Hz, 1H, C_6H_4), 7.10-7.00 (m, 2H, C_6H_4), 2.05 (s, 6H), 1.83 (s, 6H), 1.69 (s, 6H), 1.28-1.16 (m, 4H, NCH_2), 0.63 (s, 2H, $NiCH_2$). ESI-MS data for this complex was unsuccessful due to high O_2-sensitivity and thermal instability at room temperature. Raman (powder, 25 °C, λ_{ext} = 633 nm): ν(Ni–S) = 416, ν(Ni–C) = 653, ν(C–S) = 765 cm^{-1}.

Ni(tmeda)(OC) (**2$_{tmeda}$**). **3$_{tmeda}$** (100 mg, 0.33 mmol) dissolved in 15 mL benzene was exposed to 1 atm N_2O. The solution was stirred for 3 days at room temperature. The solid obtained after removing the solvent was washed with 1 mL *n*-pentane twice and then 1 mL diethyl ether twice, and dried in vacuo. Yield: 65 mg (62 %). Elemental analysis for this complex was unsuccessful due to O_2 sensitivity. UV-Vis (C_6H_6, 25 °C): λ_{max}, nm (ε, M^{-1} cm^{-1}) = 441 (320), 304 (4410). ^{1}H NMR (400 MHz, C_6D_6, 25 °C): δ = 7.46 (d, *J* = 7.5 Hz, 1H, C_6H_4), 7.24 (t, *J* = 7.5 Hz, 1H, C_6H_4), 7.03 (d, *J* = 8.0 Hz, 1H, C_6H_4), 6.85 (t, *J* = 7.4 Hz, 1H, C_6H_4), 2.16 (s, 6H), 1.86 (s, 6H), 1.52 (s, 6H), 1.27-1.07 (m, 4H, NCH_2), 0.75 ppm (s, 2H, $NiCH_2$). ESI-MS data for this complex was unsuccessful due to its high O_2-sensitivity and thermal instability. Raman (powder, 25 °C, λ_{ext} = 633 nm): ν(Ni–O) = 509, ν(Ni–C) = 651 cm^{-1}.

Ni(tmeda)(CC) (**3$_{tmeda}$**). This complex was synthesized from $Ni(py)_2(CC)$ and tmeda instead of previously reported method using $Ni(tmeda)(acac)_2$ and $Mg(CH_2C(CH_3)_2Ph)_2$.[13] To the benzene solution of $Ni(Py)_2(CC)$ (139 mg, 0.40 mmol), 3 equivalents of tmeda (182 uL, 1.2 mmol) were added and stirred for 2 hours. Green solid obtained after removing the solvent in vacuo was washed with diethyl ether and dissolved in benzene. After filtration of the benzene solution through Celite 545, the solvent was removed under reduced pressure. Yield: 114 mg (93 %). ^{1}H NMR (400 MHz, C_6D_6, 25 °C): δ = 8.13 (dd, *J* = 7.4, 1.8 Hz, 1H, C_6H_4), 7.43 (dd, *J* = 7.5, 1.8 Hz, 1H, C_6H_4), 7.10-7.00 (m, 2H, C_6H_4), 2.05 (s, 6H), 1.83 (s, 6H), 1.69 (s, 6H), 1.28-1.16 (m, 4H, NCH_2), 0.87-0.77 ppm (s, 2H, $NiCH_2$).

Ni(bpy)(Me)(SPh) (**4$_{bpy}$**). Thiophenol (13 uL, 0.12 mmol) was added to the vial with **6$_{bpy}$** (30 mg, 0.12 mmol) dissolved in diethyl ether (4 mL) with gentle stirring. The color of the solution was turned to dark blue and black precipitate was formed. The solution was evaporated and washed with *n*-pentane (3 mL, 3 times) and diethyl ether (1 mL, 2 times). The resulting powder was dried under vacuo to yield the title compound as a purple-colored powder. Yield: 20 mg (48 %). Elemental analysis for this complex was unsuccessful due to O_2 sensitivity. UV-Vis (C_6H_6, 25 °C): λ_{max}, nm (ε, M^{-1} cm^{-1}) = 529 (2940), 367 (3320). ^{1}H NMR (400 MHz, CD_3CN, 25 °C): δ = 9.04 (s, 1H), 8.56 (s, 1H), 8.13-8.00 (m, 4H), 7.62-7.47 (m, 4H), 7.04-6.92 (m, 3H), –0.14 ppm (s, 3H, $NiCH_3$). MS (*m/z*): Calcd. for $C_{13}H_{14}N_3Ni$ $[M - SC + CH_3CN]^+$: 270.05; found: 270.05. Raman analysis for this complex was unsuccessful due to its photodecay during the Raman spectral measurement.

Ni(bpy)Me$_2$ (**6$_{bpy}$**). This complex was synthesized from $Ni(bpy)Cl_2$ and methyllithium instead of previously reported method using Ni(tmeda)(acac), $Mg(tmeda)(CH_3)_2$, and bpy.[14] $Ni(bpy)Cl_2$ (250 mg, 0.88 mmol) was dispersed in diethyl ether (20 mL) and cooled to −78 °C. 1.6 M methyllithium solution in diethyl ether (1.09 mL, 1.75 mmol) was cooled to −78 °C and added to $Ni(bpy)Cl_2$ solution with vigorous stirring. The solution was stirred for 30 minutes at −78 °C, and warmed to 25 °C, and stirred for 1 hour. The solution was evaporated under vacuo

and washed with diethyl ether (1 mL, 2 times). The resulting powder was dried under vacuo to yield the title compound as a dark blue powder. Yield: 190 mg (89 %). ^{1}H NMR (400 MHz, C_6D_6, 25 °C): δ = 9.14 (s, 2H, bpy), 6.94 (s, 2H, bpy), 6.71 (s, 2H, bpy), 6.52 (s, 2H, bpy), 1.00 ppm (s, 6H, $NiCH_3$).

Ni(dmpe)(Me)(SPh) (**4$_{dmpe}$**). Sodium thiophenolate (21 mg, 0.17 mmol) dissolved in tetrahydrofuran was added to Ni(dmpe)MeCl (44 mg, 0.17 mmol) dissolved in tetrahydrofuran. The solution was stirred for 30 minutes and the solvent was evaporated under vacuo. The resulting solid was washed with *n*-pentane (2 mL, 2 times) and diethyl ether (1 mL, 5 times). Yield: 52 mg (98 %). Elemental analysis for this complex was unsuccessful due to O_2 sensitivity. UV-Vis (CH_3CN, 25 °C): λ_{max}, nm (ε, M^{-1} cm^{-1}) = 345 (3390), 290 (14480). ^{1}H NMR (400 MHz, CD_3CN, 25 °C): δ = 7.24 (d, *J* = 7.3 Hz, 2H, C_6H_5), 7.03 (t, *J* = 7.5 Hz, 2H, C_6H_5), 6.97 (d, *J* = 7.5 Hz, 1H, C_6H_5), 1.84-1.54 (m, 4H, PCH_2), 1.39 (d, *J* = 9.7 Hz, 6H, PCH_3), 1.23 (d, *J* = 8.7 Hz, 6H, PCH_3), –0.51 ppm (dd, *J* = 7.5, 4.4 Hz, 3H, $NiCH_3$). ^{31}P NMR (162 MHz, CD_3CN, 25 °C): 41.9 (d, *J* = 16.4 Hz), 33.6 ppm (d, *J* = 16.3 Hz). MS (*m/z*): Calcd. for $C_7H_{19}NiP_2$ $[M - SPh]^+$: 223.03; found: 223.03; Calcd. for $C_{12}H_{21}NiP_2S$ $[M - CH_3]^+$: 317.02; found: 317.02. Raman (powder, 25 °C, λ_{ext} = 514 nm): ν(Ni–S) = 400, ν(C–S) = 432, ν(Ni–C) = 507 cm^{-1}.

Ni(dmpe)(Me)(OPh) (**5$_{dmpe}$**). Phenol (30 mg, 0.31 mmol) was dissolved in diethyl ether and mixed with the diethyl ether solution of **6$_{dmpe}$** (75 mg, 0.31 mmol). Upon mixing, the color of the Ni-containing solution immediately changed from bright yellow to orange-yellow, and the mixture was stirred for 20 minutes. The precipitate obtained by removing supernatant was washed with *n*-pentane (1 mL, 2 times) and diethyl ether (1 mL, 2 times). The resulting powder was dried under vacuo to yield the title compound. Yield: 78 mg (79 %). Elemental analysis for this complex was unsuccessful due to O_2 sensitivity. UV-Vis (CH_3CN, 25 °C): λ_{max}, nm (ε, M^{-1} cm^{-1}) = 399 (1750), 308 (7300), 267 (22830). ^{1}H NMR (400 MHz, CD_3CN, 25 °C): δ = 6.91 (t, *J* = 7.7 Hz, 2H, C_6H_5), 6.69 (d, *J* = 7.9 Hz, 2H, C_6H_5), 6.29 (s, 1H, C_6H_5), 1.79-1.42 (m, 4H, PCH_2), 1.41 (d, *J* = 9.7 Hz, 6H, PCH_3), 1.16 (d, *J* = 8.6 Hz, 6H, PCH_3), –0.35 ppm (dd, *J* = 6.4, 5.2 Hz, 3H, $NiCH_3$). ^{31}P NMR (162 MHz, CD_3CN, 25 °C): 38.4 (br, s), 26.8 ppm (br, s). MS (*m/z*): Calcd. for $C_7H_{19}NiP_2$ $[M - OPh]^+$: 223.03; found: 223.03; Calcd. for $C_9H_{22}NNiP_2$ $[M - OPh + CH_3CN]^+$: 264.06; found: 264.05. Raman (powder, 25 °C, λ_{ext} = 514 nm): ν(Ni–C) = 506, ν(Ni–O) = 572 cm^{-1}.

Ni(dmpe)Me$_2$ (**6$_{dmpe}$**). This complex was synthesized from Ni(dmpe)Cl_2 and methyllithium instead of previously reported method using Ni(tmeda)(acac), Mg(tmeda)$(CH_3)_2$, and dmpe.[14] Ni(dmpe)Cl_2 (274 mg, 0.98 mmol) was dispersed in diethyl ether (20 mL) and cooled to −78 °C. To this mixture, 1.6 M methyllithium solution in diethyl ether (1.53 mL, 2.45 mmol) was added dropwise with vigorous stirring at −78 °C. The solution mixture was stirred for 30 minutes at −78 °C and then another 1 hour at 25 °C. The solvent was evaporated under vacuo and the title compound was extracted with diethyl ether (20 mL, 2 times). After evaporation of diethyl ether under vacuo, the resulting yellow powder was washed with *n*-pentane (3 mL, 3 times) and diethyl ether (2 mL, 2 times), and dried under vacuo. Yield: 162 mg (67 %). ^{1}H NMR (400 MHz, CD_3CN, 25 °C): δ = 1.65-1.51 (m, 4H, PCH_2), 1.25 (dd, *J* = 7.6, 0.4 Hz, 12H, PCH_3), –0.38 ppm (dd, *J* = 11.2, 4.4 Hz, 6H, $NiCH_3$). ^{31}P NMR (162 MHz, CD_3CN, 25 °C): 36.7 ppm (s).

Photoreactions. All samples were prepared anaerobically and placed in J-Young NMR tubes. Acetonitrile-d_3 was used for $\mathbf{1}_{\mathbf{bpy}}$, $\mathbf{1}_{\mathbf{Py_3CH}}$, and $\mathbf{1}_{\mathbf{dmpe}}$, while $\mathbf{1}_{\mathbf{dppe}}$ and $\mathbf{1}_{\mathbf{tmeda}}$ have limited solubility in acetonitrile and thus benzene-d_6 and the toluene-d_8:benzene-d_6=1:1 mixed solvent were used, respectively. Water baths installed with suprasil fused silica windows were used during irradiation and the temperature was kept at 20 ℃, except for $\mathbf{1}_{\mathbf{tmeda}}$ that required a 0 ℃ ice-water bath. Changchun New Industries optoelectronics 532, 515, 488, 473, 457, 405, and 355 nm lasers, Innovative Photonic Solutions 830, 785, and 633 nm lasers, and Kimmon Koha Co., LTD. He-Cd IK 5751I-G 325/442 nm dual 442 and 325 nm laser were used with the 50 % ND filter to reduce the power of lasers to 50 mW. The power of laser light was measured before and after the reaction to ensure the stability, by using Thorlabs PM160T laser power meter with a thermal sensor within 5 % measurement errors. With 52 W 390 LED, the water bath that contained the J-Young NMR tube was placed at 5 cm from the light source.

Protocol for ferrioxalate actinometry. Potassium ferrioxalate was synthesized as reported.[15] 350 μL 12 mM potassium ferrioxalate solution was prepared with the 50 mM H_2SO_4 aqueous solution, and placed in a J-Young NMR tube. After exposure to 50 mW 405 nm irradiation for a given time, 2 mL 0.2 % 1,10-phenanthroline (phen) aqueous solution and 250 μL 100 mM sodium acetate/1 % H_2SO_4 aqueous solution were added to the 250 μL irradiated ferrioxalate solution, and distilled water was filled to make the entire volume as 5 mL. The final concentration of iron complex after dilution was 0.6 mM. After waiting for 30 min, the quantity of the $[Fe(phen)_3]^{2+}$ complex produced was estimated by using electronic absorption at 510 nm and the extinction coefficient of 11,100 M^{-1} cm^{-1}.[16] The photo-induced conversion ratios were used to assess the effectiveness of our irradiation setup, given quantum yields reported in the literature.[15]

Spectroscopic details. *Magnetic circular dichroism (MCD) and electronic absorption (Abs) spectroscopies.* The JASCO J-1500 CD spectrometer was used for collecting both Abs and MCD spectra. For MCD spectroscopy, the solenoid core bore of the Cryomagnetics 5T cryogen-free superconducting magnet was used, providing a longitudinal magnetic field parallel to the light propagation direction.

Nuclear Magnetic Resonance (NMR) spectroscopy. ^{1}H and ^{31}P NMR spectra were recorded on the Bruker 400 MHz Avance III NMR spectrometer equipped with a BBFO probe.

Resonance Raman (rR) spectroscopy. The Uninanotech resonance Raman spectrometer consisting of an Andor SR-500i imaging spectrometer equipped with an 1800 l/mm grating, an Andor iDUS DU420A-BU2 detector, and Kimmon Koha Co., LTD. He-Cd IK 5751I-G 325/442 nm dual 442 and 325 nm laser were used for rR spectra obtained with 442 nm excitation. Data with visible excitation were measured on an Andor SR-750-A-R spectrometer equipped with 1200 and 1800 l/mm gratings, an Andor iVac DR-316B-LDCDD-RES detector, and the above-mentioned visible-light lasers. Spectra obtained with NIR excitations were collected with an Andor SR-303i spectrometer equipped with a 1200 l/mm grating, an Andor iVac DR-324B-FI-RES detector, and the above-mentioned near IR lasers.

Electron Paramagnetic Resonance (EPR) Spectroscopy. EPR spectra were collected at 100 K with a Bruker EMXplus X-band EPR spectrometer equipped with an ER4141VT variable temperature controller and an ER4119HS cavity liquid nitrogen cryostat.

Electrospray Ionization Mass Spectrometry (ESI–MS). Mass spectrometric analyses of the synthesized Ni(II) complexes were conducted by an Agilent 6530 Accurate Mass quadrupole time-of-flight (Q-TOF) mass spectrometer (Agilent Technologies, Santa Clara, USA) equipped with an ESI source in a positive ion mode. The capillary voltage, fragmentor voltage, gas temperature, and drying gas flow were set to 3 kV, 50 V, 300 ^{o}C, and 12 L/min, respectively.

Elemental Analysis. Elemental analysis was carried out at the KAIST Research Analysis Center on a Thermo Scientific Flash 2000 CHNS elemental analyzer.

Computational details. All DFT calculations were conducted by utilizing the Gaussian 09-d.01[17] package, with the LC-ωPBE functional[18] tuned to ω = 0.15, the 6-311g(d,p) basis set[19] and the CPCM solvation model.[20] The ground-state and excited-state potential energy surfaces were calculated by performing TDDFT calculations.[21] Mulliken population analysis and Mayer bond order calculations were performed with the QMForge 2.4 software.[22]

Table S1. RE conversion ratios of **1**, **2**, and **3** under dark conditions.

Ni complex	T (℃)	Time (h)	Conversion (%)	Ni complex	T (℃)	Time (h)	Conversion (%)
$\mathbf{1}_{bpy}$	20	8	0	$\mathbf{1}_{bpy}$	65	2	86
					100	24	82[a]
$\mathbf{2}_{bpy}$	20	96	0	$\mathbf{2}_{bpy}$	75	8	0
$\mathbf{3}_{bpy}$	20	96	0	$\mathbf{3}_{bpy}$	75	8	0
$\mathbf{1}_{dmpe}$	20	8	0	$\mathbf{1}_{dmpe}$	75	8	<2
					100	24	75[a]
$\mathbf{2}_{dmpe}$	20	24	0	$\mathbf{2}_{dmpe}$	75	8	0
$\mathbf{3}_{dmpe}$	20	48	0	$\mathbf{3}_{dmpe}$	75	8	<2
$\mathbf{1}_{dppe}$	20	2	<2	$\mathbf{1}_{dppe}$	20	8	15
	20	8	15		75	10 min	99
$\mathbf{2}_{dppe}$	20	48	0	$\mathbf{2}_{dppe}$	75	8	0
$\mathbf{3}_{dppe}$	20	48	<2	$\mathbf{3}_{dppe}$	75	8	42
$\mathbf{1}_{Py_3CH}$	20	8	0	$\mathbf{1}_{Py_3CH}$	75	8	78
$\mathbf{2}_{Py_3CH}$	20	48	0	$\mathbf{2}_{Py_3CH}$	75	8	0
$\mathbf{3}_{Py_3CH}$	20	96	0	$\mathbf{3}_{Py_3CH}$	75	8	0
$\mathbf{1}_{tmeda}$	0	8	4	$\mathbf{1}_{tmeda}$	20	8	46
					75	8	49
$\mathbf{2}_{tmeda}$	20	8	0	$\mathbf{2}_{tmeda}$	75	8	0
$\mathbf{3}_{tmeda}$	20	48	0	$\mathbf{3}_{tmeda}$	75	9	6

[a] Reported in ref 4. Other conditions are tested in this study.

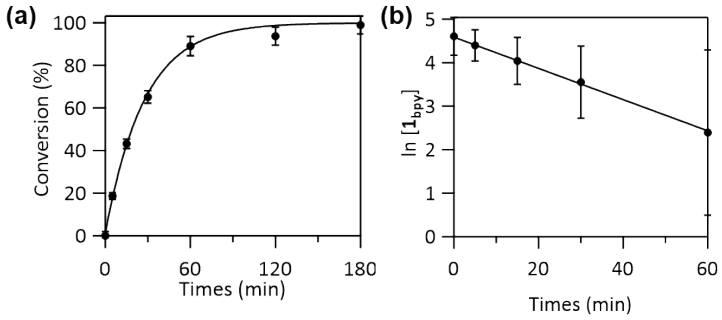

Figure S1. (a) ^{1}H NMR-monitored conversion of $\mathbf{1}_{\mathbf{bpy}}$ as a function of 52 W 390 nm LED irradiation time. (b) Plot of ln[$\mathbf{1}_{\mathbf{bpy}}$] vs. irradiation time to show the 1st-order kinetics. The fit curve in (a) was obtained with the 1st-order rate constant $k_{390} = 3.6\ (\pm\ 0.2) \times 10^{-2}$ min^{-1} obtained from (b).

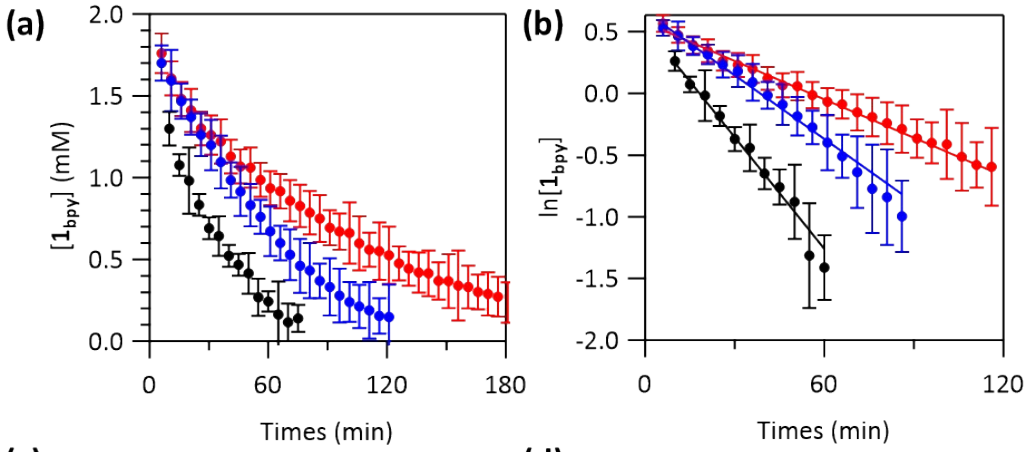

(c)

Temperature (°C)	k_{dark} (min^{-1})
60	1.0 (± 0.3) × 10^{-2}
65	1.7 (± 0.3) × 10^{-2}
70	3.0 (± 0.4) × 10^{-2}
20	1.5 (± 1.0) × 10^{-6} (predicted)

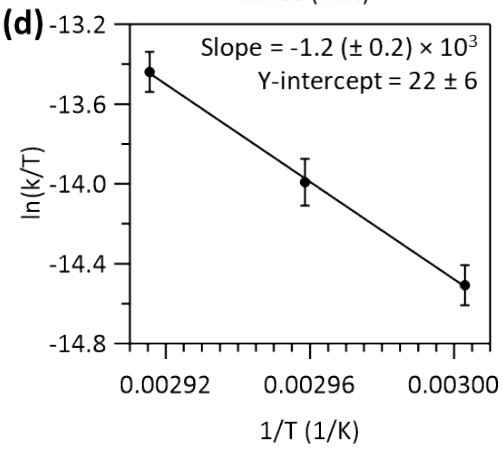

(e)

	$\Delta H^{\ddagger}$	$\Delta S^{\ddagger}$	$\Delta G^{\ddagger}_{20\,°C}$
Activation barrier	24 (± 4) kcal/mol	–4 (± 10) cal/mol K	25 (± 5) kcal/mol

Figure S2. (a) Decay of $\mathbf{1}_{\mathbf{bpy}}$ under dark condition at 70 (black), 65 (blue), and 60 (red) °C. (b) Plots of ln[$\mathbf{1}_{\mathbf{bpy}}$] vs. reaction time to show the 1st-order kinetics. (c) Rate constants k's obtained from (b). (d) Eyring plot with k's in s^{-1}. (e) $\Delta H^{\ddagger}$, $\Delta S^{\ddagger}$, and $\Delta G^{\ddagger}$ obtained from the Eyring plot.

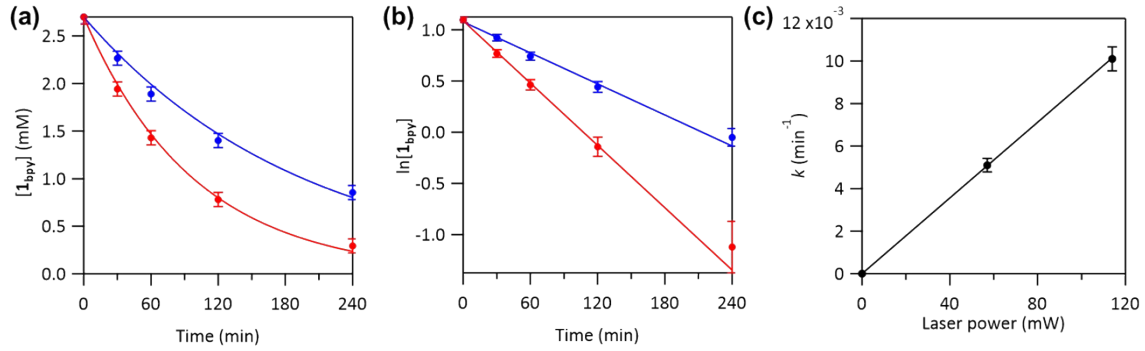

Figure S3. (a) 405 nm-induced decay of $\mathbf{1_{bpy}}$ as a function of irradiation time with the laser power of 57 mW (blue) and 114 mW (red). (b) Plots of ln[$\mathbf{1_{bpy}}$] vs. irradiation time to show the 1st-order kinetics. (c) 1st-order rate constants (k's) vs. laser power. Given this linear relationship, the rate constants obtained with different laser powers in Fig. S4 were normalized for 50 mW.

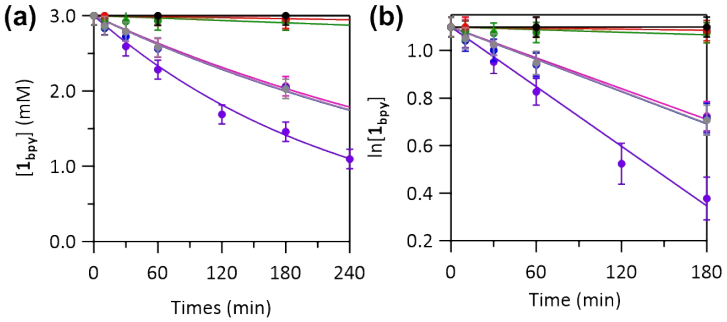

Figure S4. (a) Decay of $\mathbf{1_{bpy}}$ as a function of the irradiation time of 50 mW 830 (black), 633 (red), 532 (green), 442 (blue), 405 (purple), 355 (pink), and 325 (gray) nm laser lights. (b) Plots of ln[$\mathbf{1_{bpy}}$] vs. irradiation time to show the 1st-order kinetics of the photo-induced RE reaction. Rate constants obtained from these plots were used to construct the fitting curves in (a).

Table S2. 1st-order rate constants (k, in min^{-1}) for the photo-induced C–S bond-forming RE reactions of $\mathbf{1_{bpy}}$ measured with 50 mW laser lines.

Excitation wavelength	Related Abs bands	k (min^{-1})
830 nm	N.A.	0
633 nm	Band 1	0
532 nm	Band 2	$2 (\pm 2) \times 10^{-4}$
442 nm	Band 3	$2.3 (\pm 0.3) \times 10^{-3}$
405 nm		$4.2 (\pm 0.4) \times 10^{-3}$
355 nm	Band 4	$2.2 (\pm 0.3) \times 10^{-3}$
325 nm	Band 5	$2.3 (\pm 0.3) \times 10^{-3}$

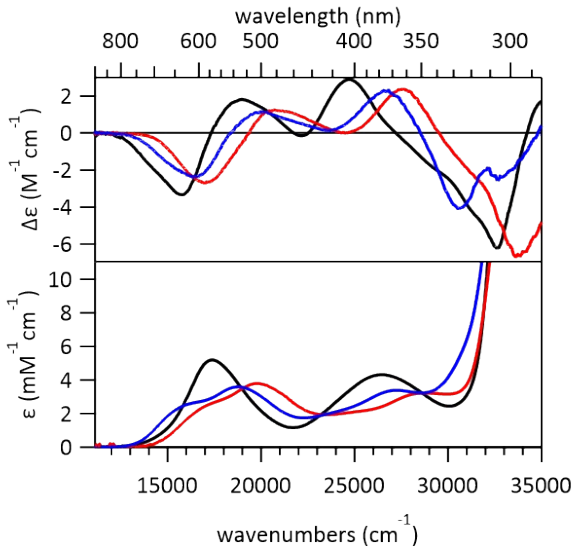

Figure S5. 5 T MCD (top) and Abs (bottom) spectra collected at 298 K of $\mathbf{1}_{\mathbf{bpy}}$ (blue), $\mathbf{2}_{\mathbf{bpy}}$ (red), and $\mathbf{3}_{\mathbf{bpy}}$ (black), indicating the equivalent frontier electronic structures of the three species.

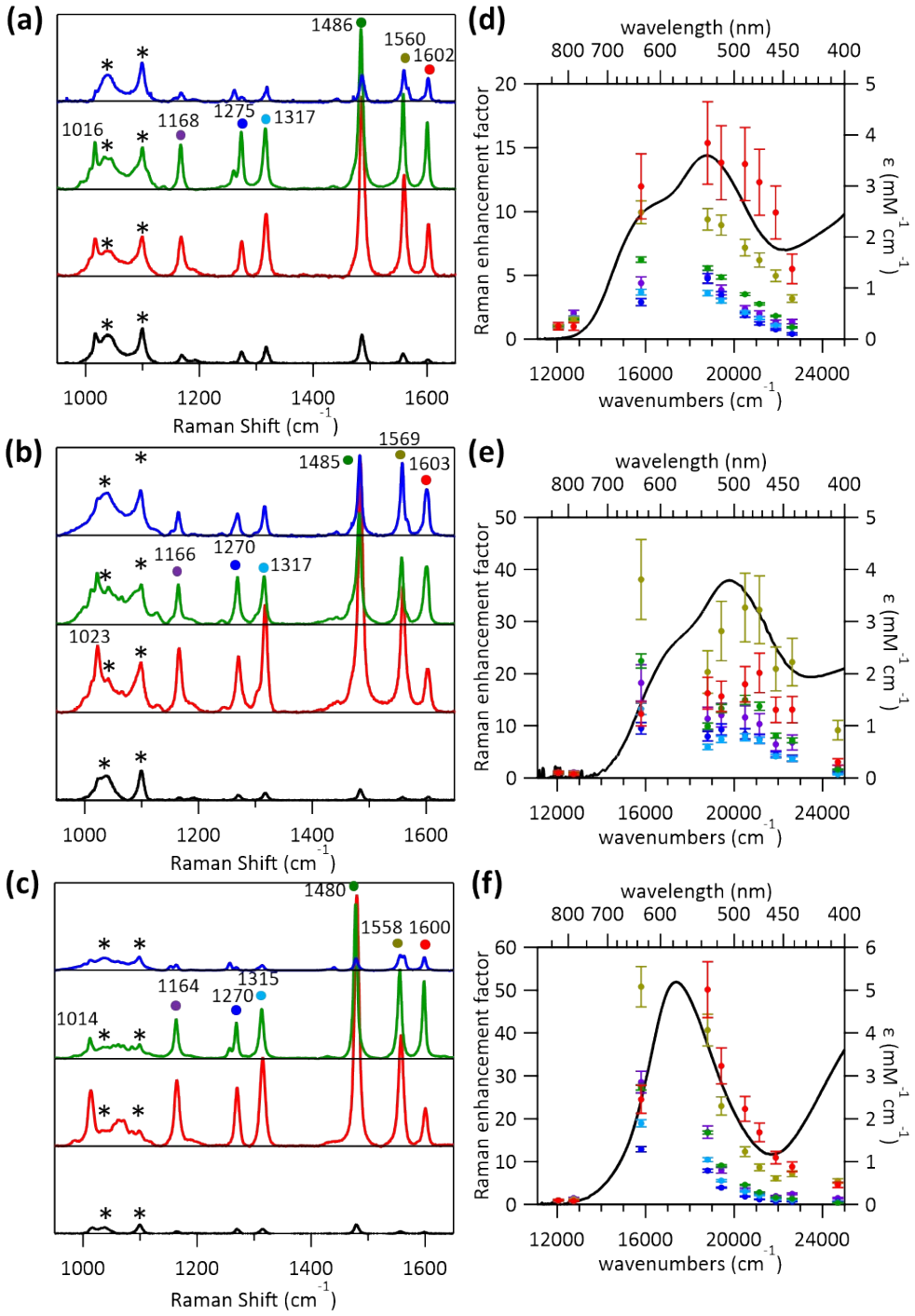

Figure S6. (a-c) rR spectra of (a) $\mathbf{1}_{\mathbf{bpy}}$, (b) $\mathbf{2}_{\mathbf{bpy}}$, and (c) $\mathbf{3}_{\mathbf{bpy}}$ obtained with 442 (blue), 532 (green), 633 (red), and 830 nm (black) laser excitations. Peaks with asterisks are from acetonitrile-d_3 solvent and used for intensity calibration. (d-f) rR intensity profiles of (d) $\mathbf{1}_{\mathbf{bpy}}$, (e) $\mathbf{2}_{\mathbf{bpy}}$, and (f) $\mathbf{3}_{\mathbf{bpy}}$. The rR features labeled with colored dots in (a-c) show resonance enhancements. For $\mathbf{1}_{\mathbf{bpy}}$, higher-energy laser excitations to bands 3 and 4 in Fig. 2 induced the RE reaction even under liquid nitrogen conditions. Thus, only the rR profile on bands 1 and 2 could be obtained.

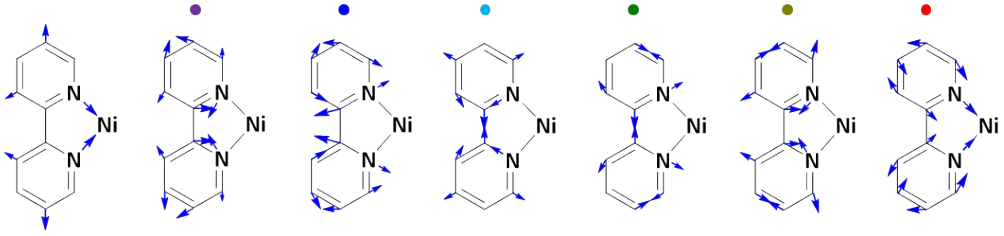

		-	●	●	●	●	●	●
$\mathbf{1}_{bpy}$	**Exp.**	1016	1168	1275	1317	1486	1560	1602
	DFT	1105	1304	1388	1456	164	1698	1763
$\mathbf{2}_{bpy}$	**Exp.**	1023	1166	1270	1317	1485	1569	1603
	DFT	1110	1305	1386	1460	1643	1697	1765
$\mathbf{3}_{bpy}$	**Exp.**	1014	1164	1270	1315	1480	1558	1600
	DFT	1105	1304	1388	1456	1641	1698	1762

Figure S7. DFT-calculated bpy-based normal modes and their energies in comparison to resonance-enhanced Raman features of $\mathbf{1}_{bpy}$~$\mathbf{3}_{bpy}$.

Table S3. Fit parameters from Gaussian deconvolution of the MCD and Abs spectra of $\mathbf{1}_{\mathbf{bpy}}$, and related TDDFT-calculated transitions.

Band	Abs		MCD		TDDFT assignment	
	Energy (cm^{-1})	ε (M^{-1} cm^{-1})	Energy (cm^{-1})	Δε (M^{-1} cm^{-1})		
1	16,100	2,200	16,300	–2.5	#1: 99 → 100 (77 %), 97 → 100 (17 %)	Ni $3d_{yz}$-S_{3p} → bpy π*
2	19,200	3,200	19,500	1.3	#3: 97 → 100 (71 %), 99 → 100 (15 %)	Ni $3d_{xz}$ → bpy π*
3	23,500	1,800	23,200	0.06	#8: 99 → 102 (56 %), 98 → 102 (20 %)	Ni $3d_{yz}$-S_{3p} → bpy π*
4	27,000	3,100	27,100	2.4	#11: 97 → 101 (35 %), 97 → 102 (14 %), 99 → 102 (14 %), 98 → 102 (12 %)	Ni $3d_{xz}$ → bpy π*
5	30,500	3,500	30,500	–4.0	#13: 97 → 102 (62 %), 98 → 103 (12 %)	Ni $3d_{xz}$ → bpy π*
d-d	-	-	-	-	#6: 99 → 103 (46 %), 96 → 100 (27 %) #10: 98 → 103 (70 %), 97 → 102 (14 %) #12: 97 → 103 (81 %) #15: 96 → 103 (71 %), 95 → 103 (20 %)	Ni $3d_{yz}$-S_{3p} → $3d_{x^2-y^2}$ Ni $3d_{z^2}$ → $3d_{x^2-y^2}$ Ni $3d_{xz}$ → $3d_{x^2-y^2}$ Ni $3d_{xy}$ → $3d_{x^2-y^2}$

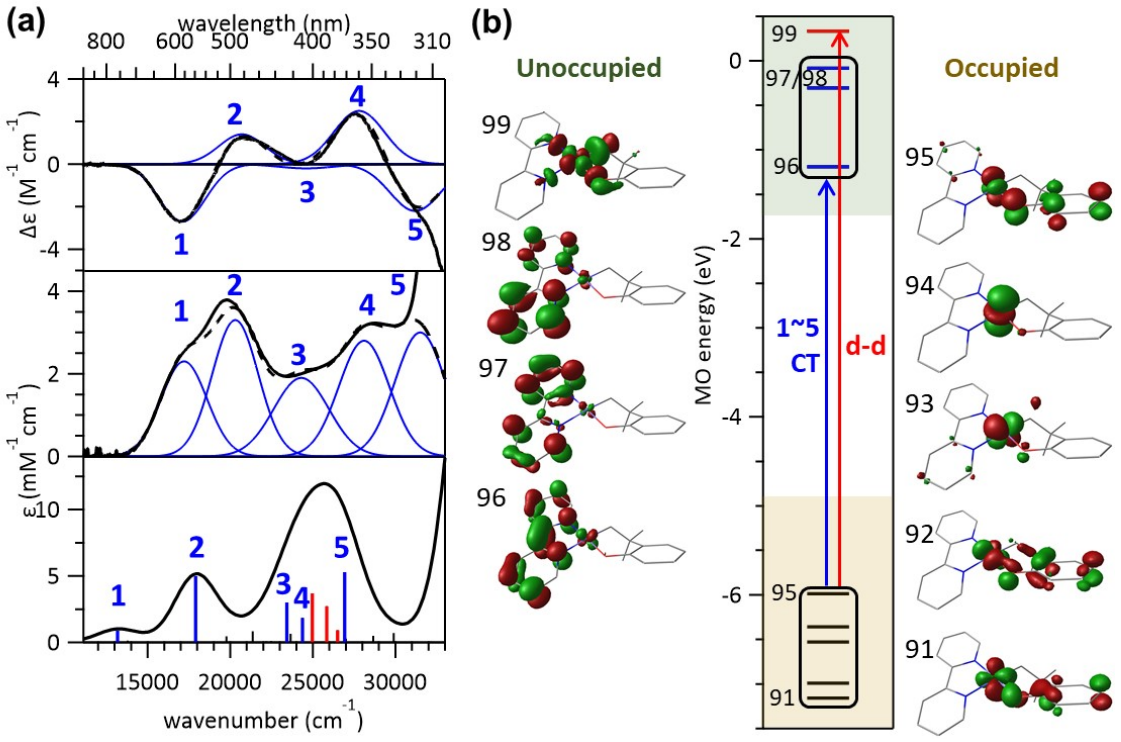

Figure S8. (a) 5 T MCD (top) and Abs (middle) collected at 298 K and TDDFT-simulated Abs (bottom) spectra of $\mathbf{2}_{\mathbf{bpy}}$. Gaussian deconvolution bands and their relevant TDDFT-calculated states are highlighted in color. The sums of Gaussian bands are shown in black dashed lines. (b) FMOs associated with the TDDFT-calculated transitions.

Table S4. Fit parameters from Gaussian deconvolution of the MCD and Abs spectra of $\mathbf{2}_{\mathbf{bpy}}$, and related TDDFT-calculated transitions.

Band	Abs		MCD		TDDFT assignment	
	Energy (cm^{-1})	ε (M^{-1} cm^{-1})	Energy (cm^{-1})	Δε (M^{-1} cm^{-1})		
1	17,200	2,300	17,100	–2.7	#1: 95 → 96 (71 %), 93 → 96 (15 %)	Ni $3d_{yz}$-O_{2p} → bpy π*
2	20,300	3,300	20,700	1.4	#3: 93 → 96 (66 %), 95 → 96 (15 %)	Ni $3d_{xz}$ → bpy π*
3	24,300	1,900	24,600	–0.2	#8: 95 → 98 (42 %), 93 → 97 (20 %), 94 → 98 (19 %)	Ni $3d_{yz}$-O_{2p} → bpy π*
4	28,100	2,800	27,800	2.5	#10: 93 → 97 (41 %), 94 → 99 (23 %), 93 → 98 (18 %)	Ni $3d_{xz}$ → bpy π*
5	31,500	3,000	31,200	–2.2	#14: 93 → 98 (34 %), 91 → 96 (15 %), 92 → 96 (12 %)	Ni $3d_{xz}$ → bpy π*
d-d	-	-	-	-	#11: 94 → 99 (32 %), 91 → 96 (18 %), 92 → 96 (12 %) #12: 93 → 99 (50 %), 93 → 98 (21 %), 94 → 99 (12 %) #13: 93 → 99 (27 %), 94 → 99 (23 %) #15: 92 → 99 (45 %), 91 → 99 (30 %)	Ni $3d_{yz}$-O_{2p} → $3d_{x^2-y^2}$ Ni $3d_{z^2}$ → $3d_{x^2-y^2}$ Ni $3d_{xz}$ → $3d_{x^2-y^2}$ Ni $3d_{xy}$ → $3d_{x^2-y^2}$

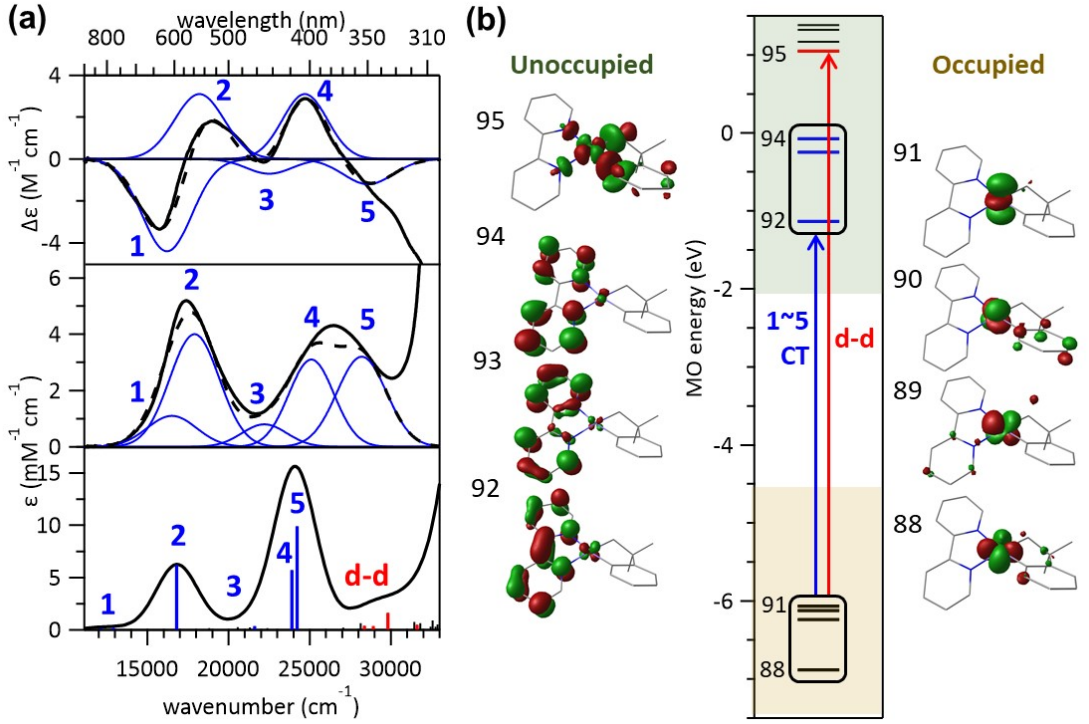

Figure S9. (a) 5 T MCD (top) and Abs (middle) collected at 298 K and TDDFT-simulated Abs (bottom) spectra of $\mathbf{3}_{\mathbf{bpy}}$. Gaussian deconvolution bands and their relevant TDDFT-calculated states are highlighted in color. The sums of Gaussian bands are shown in black dashed lines. (b) FMOs associated with the TDDFT-calculated transitions.

Table S5. Fit parameters from Gaussian deconvolution of the MCD and Abs spectra of $\mathbf{3}_{\mathbf{bpy}}$, and related TDDFT-calculated transitions.

Band	Abs		MCD		TDDFT assignment	
	Energy (cm^{-1})	ε (M^{-1} cm^{-1})	Energy (cm^{-1})	Δε (M^{-1} cm^{-1})		
1	16,500	1,100	16,200	–4.4	#1: 91 → 92 (94 %) #2: 90 → 92 (73 %), 89 → 92 (21 %)	Ni $3d_{z^2/yz}$ → bpy π*
2	17,900	4,000	18,200	3.1	#3: 89 → 92 (70 %), 90 → 92 (20 %)	Ni $3d_{xz}$ → bpy π*
3	22,200	800	22,500	–0.7	#7: 91 → 94 (68 %), 90 → 94 (22 %)	Ni $3d_{z^2}$ → bpy π*
4	25,100	3,100	24,700	3.1	#9: 89 → 94 (53 %), 90 → 94 (29 %)	Ni $3d_{xz}$ → bpy π*
5	28,200	3,200	28,600	–1.2	#10: 89 → 93 (34 %), 89 → 94 (26 %), 91 → 94 (14 %)	Ni $3d_{xz}$ → bpy π*
d-d	-	-	-	-	#14: 91 → 95 (60 %), 90 → 95 (13 %) #15: 90 → 95 (50 %), 89 → 95 (18 %) #16: 89 → 95 (57 %), 90 → 95 (10 %) #18: 88 → 95 (84 %)	Ni $3d_{yz}$ → $3d_{x^2-y^2}$ Ni $3d_{z^2}$ → $3d_{x^2-y^2}$ Ni $3d_{xz}$ → $3d_{x^2-y^2}$ Ni $3d_{xy}$ → $3d_{x^2-y^2}$

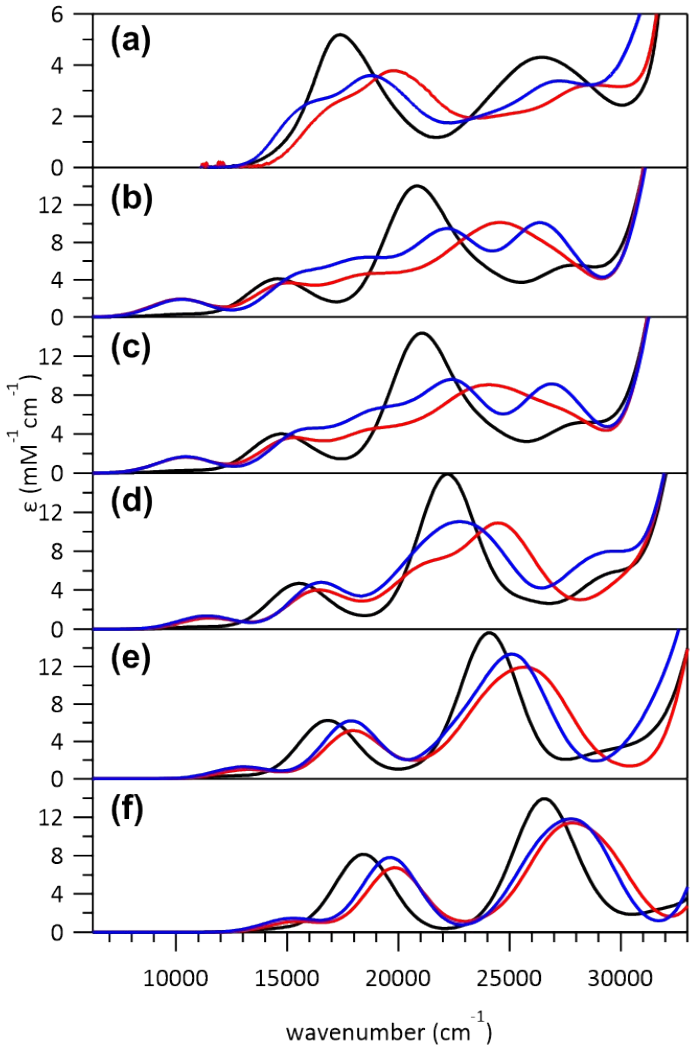

Figure S10. Validation of TDDFT methods. (a) Experimental and (b~f) TDDFT-simulated Abs spectra of $\mathbf{1}_{bpy}$ (blue), $\mathbf{2}_{bpy}$ (red), and $\mathbf{3}_{bpy}$ (black). With the LC-ωPBE functional and the 6-311g(d,p) basis set, the effects of ω values were tested for the best reproduction of the data. The ω values of (b) 0, (c) 0.05, (d) 0.10, (e) 0.15, and (f) 0.20 were tested and ω = 0.15 was chosen because it reproduces the experimental order of transition energies in $\mathbf{1}_{bpy}$~$\mathbf{3}_{bpy}$ complexes.

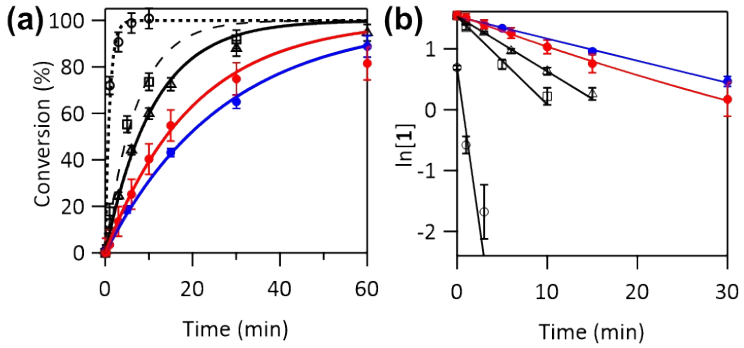

Figure S11. (a) 390 nm LED-induced formation of the C–S coupled product and the fitting curve of $\mathbf{1}_{\mathbf{bpy}}$ (●, blue solid), $\mathbf{1}_{\mathbf{tmeda}}$ (●, red solid), $\mathbf{1}_{\mathbf{Py_3CH}}$ (□, black dashed), $\mathbf{1}_{\mathbf{dppe}}$ (○, black dotted), and $\mathbf{1}_{\mathbf{dmpe}}$ (△, black solid). (b) Plots of ln[**1**] vs. irradiation time to show the 1st-order kinetics.

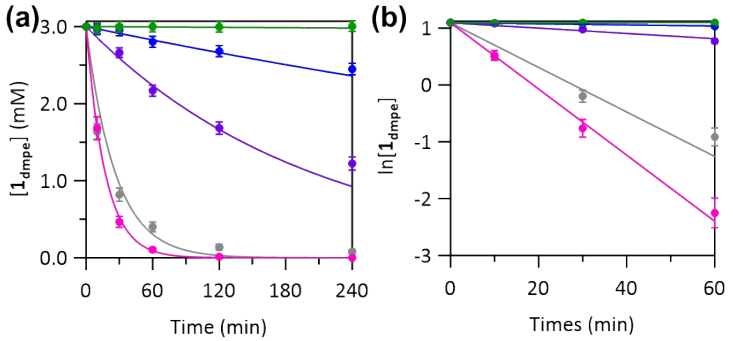

Figure S12. (a) Decay of $\mathbf{1}_{\mathbf{dmpe}}$ as a function of irradiation time of the 50 mW 532 (green), 442 (blue), 405 (purple), 355 (pink), and 325 (gray) nm lasers. (b) Plots of ln[$\mathbf{1}_{\mathbf{dmpe}}$] vs. irradiation time to show the 1st-order kinetics of the reaction. Rate constants obtained from these plots were used to construct the fitting curves in (a).

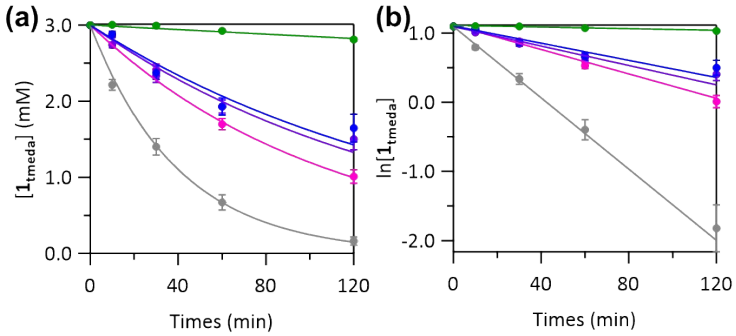

Figure S13. (a) Decay of $\mathbf{1}_{\mathbf{tmeda}}$ as a function of irradiation time of the 50 mW 532 (green), 442 (blue), 405 (purple), 355 (pink), and 325 (gray) nm lasers. (b) Plots of ln[$\mathbf{1}_{\mathbf{tmeda}}$] vs. irradiation time to show the 1st-order kinetics of the reaction. Rate constants obtained from these plots were used to construct the fitting curves in (a).

Table S6. 390 nm LED-induced RE activities of nickelacycles.

Ni complex	Temp. (°C)	*k* (min^{-1})	Conversion (%)	Reaction time (h)
$\mathbf{1}_{bpy}$	20	3.6×10^{-2}	93	2
	20		99	3
	20	8.4×10^{-7} a)	0	8 (dark)
	65	1.6×10^{-2}	86	2 (dark)
$\mathbf{1}_{Py_3CH}$	20	1.4×10^{-1}	100	2
	20	2×10^{-6} a)	0	8 (dark)
	75	2×10^{-3}	78	8 (dark)
$\mathbf{1}_{tmeda}$	0	5.0×10^{-2}	85	2
	0	9×10^{-5}	4	8 (dark)
$\mathbf{1}_{dmpe}$	20	9.1×10^{-2}	97	2
	75	-	2	8 (dark)
$\mathbf{1}_{dppe}$	20	1.0×10^{0}	100	2
	20	3.6×10^{-4}	15	8 (dark)
$\mathbf{2}_{bpy}$	20	N.A.	0	24
$\mathbf{2}_{Py_3CH}$	20	N.A.	0	2
$\mathbf{2}_{tmeda}$	20	N.A.	0	2
$\mathbf{2}_{dmpe}$	20	N.A.	0	2
$\mathbf{2}_{dppe}$	20	N.A.	0	2
$\mathbf{3}_{bpy}$	20	N.A.	0	24
$\mathbf{3}_{Py_3CH}$	20	N.A.	0	2
$\mathbf{3}_{tmeda}$	20	N.A.	0	2
$\mathbf{3}_{dmpe}$	20	N.A.	0	2
$\mathbf{3}_{dppe}$	20	N.A.	2	2

a) Extrapolated with Eyring equation from high-temperature experiments.

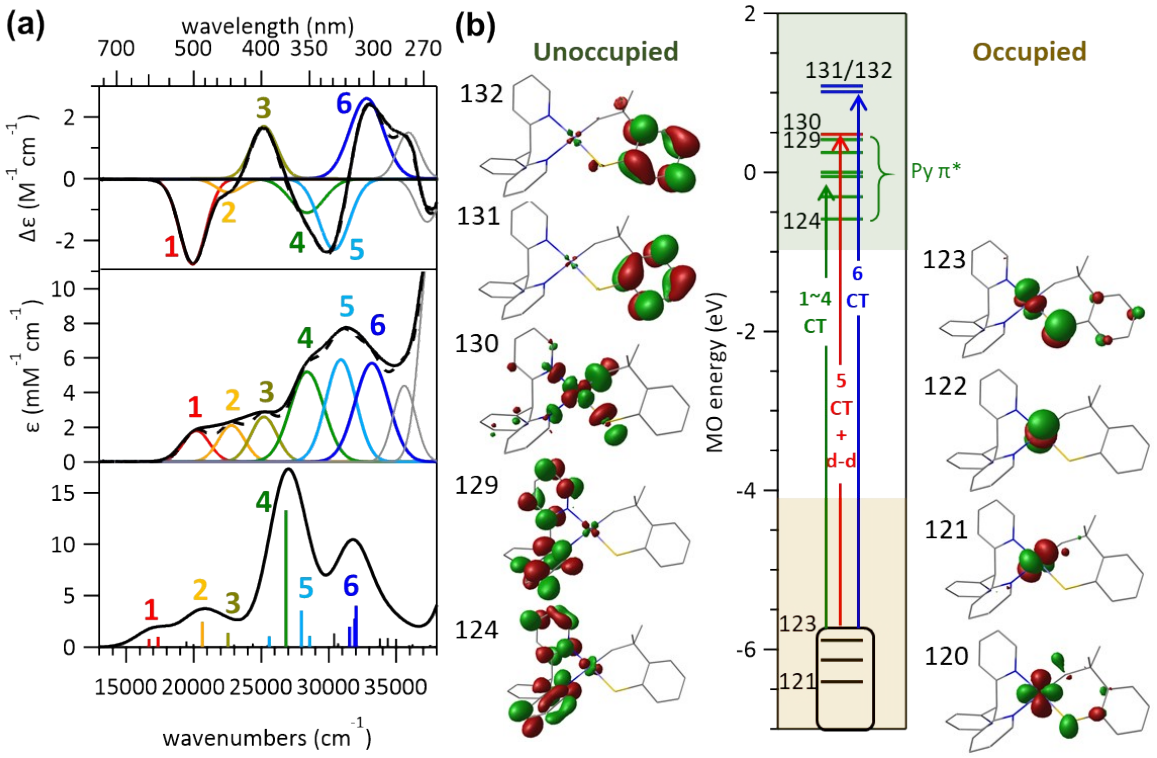

Figure S14. (a) 5 T MCD (top) and Abs (middle) collected at 298 K and TDDFT-simulated Abs (bottom) spectra of $\mathbf{1}_{\mathbf{Py_3CH}}$. Gaussian deconvolution bands and their relevant TDDFT-calculated states are highlighted in color. The sums of Gaussian bands are shown in black dashed lines. (b) FMOs associated with the TDDFT-calculated transitions.

Table S7. Fit parameters from Gaussian deconvolution of the MCD and Abs spectra of $\mathbf{1}_{\mathbf{Py_3CH}}$, and related TDDFT-calculated transitions.

Band	Abs		MCD		TDDFT assignment	
	Energy (cm^{-1})	ε (M^{-1} cm^{-1})	Energy (cm^{-1})	Δε (M^{-1} cm^{-1})		
1	20,200	1,800	19,920	−2.8	#1: 123 → 124 (58 %), 122 → 124 (35 %) #2: 122 → 124 (61 %), 123 → 124 (28 %)	Ni $3d_{z^2/yz}$ → Py π* + Ni $3d_{x^2-y^2}$
2	22,800	2,100	22,600	−0.44	#5: 123 → 125 (38 %), 121 → 124 (30 %), 122 → 125 (12 %)	Ni $3d_{xz/yz}$ → Py π*
3	25,200	2,600	25,200	+1.7	#8: 121 → 125 (72 %)	Ni $3d_{xz}$ → Py π*
4	28,400	5,200	28,400	−1.1	#13: 123 → 129 (39 %), 121 → 130 (32 %)	Ni $3d_{yz}$ → Py π* Ni $3d_{xz}$ → $3d_{x^2-y^2}$
5	30,900	5,900	30,400	−2.3	#15: 120 → 124 (65 %) #16: 120 → 125 (57 %), 120 → 130 (14 %) #19: 120 → 130 (58 %), 120 → 125 (23 %) #21: 120 → 127 (47 %), 119 → 124 (34 %)	Ni $3d_{xy}$ → Py π* Ni $3d_{xy}$ → $3d_{x^2-y^2}$
6	33,200	5,700	32,800	+2.6	#26: 123 → 131 (79 %), 123 → 132 (15 %) #27: 118 → 124 (58 %), 123 → 132 (31 %) #28: 123 → 132 (48 %), 118 → 124 (32 %)	Ni 3d → C_6H_4 π*

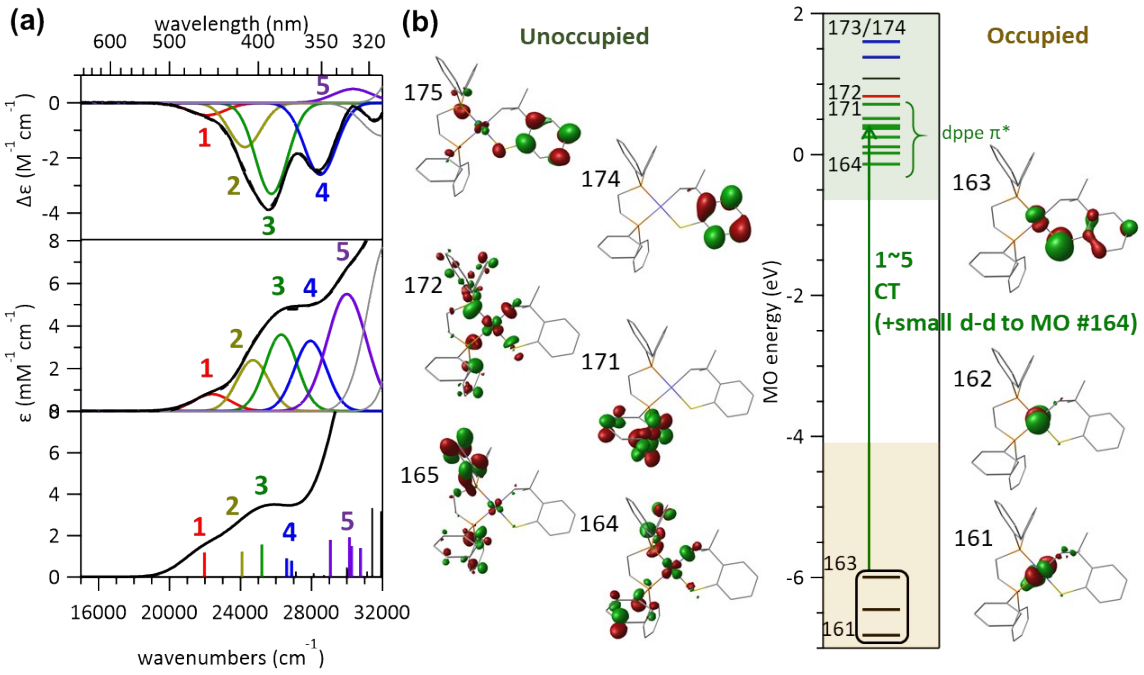

Figure S15. (a) 5 T MCD (top) and Abs (middle) collected at 298 K and TDDFT-simulated Abs (bottom) spectra of $\mathbf{1}_{\mathbf{dppe}}$. Gaussian deconvolution bands and their relevant TDDFT-calculated states are highlighted in color. The sums of Gaussian bands are shown in black dashed lines. (b) FMOs associated with the TDDFT-calculated transitions.

Table S8. Fit parameters from Gaussian deconvolution of the MCD and Abs spectra of $\mathbf{1}_{\mathbf{dppe}}$, and related TDDFT-calculated transitions.

Band	Abs		MCD		TDDFT assignment	
	Energy (cm^{-1})	ε (M^{-1} cm^{-1})	Energy (cm^{-1})	Δε (M^{-1} cm^{-1})		
1	22,400	800	22,100	–0.45	#1: 163 → 164 (67 %), 163 → 165 (11 %)	Ni $3d_{yz}$-S_{3p} → dppe π*
2	24,700	2,400	24,250	–1.6	#2: 162 → 164 (74 %)	Ni $3d_{z^2}$ → dppe π*
3	26,300	3,600	25,750	–3.3	#3: 163 → 165 (30 %), 163 → 166 (22 %), 162 → 164 (15 %), 163 → 164 (11 %)	Ni $3d_{z^2/yz}$ → dppe π*
4	27,950	3,300	28,500	–2.6	#4: 162 → 165 (20 %), 161 → 164 (19 %), 162 → 166 (14 %), 163 → 165 (12 %) #5: 161 → 164 (25 %), 162 → 165 (20 %), 163 → 166 (13 %)	Ni $3d_{z^2/xz}$ → dppe π*
5	30,000	5,500	30,350	+0.5	#9: 163 → 170 (20 %), 163 → 167 (17 %), 163 → 168 (14 %) #12: 162 → 167 (31 %), 163 → 169 (14 %) #13: 163 → 169 (31 %), 161 → 165 (28 %) #14: 162 → 170 (30 %), 162 → 168 (20 %), 162 → 166 (15 %)	Ni 3d → dppe π*
6	22,400	800	22,100	–0.45	#1: 163 → 164 (67 %), 163 → 165 (11 %)	Ni $3d_{yz}$-S_{3p} → dppe π*

Table S9. Fit parameters from Gaussian deconvolution of the MCD and Abs spectra of $\mathbf{1}_{\mathbf{tmeda}}$, and related TDDFT-calculated transitions.

Band	Abs		MCD		TDDFT assignment	
	Energy (cm^{-1})	ε ($M^{-1}\ cm^{-1}$)	Energy (cm^{-1})	Δε ($M^{-1}\ cm^{-1}$)		
1	17,000	40	-	-	#4: 91 → 92 (99 %)	Ni $3d_{yz}$-S_{3p} → $3d_{x^2-y^2}$
2	19,700	100	-	-	#6: 90 → 92 (99 %)	Ni $3d_{z^2}$ → $3d_{x^2-y^2}$
3	22,400	360	22,300	–0.34	#8: 88 → 92 (97 %)	Ni $3d_{xy}$ → $3d_{x^2-y^2}$
4	26,300	155	26,300	–0.035	#7: 89 → 92 (99 %)	Ni $3d_{xz}$ → $3d_{x^2-y^2}$
5	30,200	7,200	29,900	–6.4	#13: 91 → 93 (83 %), 91 → 94 (13 %)	Ni $3d_{yz}$-S_{3p} → C_6H_4 π*

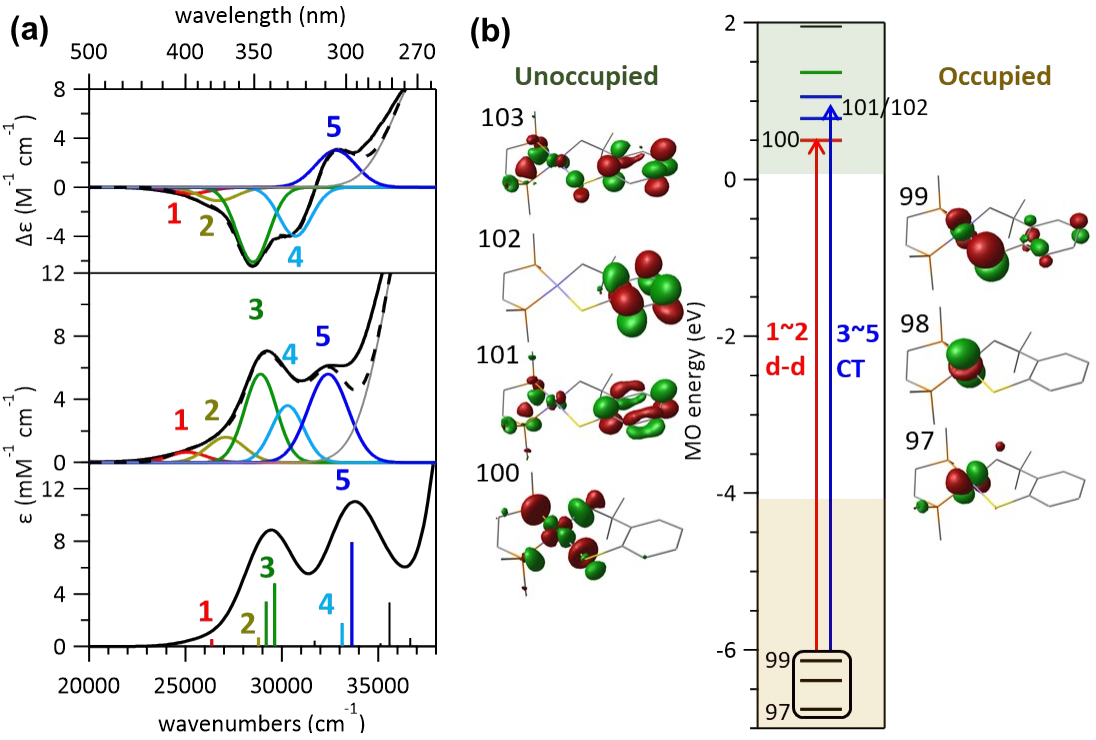

Figure S16. (a) 5 T MCD (top) and Abs (middle) collected at 298 K and TDDFT-simulated Abs (bottom) spectra of $\mathbf{1}_{\mathbf{dmpe}}$. Gaussian deconvolution bands and their relevant TDDFT-calculated states are highlighted in color. The sums of Gaussian bands are shown in black dashed lines. (b) FMOs associated with the TDDFT-calculated transitions.

Table S10. Fit parameters from Gaussian deconvolution of the MCD and Abs spectra of $\mathbf{1}_{\mathbf{dmpe}}$, and related TDDFT-calculated transitions.

Band	Abs		MCD		TDDFT assignment	
	Energy (cm^{-1})	ε (M^{-1} cm^{-1})	Energy (cm^{-1})	Δε (M^{-1} cm^{-1})		
1	25,100	650	25,300	–0.5	#6: 98 → 100 (88 %)	Ni $3d_{z^2}$ → $3d_{x^2-y^2}$
2	27,100	1,600	26,700	–1.1	#10: 97 → 100 (73 %), 98 → 101 (12 %)	Ni $3d_{xz}$ → $3d_{x^2-y^2}$
3	28,900	5,600	28,500	–6.1	#11: 98 → 101 (33 %), 99 → 101 (28 %), 97 → 100 (23 %) #13: 99 → 101 (45 %), 98 → 101 (30 %)	Ni $3d_{yz/z^2}$ → C_6H_4 π*
4	30,300	3,600	30,700	–4.0	#18: 99 → 102 (92 %)	Ni $3d_{yz/z^2}$ → C_6H_4 π*
5	32,400	5,600	32,800	+3.0	#19: 97 → 101 (68 %), 97 → 103 (13 %)	Ni $3d_{xz}$ → C_6H_4 π*

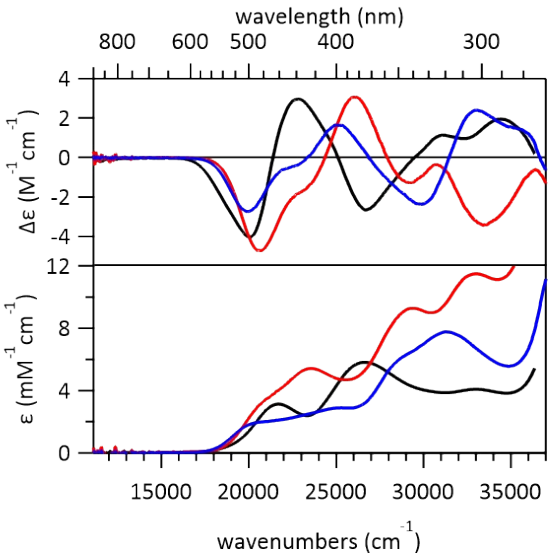

Figure S17. 5 T MCD (top) and Abs (bottom) spectra collected at 298 K of $\mathbf{1}_{\mathbf{Py_3CH}}$ (blue), $\mathbf{2}_{\mathbf{Py_3CH}}$ (red), and $\mathbf{3}_{\mathbf{Py_3CH}}$ (black).

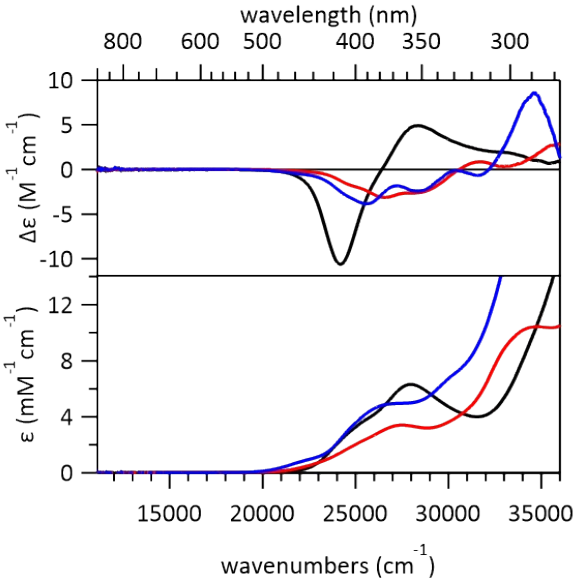

Figure S18. 5 T MCD (top) and Abs (bottom) spectra collected at 298 K of $\mathbf{1}_{\mathbf{dppe}}$ (blue), $\mathbf{2}_{\mathbf{dppe}}$ (red), and $\mathbf{3}_{\mathbf{dppe}}$ (black).

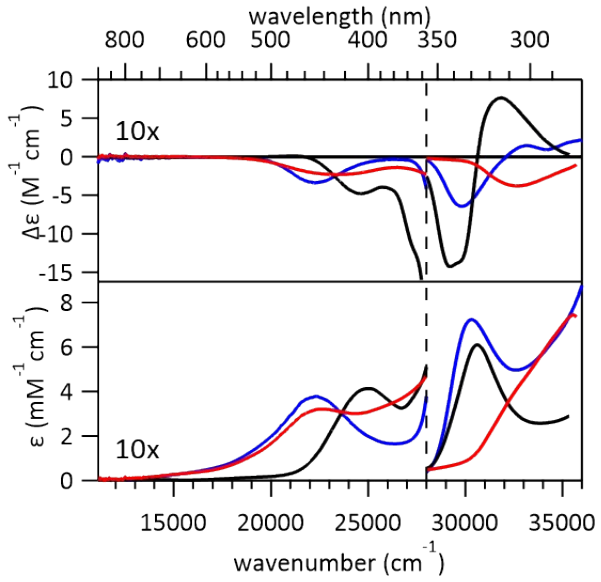

Figure S19. 5 T MCD (top) and Abs (bottom) spectra collected at 298 K of $\mathbf{1}_{\mathbf{tmeda}}$ (blue), $\mathbf{2}_{\mathbf{tmeda}}$ (red), and $\mathbf{3}_{\mathbf{tmeda}}$ (black).

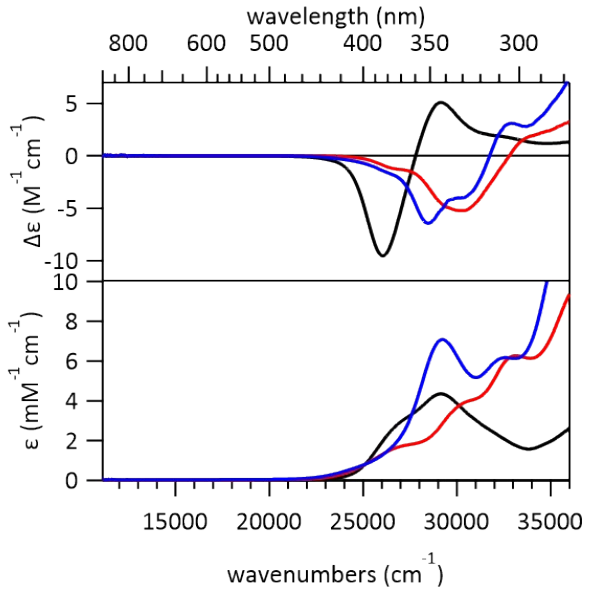

Figure S20. 5 T MCD (top) and Abs (bottom) spectra collected at 298 K of $\mathbf{1}_{\mathbf{dmpe}}$ (blue), $\mathbf{2}_{\mathbf{dmpe}}$ (red), and $\mathbf{3}_{\mathbf{dmpe}}$ (black).

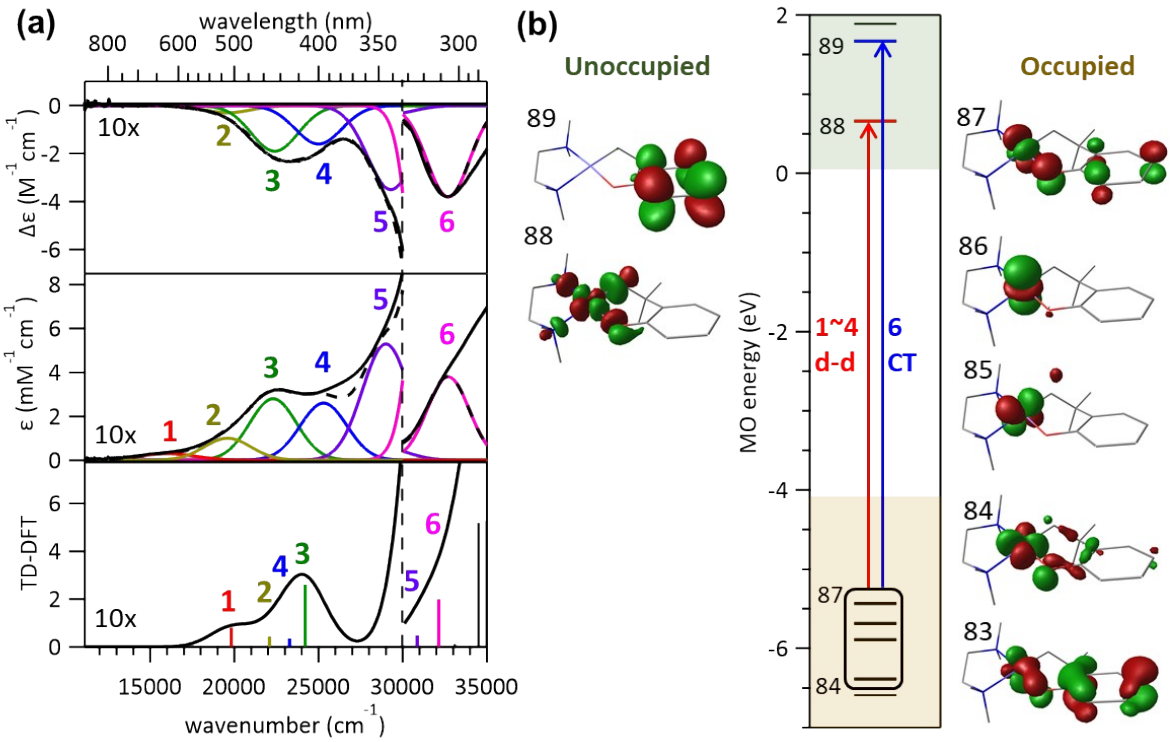

Figure S21. (a) 5 T MCD (top) and Abs (middle) collected at 298 K and TDDFT-simulated Abs (bottom) spectra of $\mathbf{2}_{\mathbf{tmeda}}$. Gaussian deconvolution bands and their relevant TDDFT-calculated states are highlighted in color. The sums of Gaussian bands are shown in black dashed lines. (b) FMOs associated with the TDDFT-calculated transitions.

Table S11. Fit parameters from Gaussian deconvolution of the MCD and Abs spectra of $\mathbf{2}_{\mathbf{tmeda}}$, and related TDDFT-calculated transitions.

Band	Abs		MCD		TDDFT assignment	
	Energy (cm^{-1})	ε (M^{-1} cm^{-1})	Energy (cm^{-1})	Δε (M^{-1} cm^{-1})		
1	16,000	30	-	-	#5: 87 → 88 (97 %)	Ni $3d_{yz}$-O_{2p} → $3d_{x^2-y^2}$
2	19,600	100	19,600	–0.03	#6: 86 → 88 (99 %)	Ni $3d_{z^2}$ → $3d_{x^2-y^2}$
3	22,300	280	22,400	–0.19	#8: 84 → 88 (87 %)	Ni $3d_{xy}$ → $3d_{x^2-y^2}$
4	25,300	260	25,000	–0.16	#7: 85 → 88 (99 %)	Ni $3d_{xz}$ → $3d_{x^2-y^2}$
5	29,000	530	29,300	–0.35	#13: 83 → 88 (86 %)	O_{2p}+Ni $3d_{yz}$ → Ni $3d_{x^2-y^2}$
6	32,700	3,800	32,700	–3.8	#14 : 87 → 89 (97 %)	Ni $3d_{yz}$ → C_6H_4 π*

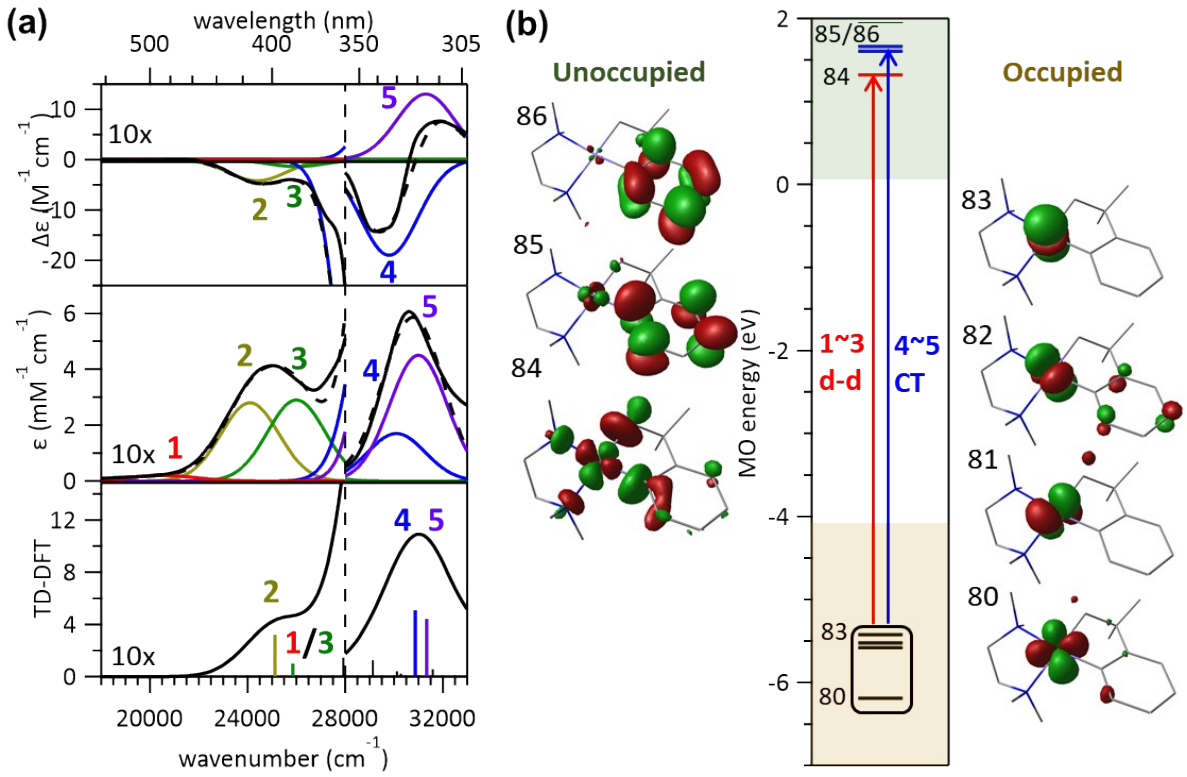

Figure S22. (a) 5 T MCD (top) and Abs (middle) collected at 298 K and TDDFT-simulated Abs (bottom) spectra of $\mathbf{3}_{\mathbf{tmeda}}$. Gaussian deconvolution bands and their relevant TDDFT-calculated states are highlighted in color. The sums of Gaussian bands are shown in black dashed lines. (b) FMOs associated with the TDDFT-calculated transitions.

Table S12. Fit parameters from Gaussian deconvolution of the MCD and Abs spectra of $\mathbf{3}_{\mathbf{tmeda}}$, and related TDDFT-calculated transitions.

Band	Abs		MCD		TDDFT assignment	
	Energy (cm^{-1})	ε (M^{-1} cm^{-1})	Energy (cm^{-1})	Δε (M^{-1} cm^{-1})		
1	20,500	20	20,500	+0.01	#6: 82 → 84 (52 %), 81 → 84 (34 %)	Ni $3d_{yz}$ → $3d_{x^2-y^2}$
2	24,100	280	24,400	–0.42	#5: 83 → 84 (85 %)	Ni $3d_{z^2}$ → $3d_{x^2-y^2}$
3	26,000	290	26,000	–0.14	#7: 81 → 84 (54 %), 82 → 84 (38 %)	Ni $3d_{xz}$ → $3d_{x^2-y^2}$
4	30,100	1,700	29,900	–19	#18: 82 → 85 (54 %), 82 → 86 (15 %)	Ni $3d_{yz}$ → C_6H_4 π*
5	31,000	4,500	31,300	+13	#20: 82 → 86 (69 %)	Ni $3d_{yz}$ → C_6H_4 π*

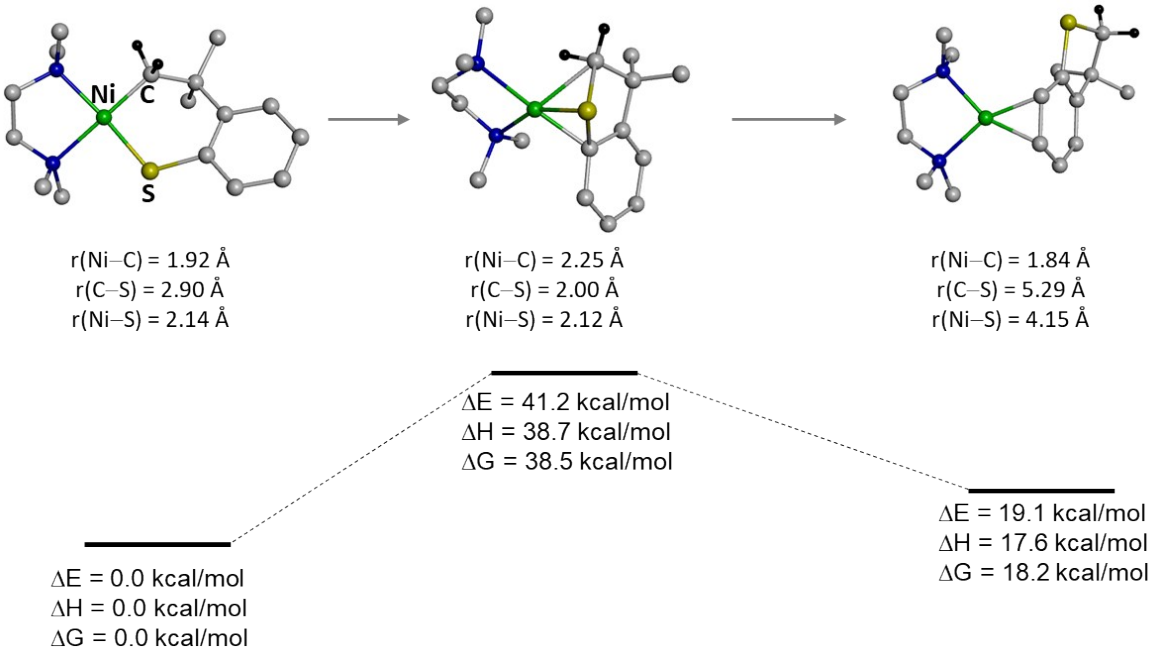

Figure S23. DFT-calculated energy profile for the ground-state C–S bond-forming RE reaction of $\mathbf{1}_{\mathbf{tmeda}}$.

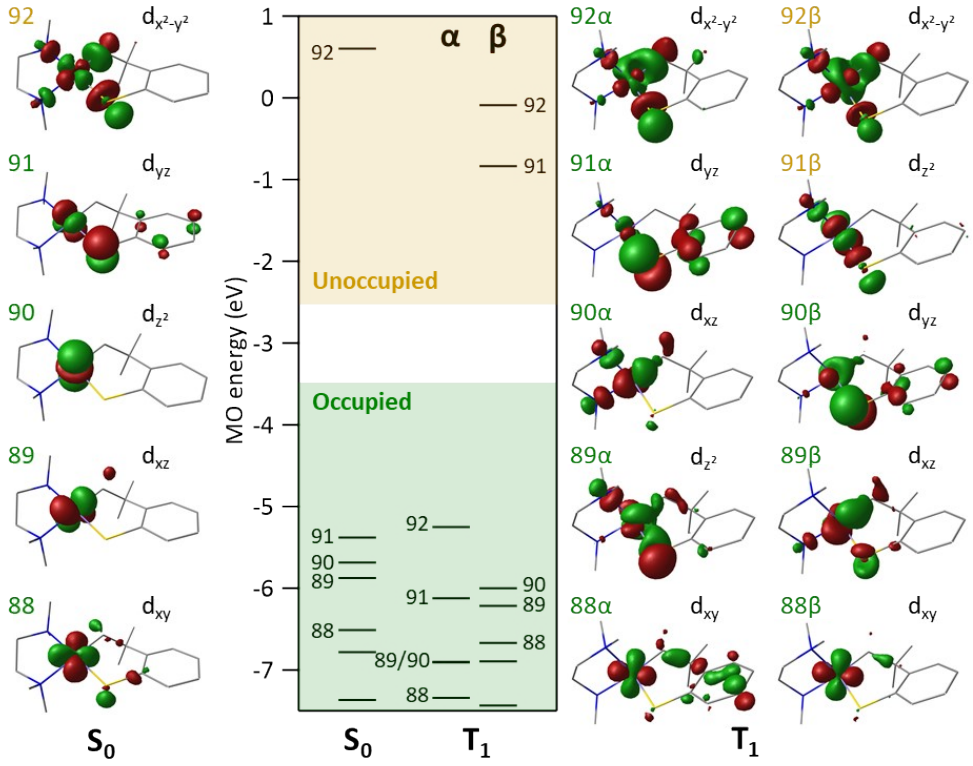

Figure S24. MO diagrams of $\mathbf{1}_{\mathbf{tmeda}}$ in the (a) S_0 and (b) T_1 states.

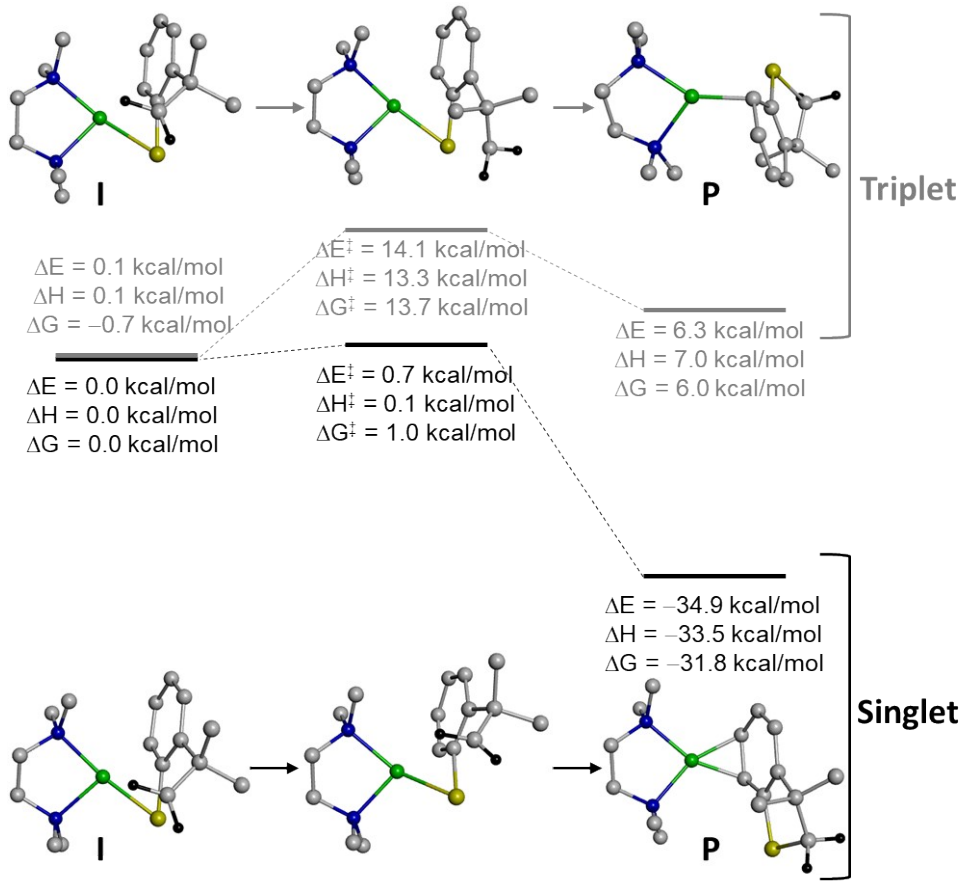

Figure S25. Energy profile for the C–S bond formation of intermediate **I** of $\mathbf{1}_{\mathbf{tmeda}}$ in the singlet (black) and triplet (grey) states.

Table S13. DFT-calculated thermodynamics for the Ni–C bond homolysis of **R** in the T_1 excited state.

kcal/mol	$\mathbf{1}_{\mathbf{tmeda}}$	$\mathbf{2}_{\mathbf{tmeda}}$	$\mathbf{3}_{\mathbf{tmeda}}$	$\mathbf{1}_{\mathbf{dmpe}}$	$\mathbf{2}_{\mathbf{dmpe}}$	$\mathbf{3}_{\mathbf{dmpe}}$	$\mathbf{1}_{\mathbf{bpy}}$
ΔE	24.6	32.2	27.8	17.8	23.0	23.8	28.5
ΔH	23.2	30.7	26.1	16.5	21.7	22.5	26.9
ΔG	22.5	28.7	27.1	15.6	19.9	20.7	26.0

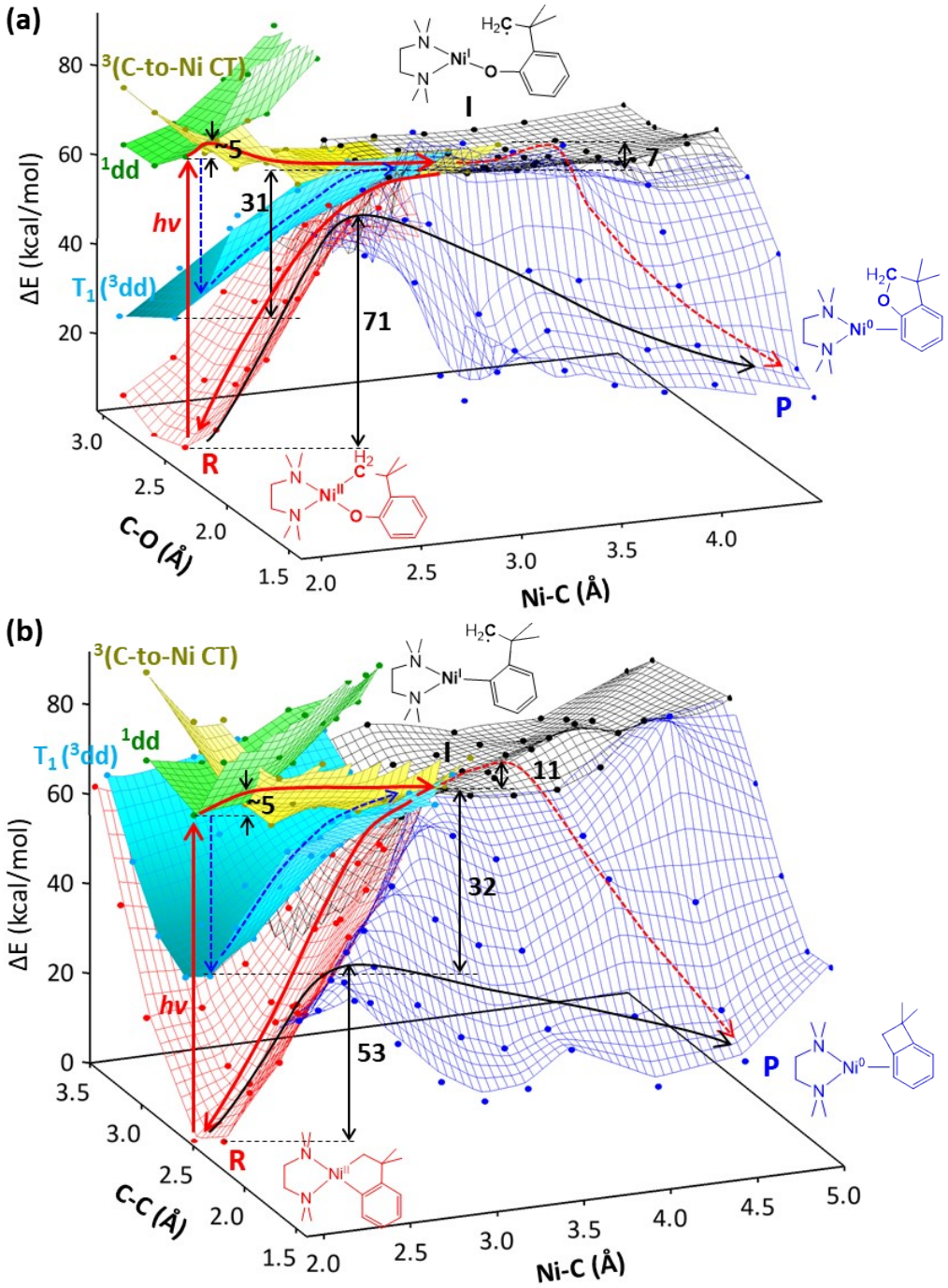

Figure S26. Ground- and excited-state PESs of (a) $\mathbf{2}_{\mathbf{tmeda}}$ and (b) $\mathbf{3}_{\mathbf{tmeda}}$. The ground-state PESs of the reactant (**R**), the Ni^{I} intermediate (**I**), and the product (**P**) are presented in red, black, and blue, respectively. The $^{1}(d_{z^2} \rightarrow d_{x^2-y^2})$, ^{3}(C-to-Ni CT), and T_1 excited states of **R** and nearby geometries are depicted in green, yellow, and cyan, respectively. The reaction coordinate consistent with experiment is shown with red solid arrows.

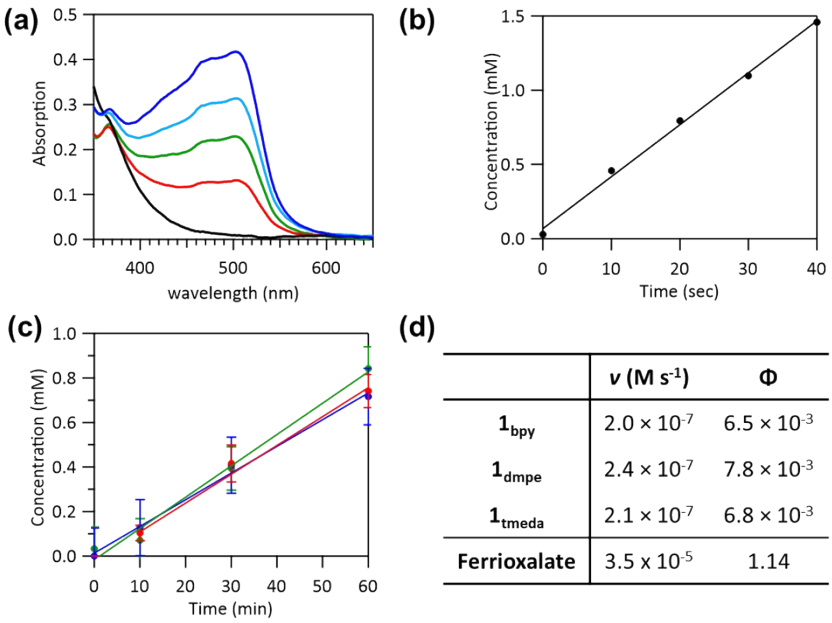

	v ($M\ s^{-1}$)	Φ
$\mathbf{1}_{bpy}$	2.0×10^{-7}	6.5×10^{-3}
$\mathbf{1}_{dmpe}$	2.4×10^{-7}	7.8×10^{-3}
$\mathbf{1}_{tmeda}$	2.1×10^{-7}	6.8×10^{-3}
Ferrioxalate	3.5×10^{-5}	1.14

Figure S27. Quantum yield determination using ferrioxalate actinometry. (a) Abs spectra obtained after adding 1,10-phenanthroline into the ferrioxalate solution that had been exposed to the 405 nm laser line for 0 (black), 10 (red), 20 (green), 30 (blue), and 40 (purple) seconds. (b) Yields of $[Fe(phen)_3]^{2+}$ as a function of irradiation time. (c) Yields of the 2,3-dihydro-3,3-dimethyl-benzo[*b*]thiophene product from $\mathbf{1}_{bpy}$ (blue), $\mathbf{1}_{dmpe}$ (green), and $\mathbf{1}_{tmeda}$ (red) as a function of irradiation time. (d) Quantum yields (Φ's) of the photo-induced C–S bond formation reactions obtained by using the equation of $\Phi_{\mathbf{1}} = v_{\mathbf{1}}/v_{ferrioxalate} \times \Phi_{ferrioxalate}$, where $\Phi_{ferrioxalate}$, $v_{ferrioxalate}$, and $v_{\mathbf{1}}$ refer to the literature reported quantum yield (1.14) of ferrioxalate,[15] and the measured photoreaction rates of ferrioxalate and **1**.

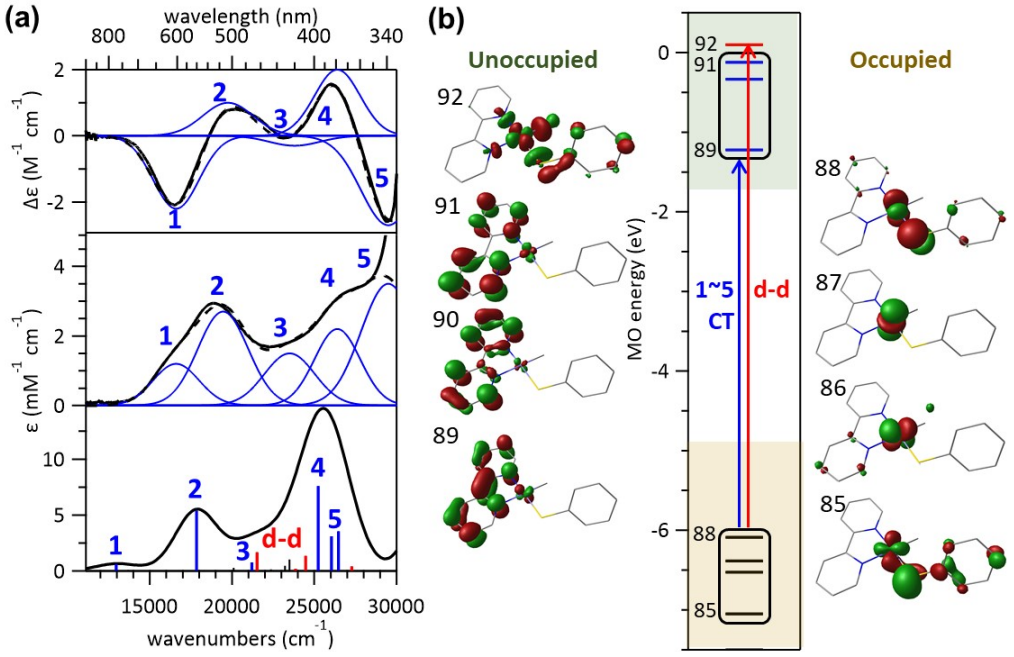

Figure S28. (a) 5 T MCD (top) and Abs (middle) collected at 298 K and TDDFT-simulated Abs (bottom) spectra of $\mathbf{4}_{\mathbf{bpy}}$. Gaussian deconvolution bands and their relevant TDDFT-calculated states are highlighted in color. The sums of Gaussian bands are shown in black dashed lines. (b) FMOs associated with the TDDFT-calculated transitions.

Table S14. Fit parameters from Gaussian deconvolution of the MCD and Abs spectra of $\mathbf{4}_{\mathbf{bpy}}$, and related TDDFT-calculated transitions.

Band	Abs		MCD		TDDFT assignment	
	Energy (cm^{-1})	ε (M^{-1} cm^{-1})	Energy (cm^{-1})	Δε (M^{-1} cm^{-1})		
1	16,600	1,200	16,600	–2.2	#3: 88 → 89 (78 %), 86 → 89 (12 %)	Ni $3d_{yz}$-S_{3p} → bpy π*
2	19,450	2,700	19,750	1.0	#9: 86 → 89 (72 %), 88 → 89 (13 %)	Ni $3d_{xz}$ → bpy π*
3	23,500	1,500	23,800	–0.3	#13: 88 → 90 (82 %)	Ni $3d_{yz}$-S_{3p} → bpy π*
4	26,400	2,200	26,400	2.0	#27: 86 → 92 (26 %), 88 → 91 (26 %), 86 → 90 (17 %)	Ni $3d_{yz}$-S_{3p}/$3d_{xz}$ → bpy π*
5	29,500	3,500	29,500	–2.7	#28: 86 → 91 (50 %), 86 → 92 (16 %), 84 → 89 (13 %) #30: 84 → 89 (36 %), 85 → 92 (16 %), 85 → 89 (13 %)	Ni $3d_{xz}$/$3d_{xy}$ → bpy π*
d-d	-	-	-	-	#16: 88 → 92 (46 %), 85 → 89 (25 %) #24: 87 → 92 (36 %), 86 → 89 (25 %), 86 → 90 (19 %) #25: 86 → 92 (32 %), 87 → 92 (31 %) #32: 85 → 92 (44 %), 84 →92 (23 %), 84 → 89 (14 %)	Ni $3d_{yz}$-S_{3p} → $3d_{x^2-y^2}$ Ni $3d_{z^2}$ → $3d_{x^2-y^2}$ Ni $3d_{xz}$ → $3d_{x^2-y^2}$ Ni $3d_{xy}$ → $3d_{x^2-y^2}$

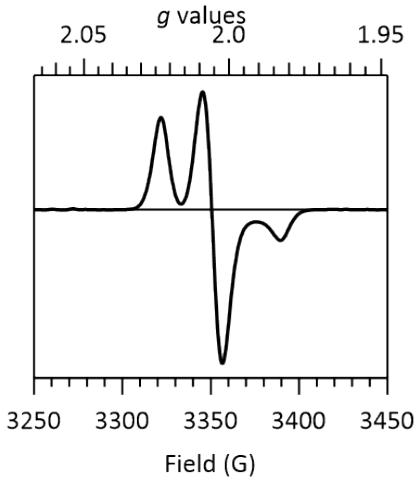

Figure S29. 100 K X-band EPR spectrum obtained from the photo-induced radical trapping experiment of $\mathbf{4}_{\mathbf{bpy}}$ with 100 equivalents of α-phenyl-tertiary-butylnitrone (PBN).

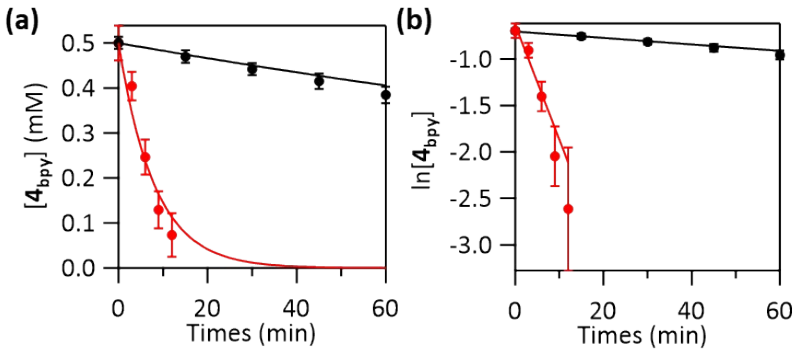

Figure S30. (a) 50 mW 405 nm (red) and 532 nm (black) laser-induced decay of $\mathbf{4}_{\mathbf{bpy}}$. (b) Plots of ln[$\mathbf{4}_{\mathbf{bpy}}$] vs. irradiation time to show the 1st-order kinetics. Rate constants obtained from logarithmic plots (k_{405} = 1.2 (± 0.2) × 10^{-1} and k_{532} = 3.5 (± 0.5) × 10^{-3} min^{-1}) were used to construct the fitting curves in (a).

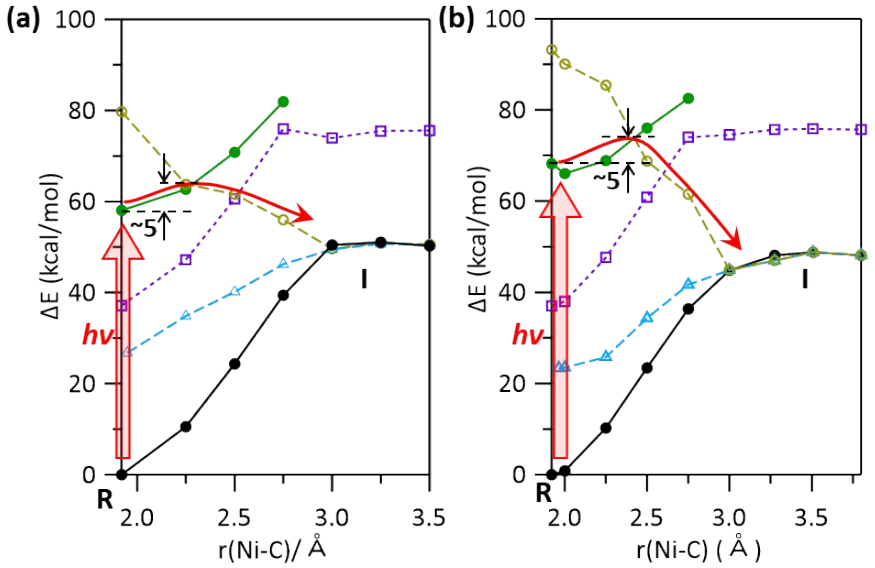

Figure S31. DFT-calculated ground- and excited-state PESs of (a) $\mathbf{1}_{\mathbf{bpy}}$ and (b) $\mathbf{4}_{\mathbf{bpy}}$. The energy profiles of the ground state (●) and the ^{1}(dd) (●), ^{3}(Ni-to-bpy π* CT) (□), ^{3}(C-to-Ni CT) (○), and T_1 (△) excited states are given along Ni–C bond homolysis**.** Upon excitation to the ^{1}(dd) excited state, both $\mathbf{1}_{\mathbf{bpy}}$ and $\mathbf{4}_{\mathbf{bpy}}$ can have the Ni-C bond dissociated with about 5 kcal/mol energy barrier via intersystem crossing to the ^{3}(C-to-Ni CT) surface. These pathways are indicated with red arrows.

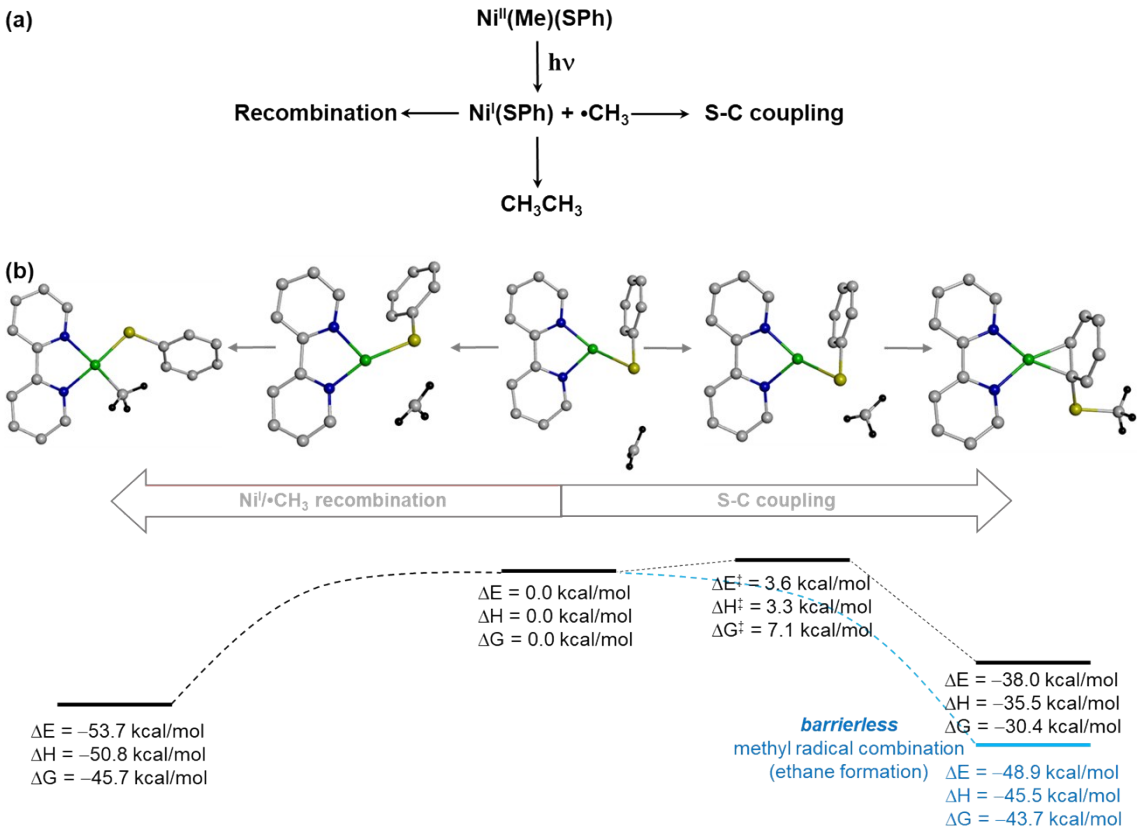

Figure S32. (a) Reaction scheme of intermediate **I** from $\mathbf{4}_{\mathbf{bpy}}$ and (b) its energy profiles along the $Ni^{I}/•CH_3$ recombination (left), C–S bond formation (right), and methyl radical combination (blue) pathways.

Table S15. ^{1}H-NMR observed major product after 390 nm LED irradiation to aliphatic nickelacycles $\mathbf{7}_{\mathbf{bpy}}$ and $\mathbf{8}_{\mathbf{bpy}}$.

	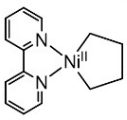 $\mathbf{7}_{\mathbf{bpy}}$	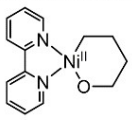 $\mathbf{8}_{\mathbf{bpy}}$
Product	 > 33 %	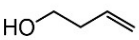 60 %

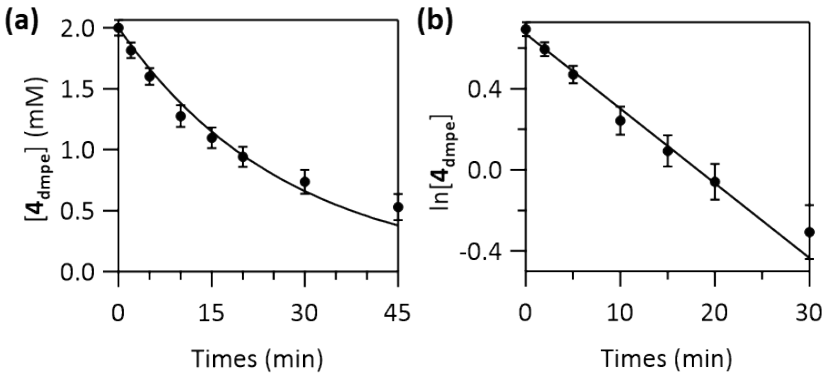

Figure S33. (a) 50 mW 405 nm laser-induced decay of $\mathbf{4}_{\mathbf{dmpe}}$. (b) Plots of ln[$\mathbf{4}_{\mathbf{dmpe}}$] vs. irradiation time to show the 1st-order kinetics. The rate constant obtained from logarithmic plots (k_{405} = 3.7 (± 0.3) × 10^{-2} min^{-1}) was used to construct the fitting curve in (a).

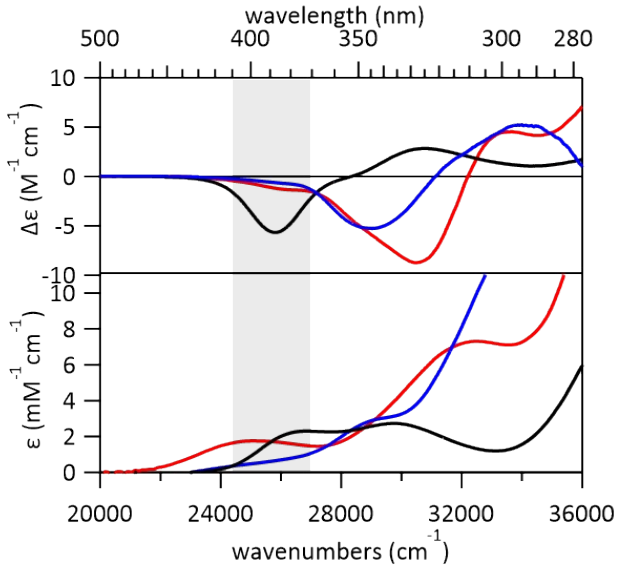

Figure S34. 5 T MCD (top) and Abs (bottom) spectra collected at 298 K of $\mathbf{4}_{\mathbf{dmpe}}$ (blue), $\mathbf{5}_{\mathbf{dmpe}}$ (red), and $\mathbf{6}_{\mathbf{dmpe}}$ (black). The energy window of 390 nm LED light is colored in gray.

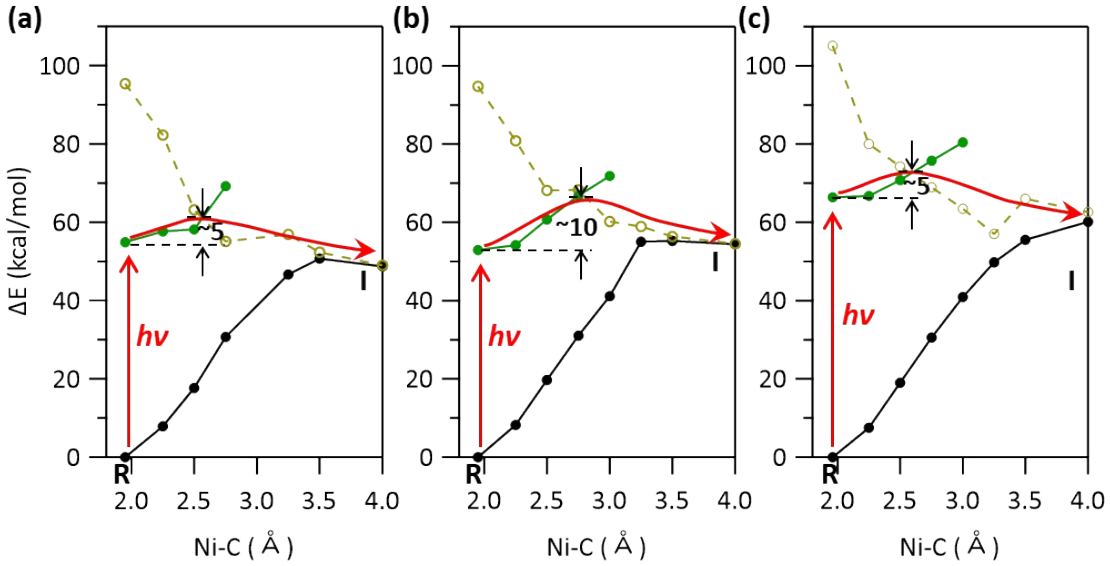

Figure S35. Energy profiles of ground state (●), ^{1}(dd) (●), and ^{3}(C-to-Ni CT) (○) excited states upon the Ni–C bond homolysis of (a) $\mathbf{4}_{\mathbf{dmpe}}$, (b) $\mathbf{5}_{\mathbf{dmpe}}$, and (c) $\mathbf{6}_{\mathbf{dmpe}}$. Upon excitation to ^{1}(dd) excited state, the reactant (**R**) can convert to intermediate (**I**) with discernible barrier via ISC to ^{3}(C-to-Ni CT) surface (Red pathway).

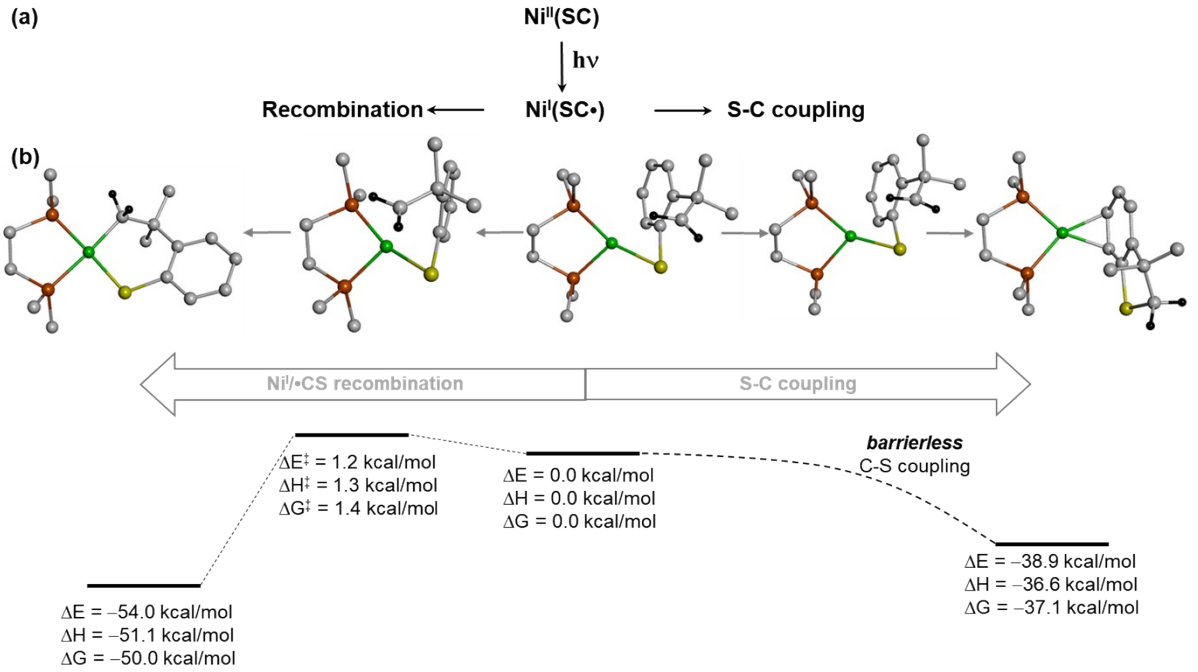

Figure S36. (a) Reaction scheme of intermediate **I** from $\mathbf{1}_{\mathbf{dmpe}}$ and (b) its energy profiles along the Ni^{I}/(•CS) recombination (left) and C–S bond formation (right) pathways.

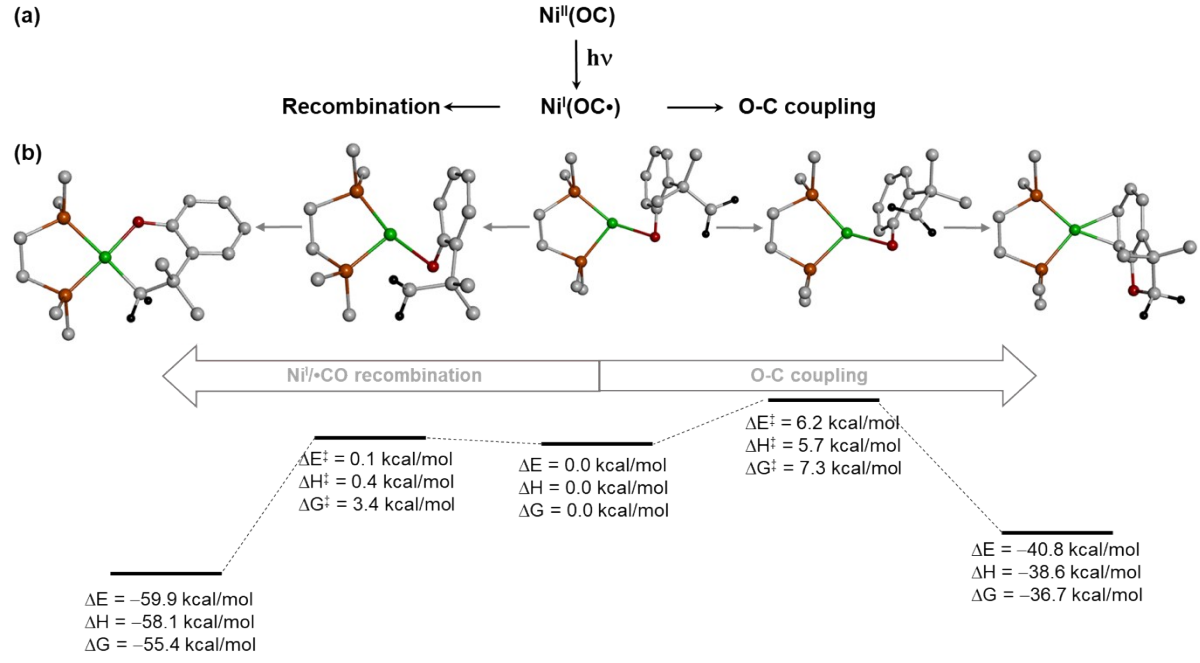

Figure S37. (a) Reaction scheme of intermediate **I** from $\mathbf{2}_{\mathbf{dmpe}}$ and (b) its energy profiles along the Ni^{I}/(•CO) recombination (left) and C–O bond formation (right) pathways.

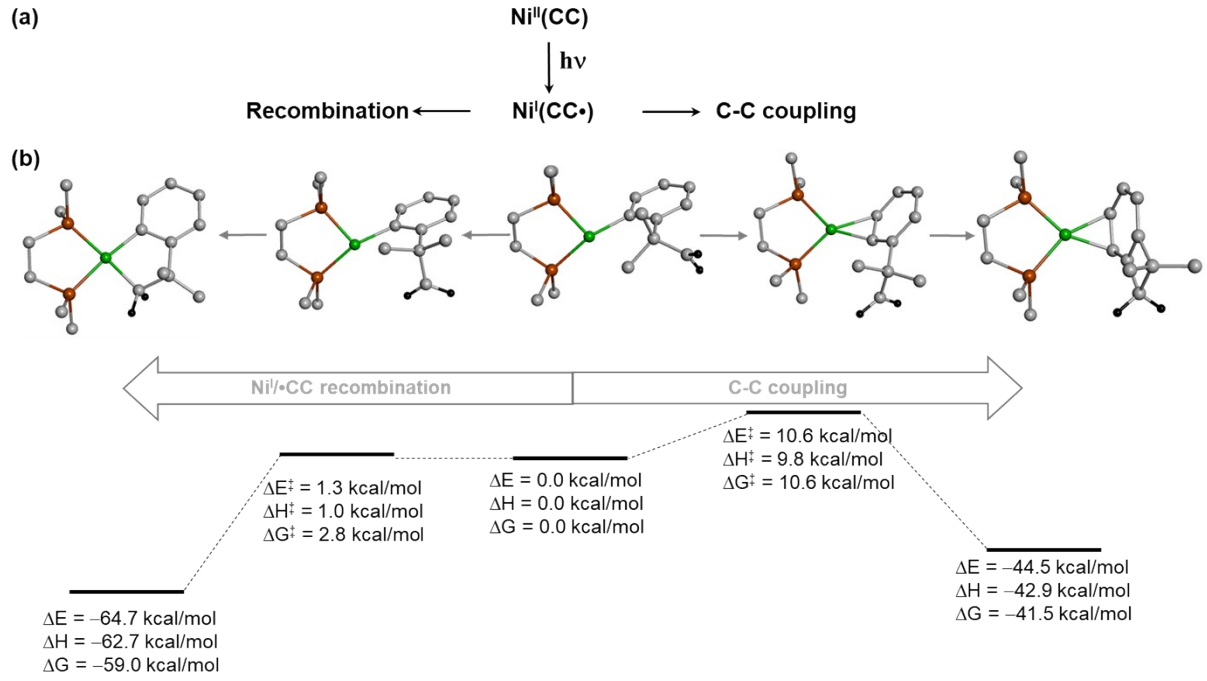

Figure S38. (a) Reaction scheme of intermediate **I** from $\mathbf{3}_{\mathbf{dmpe}}$ and (b) its energy profiles along the Ni^{I}/(•CC) recombination (left) and C–C bond formation (right) pathways.

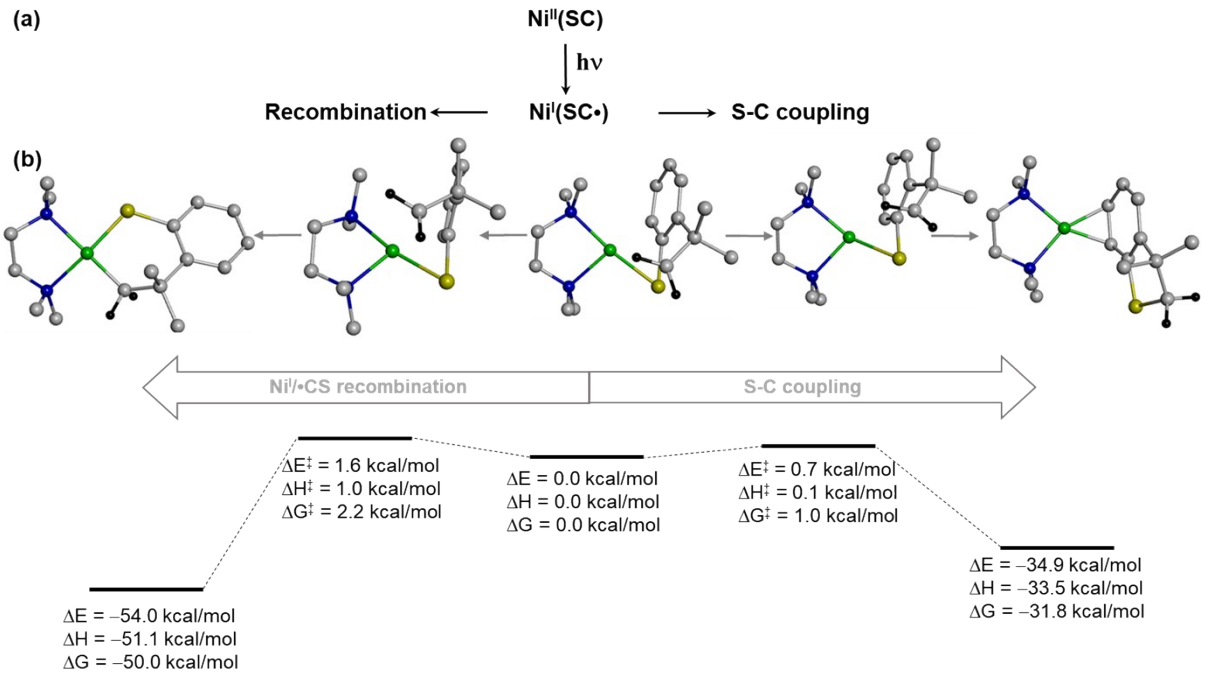

Figure S39. (a) Reaction scheme of intermediate **I** from $\mathbf{1}_{\mathbf{tmeda}}$ and (b) its energy profiles along the Ni^{I}/(•CS) recombination (left) and C–S bond formation (right) pathways.

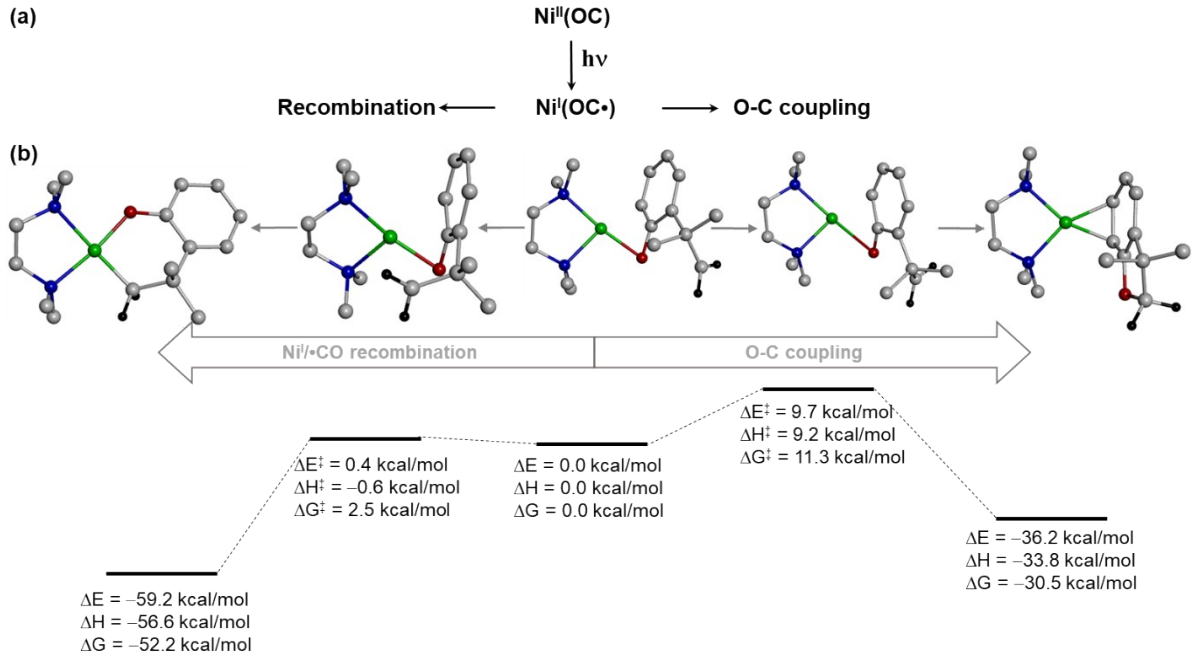

Figure S40. (a) Reaction scheme of intermediate **I** from $\mathbf{2}_{\mathbf{tmeda}}$ and (b) its energy profiles along the Ni^{I}/(•CO) recombination (left) and C–O bond formation (right) pathways.

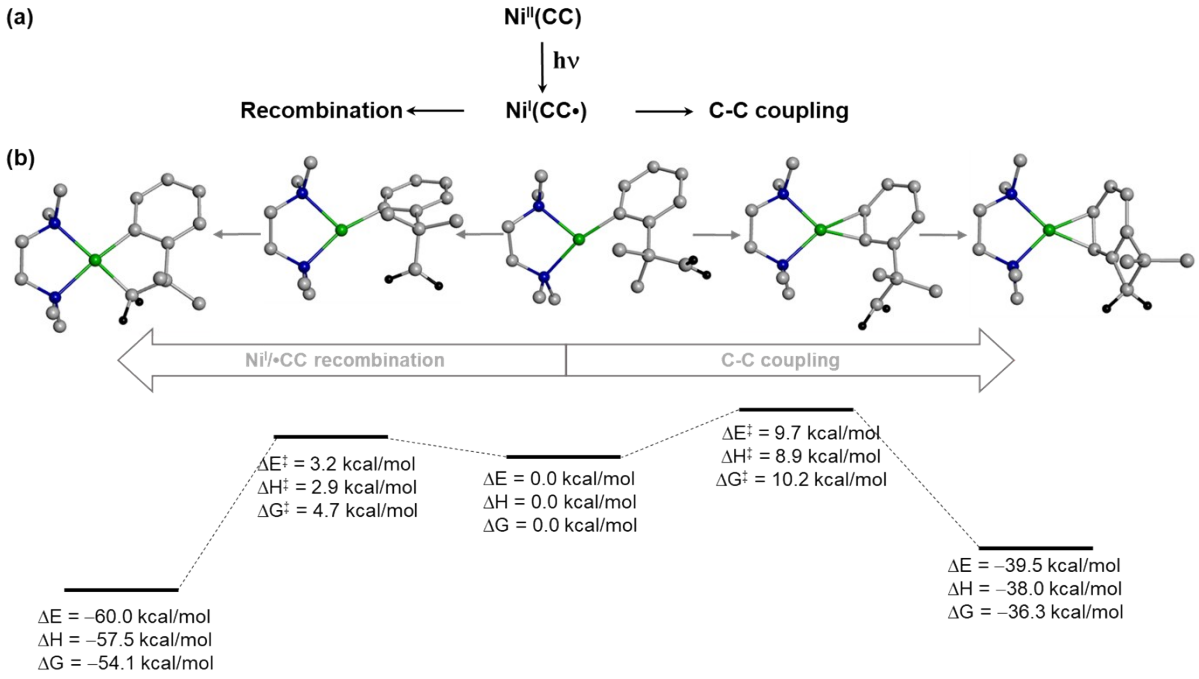

Figure S41. (a) Reaction scheme of intermediate **I** from $\mathbf{3}_{\mathbf{tmeda}}$ and (b) its energy profiles along the Ni^{I}/(•CC) recombination (left) and C–C bond formation (right) pathways.

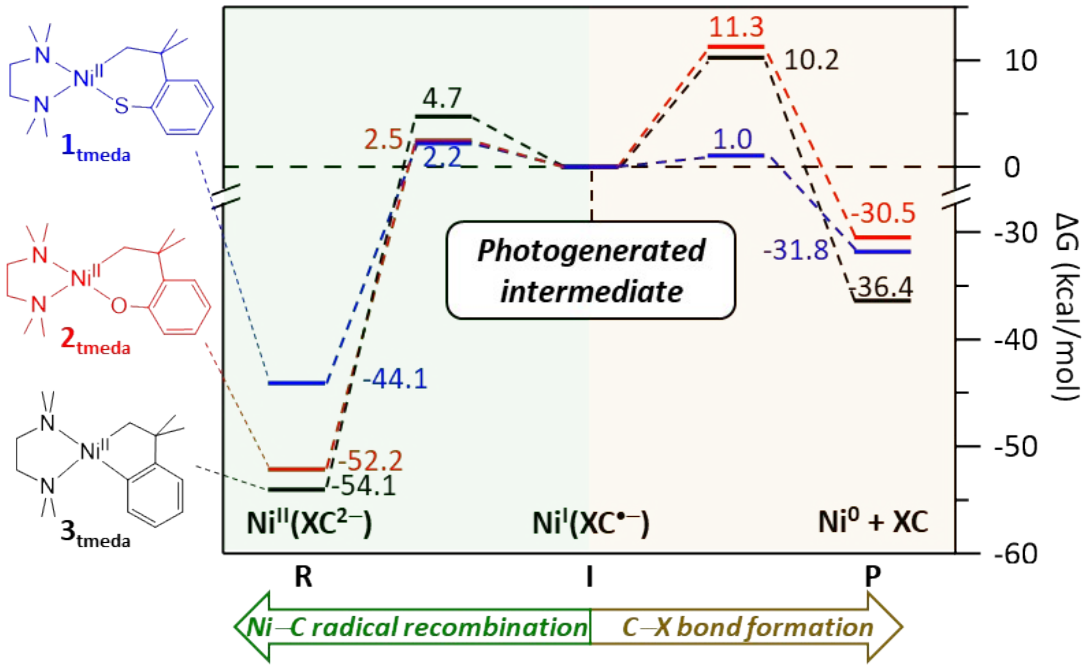

Figure S42. Energy profiles of the Ni^{I} intermediates of $\mathbf{1}_{tmeda}$~$\mathbf{3}_{tmeda}$. The Ni–C radical recombination pathway to **R** (left) and the C–X bond formation pathway to **P** (right) are compared, showing that for $\mathbf{1}_{tmeda}$, both pathways are feasible while for $\mathbf{2}_{tmeda}$ and $\mathbf{3}_{tmeda}$, the left pathway is more preferred.

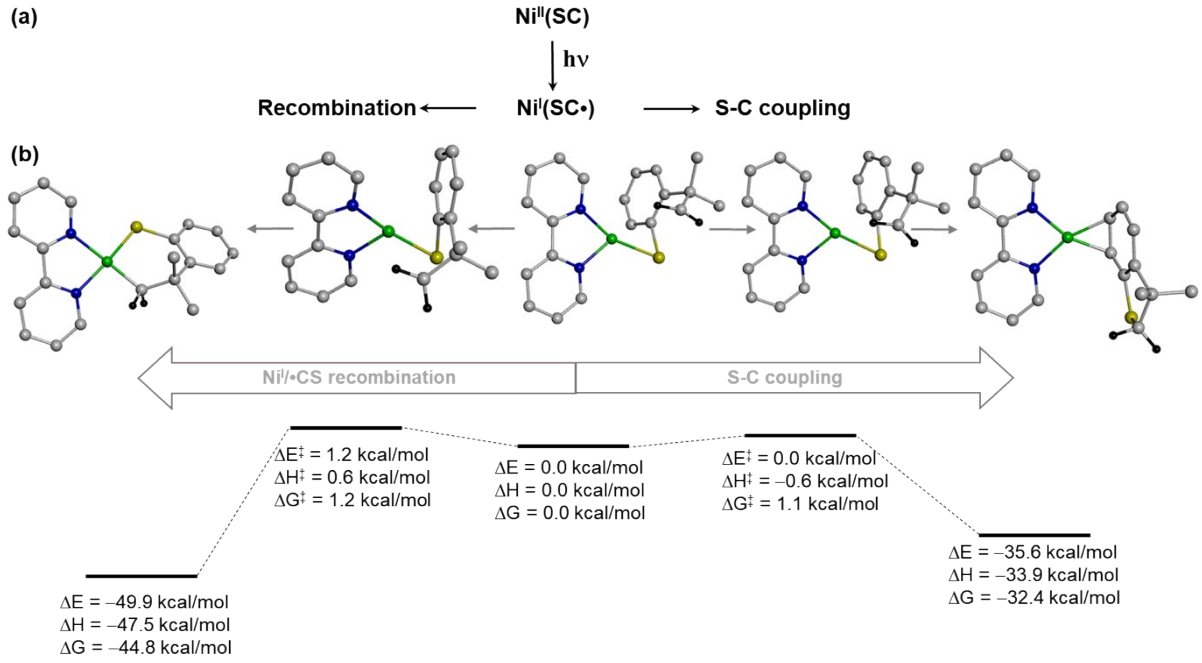

Figure S43. (a) Reaction scheme of intermediate **I** from $\mathbf{1}_{bpy}$ and (b) its energy profiles along the Ni^{I}/(•CS) recombination (left) and C–S bond formation (right) pathways.

NMR spectra of Ni complexes

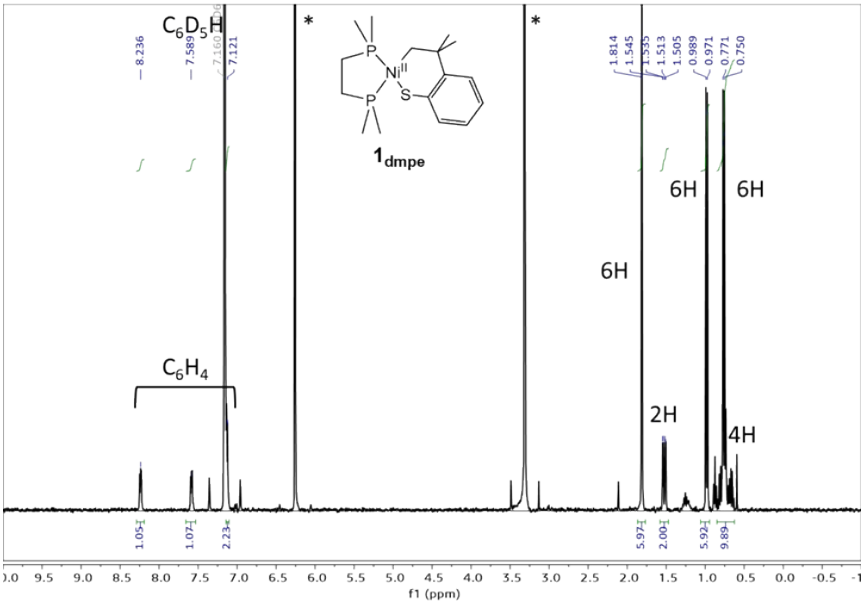

Figure S44. ^{1}H-NMR spectrum of $\mathbf{1}_{\mathbf{dmpe}}$. Peaks with asterisks are from internal standard, 1,3,5-trimethoxybenzene. ^{1}H NMR (400 MHz, C_6D_6, 25 °C): δ = 8.26-8.21 (m, 1H, C_6H_4), 7.61-7.56 (m, 1H, C_6H_4), 7.16-7.11 (m, 2H, C_6H_4), 1.81 (s, 6H, CMe_2), 1.52 (dd, *J* = 12.7, 4.0 Hz, 6H, $NiCH_2$), 0.98 (dd, *J* = 8.2, 0.7 Hz, 6H, PMe_2), 0.85-0.63 (m, 4H, PCH_2), 0.76 ppm (d, *J* = 8.4, 0.8 Hz, 6H, PMe_2).

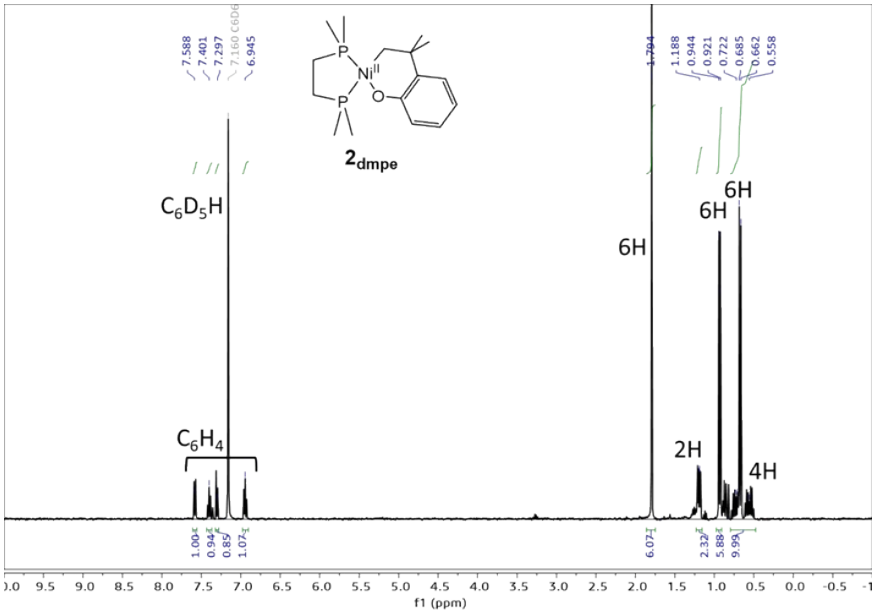

Figure S45. ^{1}H-NMR spectrum of $\mathbf{2}_{\mathbf{dmpe}}$. ^{1}H NMR (400 MHz, C_6D_6, 25 °C): δ = 7.58 (dd, *J* = 7.6, 1.8 Hz, 1H, C_6H_4), 7.43-7.37 (m, 1H, C_6H_4), 7.30 (dd, *J* = 8.0, 1.5 Hz, 1H, C_6H_4), 6.95 (td, *J* = 7.2, 1.2 Hz, 1H, C_6H_4), 1.79 (s, 6H, CMe_2), 1.19 (dd, *J* = 10.4, 4.8 Hz, 2H, $NiCH_2$), 0.93 (dd, *J* = 8.0, 0.8 Hz, 6H, PMe_2), 0.79-0.50 (m, 4H, PCH_2), 0.67 ppm (d, *J* = 9.1, 0.9 Hz, 6H, PMe_2).

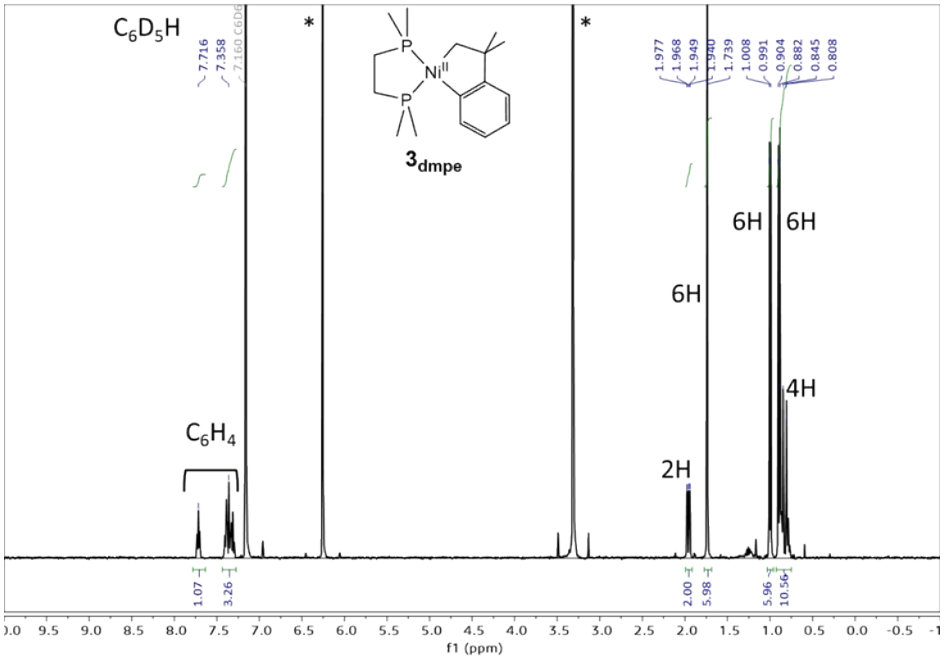

Figure S46. ^{1}H-NMR spectrum of $\mathbf{3}_{\mathbf{dmpe}}$. Peaks with asterisks are from internal standard, 1,3,5-trimethoxybenzene. ^{1}H NMR (400 MHz, C_6D_6, 25 °C): δ=7.72 (t, J = 6.6 Hz, 1H, C_6H_4), 7.42-7.28 (m, 3H, C_6H_4), 1.96 (dd, J = 11.1, 3.8 Hz, 2H, $NiCH_2$), 1.74 (s, 6H, CMe_2), 1.00 (d, J = 6.8 Hz, 6H, PMe_2), 0.89 (d, J = 8.6 Hz, 6H, PMe_2), 0.87-0.77 ppm (m, 4H, PCH_2).

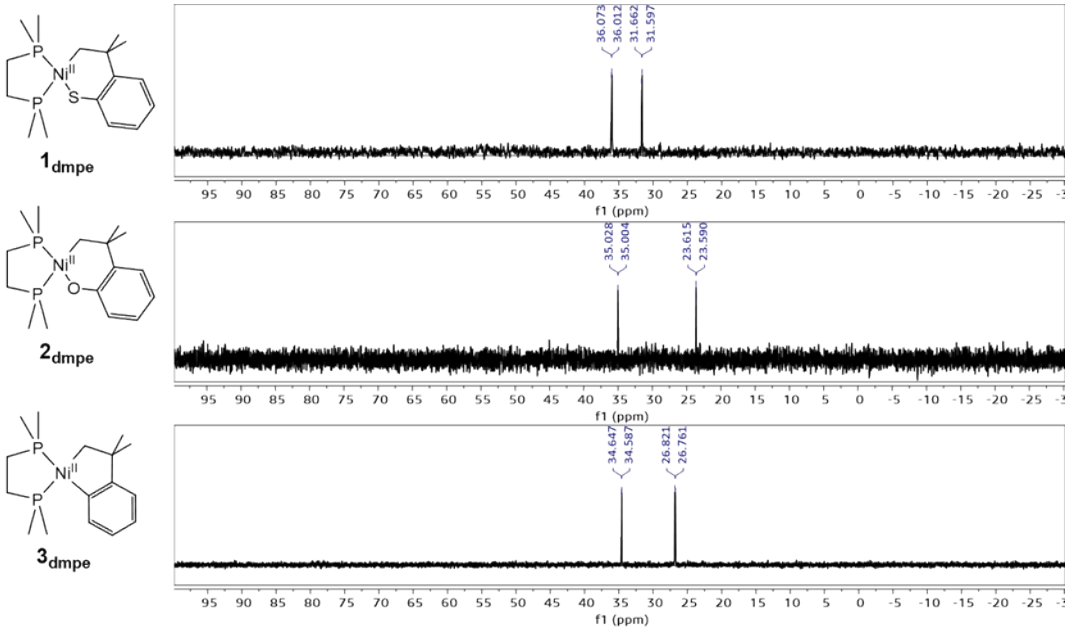

Figure S47. ^{31}P-NMR spectra of $\mathbf{1}_{\mathbf{dmpe}}$ (top), $\mathbf{2}_{\mathbf{dmpe}}$ (middle), and $\mathbf{3}_{\mathbf{dmpe}}$ (bottom).
$\mathbf{1}_{\mathbf{dmpe}}$. ^{31}P NMR (162 MHz, C_6D_6, 25 °C): δ = 36.0 (d, J = 9.9 Hz), 31.6 ppm (d, J = 10.5 Hz).
$\mathbf{2}_{\mathbf{dmpe}}$. ^{31}P NMR (162 MHz, C_6D_6, 25 °C): δ = 35.0 (d, J = 3.9 Hz), 23.6 ppm (d, J = 4.1 Hz).
$\mathbf{3}_{\mathbf{dmpe}}$. ^{31}P NMR (162 MHz, C_6D_6, 25 °C): δ = 34.6 (d, J = 9.7 Hz), 26.8 ppm (d, J = 9.7 Hz).

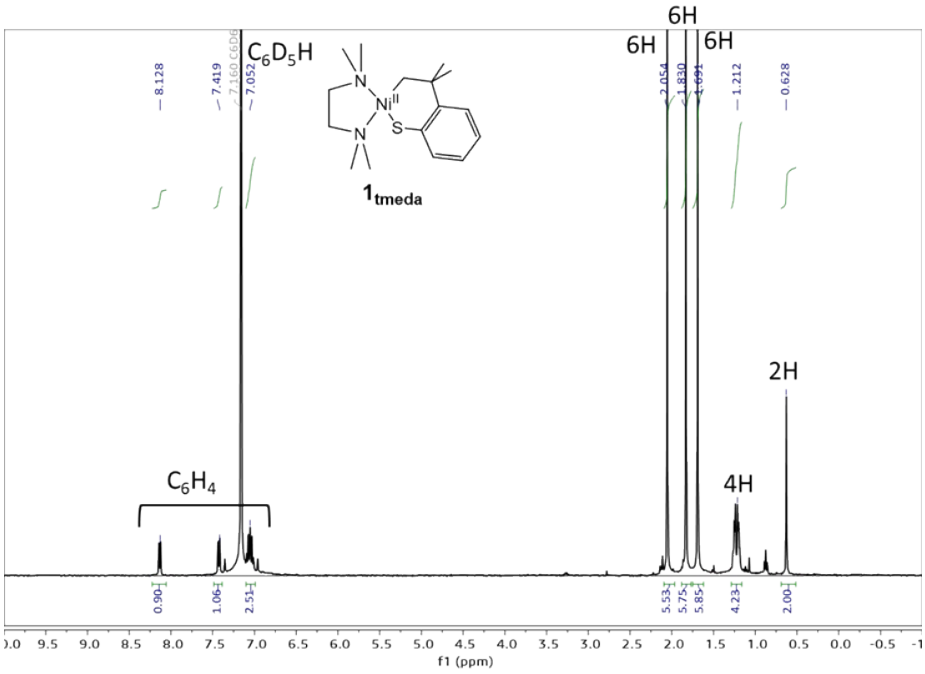

Figure S48. ^{1}H-NMR spectrum of $\mathbf{1}_{\mathbf{tmeda}}$. ^{1}H NMR (400 MHz, C_6D_6, 25 °C): δ = 8.13 (dd, *J* = 7.4, 1.8 Hz, 1H, C_6H_4), 7.43 (dd, *J* = 7.5, 1.8 Hz, 1H, C_6H_4), 7.10-7.00 (m, 2H, C_6H_4), 2.05 (s, 6H), 1.83 (s, 6H), 1.69 (s, 6H), 1.28-1.16 (m, 4H, NCH_2), 0.63 ppm (s, 2H, $NiCH_2$).

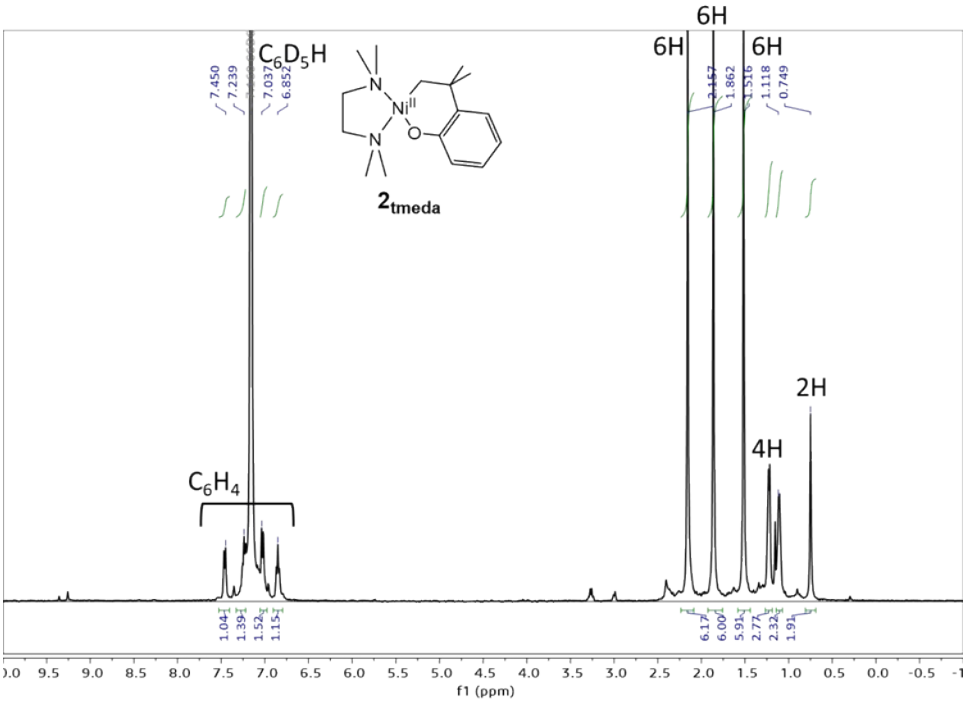

Figure S49. ^{1}H-NMR spectrum of $\mathbf{2}_{\mathbf{tmeda}}$. ^{1}H NMR (400 MHz, C_6D_6, 25 °C): δ = 7.46 (d, *J* = 7.5 Hz, 1H, C_6H_4), 7.24 (t, *J* = 7.5 Hz, 1H, C_6H_4), 7.03 (d, *J* = 8.0 Hz, 1H, C_6H_4), 6.85 (t, *J* = 7.4 Hz, 1H, C_6H_4), 2.16 (s, 6H), 1.86 (s, 6H), 1.52 (s, 6H), 1.27-1.07 (m, 4H, NCH_2), 0.75 ppm (s, 2H, $NiCH_2$).

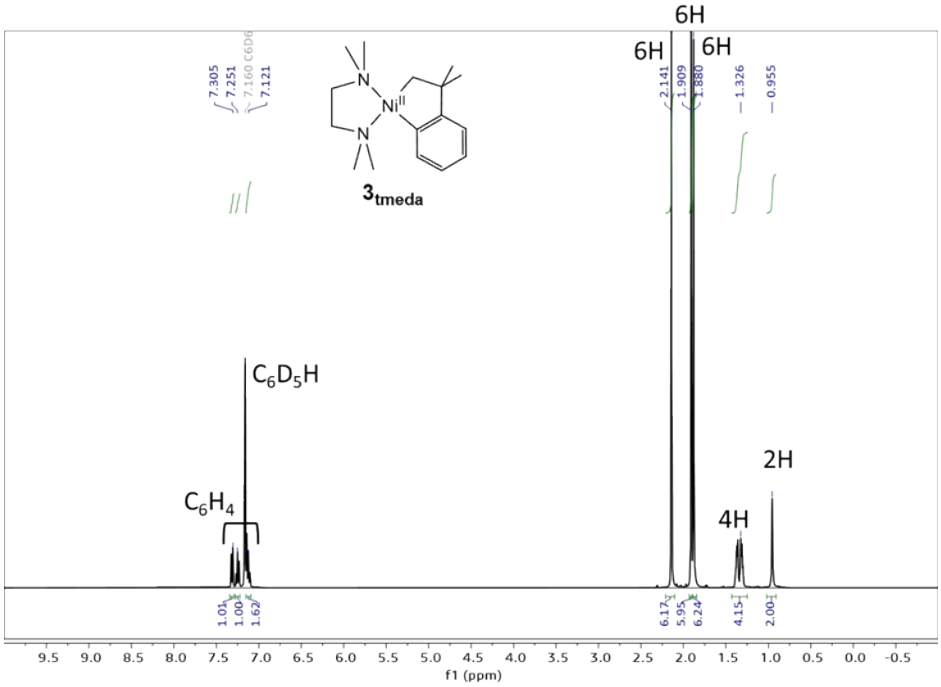

Figure S50. ^{1}H-NMR spectrum of $\mathbf{3_{tmeda}}$. ^{1}H NMR (400 MHz, C_6D_6, 25 °C): δ = 7.32 (dd, *J* = 7.6, 1.0 Hz, 1H, C_6H_4), 7.25 (td, *J* = 7.3, 1.3 Hz, 1H, C_6H_4), 7.15-7.09 (m, C_6H_4), 2.14 (s, 6H), 1.91 (s, 6H), 1.88 (s, 6H), 1.41-1.28 (m, 4H, NCH_2), 0.96 ppm (s, 2H, $NiCH_2$).

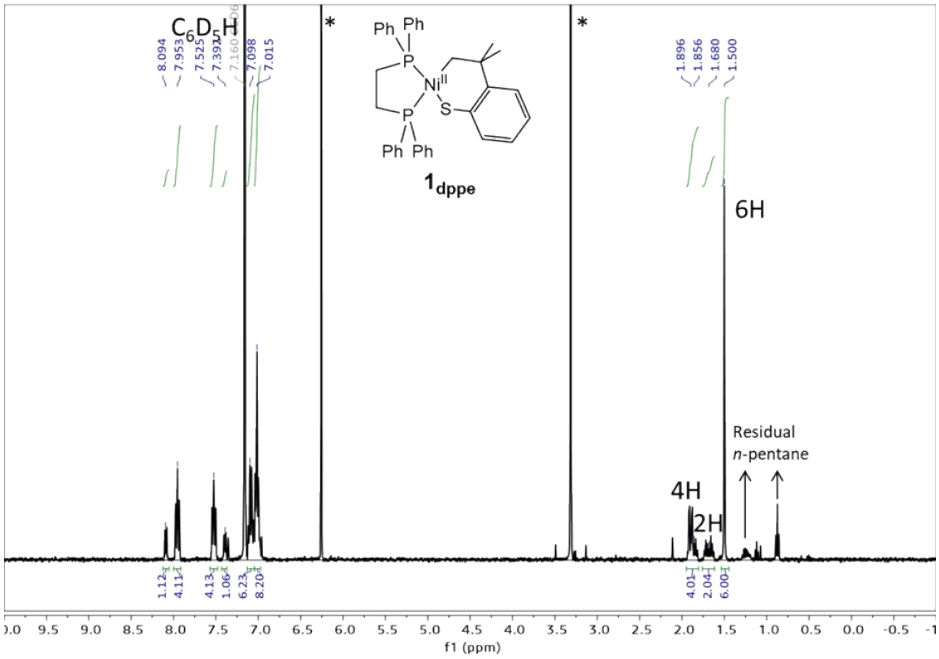

Figure S51. ^{1}H-NMR spectrum of $\mathbf{1}_{\mathbf{dppe}}$. Peaks with asterisks are from internal standard, 1,3,5-trimethoxybenzene. ^{1}H NMR (400 MHz, C_6D_6, 25 °C): δ = 8.12-8.06 (m, 1H, C_6H_4), 7.95 (ddd, *J* = 9.9, 7.9, 1.7 Hz, 4H, dppe), 7.53 (ddd, *J* = 9.8, 7.5, 1.8 Hz, 4H, dppe), 7.42-7.37 (m, 1H, C_6H_4), 7.13-6.97 (m, 14H, dppe+C_6H_4), 1.94-1.60 (m, 4H, PCH_2), 1.90 (dd, *J* = 13.2, 3.6 Hz, 2H, $NiCH_2$), 1.50 ppm (s, 6H, CMe_2).

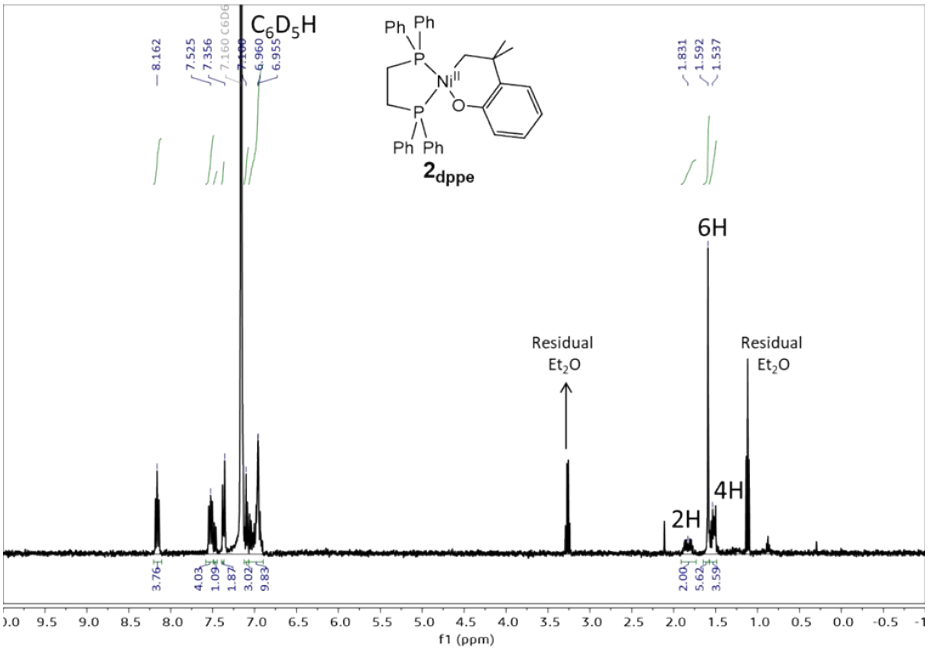

Figure S52. ^{1}H-NMR spectrum of $\mathbf{2}_{\mathbf{dppe}}$. ^{1}H NMR (400 MHz, C_6D_6, 25 °C): δ = 8.16 (ddd, *J* = 9.6, 8.2, 1.4 Hz, 4H, dppe), 7.53 (ddd, *J* = 10.4, 8.0, 1.7 Hz, 4H, dppe), 7.47 (d, *J* = 6.8 Hz, 1H, C_6H_4), 7.39-7.36 (m, 2H, C_6H_4), 7.13-6.90 (m, 13H, dppe+C_6H_4), 1.90-1.75 (m, 2H, PCH_2), 1.59 (s, 6H, CMe_2), 1.62-1.47 ppm (m, 4H, PCH_2+$NiCH_2$).

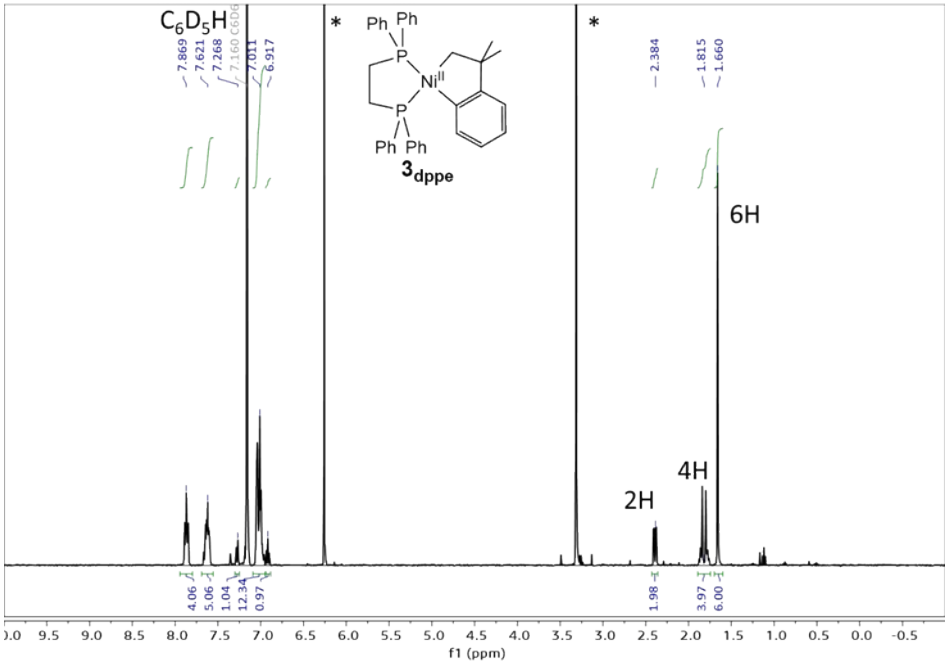

Figure S53. ^{1}H-NMR spectrum of $\mathbf{3}_{\mathbf{dppe}}$. Peaks with asterisks are from internal standard, 1,3,5-trimethoxybenzene. ^{1}H NMR (400 MHz, C_6D_6, 25 °C): δ = 7.87 (ddd, *J* = 9.6, 7.3, 2.2 Hz, 4H, C_6H_4), 7.68-7.57 (m, 4H, dppe), 7.28 (d, *J* = 7.2 Hz, 1H, C_6H_4), 7.08-6.97 (m, 12H, dppe+C_6H_4), 6.92 (tt, *J* = 7.3, 1.5 Hz, 1H, C_6H_4), 2.39 (dd, *J* = 10.8, 3.7 Hz, 2H, $NiCH_2$), 1.89-1.75 (m, 4H, PCH_2), 1.66 ppm (s, 6H, CMe_2).

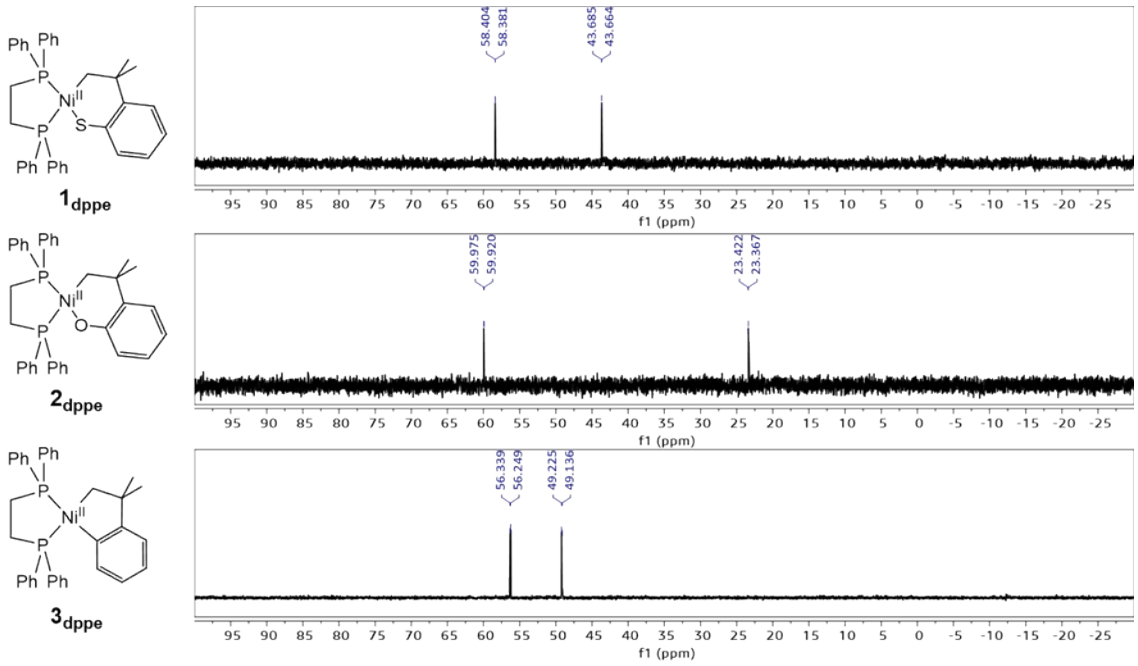

Figure S54. ^{31}P-NMR spectra of $\mathbf{1}_{\mathbf{dppe}}$ (top), $\mathbf{2}_{\mathbf{dppe}}$ (middle), and $\mathbf{3}_{\mathbf{dppe}}$ (bottom).
$\mathbf{1}_{\mathbf{dppe}}$. ^{31}P NMR (162 MHz, C_6D_6, 25 °C): δ = 58.4 (d, *J* = 3.7 Hz), 43.7 ppm (d, *J* = 3.4 Hz).
$\mathbf{2}_{\mathbf{dppe}}$. ^{31}P NMR (162 MHz, C_6D_6, 25 °C): δ = 59.9 (d, *J* = 8.9 Hz), 23.4 ppm (d, *J* = 8.9 Hz).

3_{dppe}. ^{31}P NMR (162 MHz, C_6D_6, 25 °C): δ = 56.3 (d, *J* = 14.6 Hz), 49.2 ppm (d, *J* = 14.4 Hz).

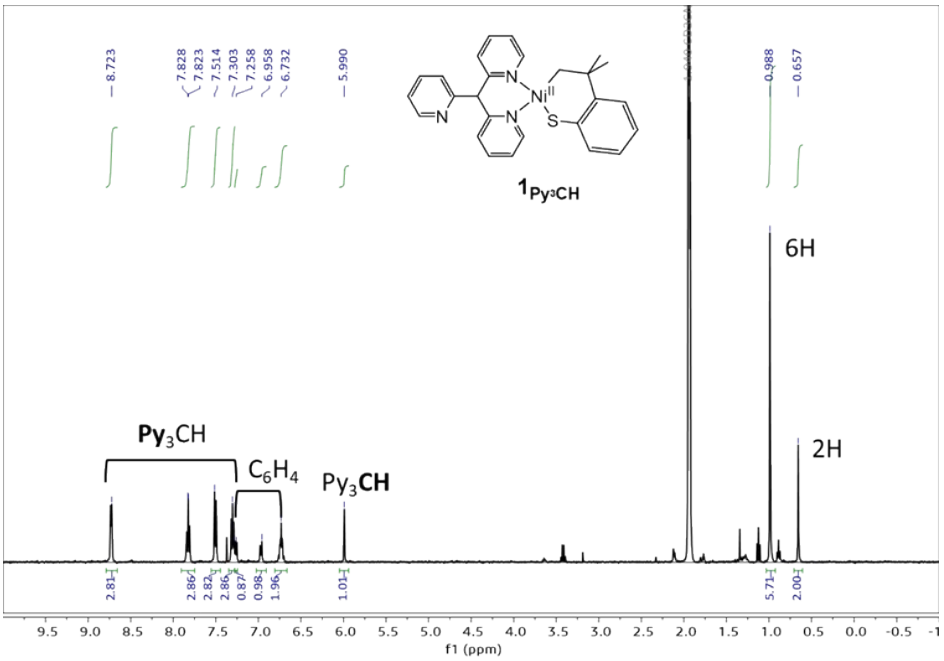

Figure S55. ^1H-NMR spectrum of **1_{Py_3CH}**. ^1H NMR (400 MHz, CD_3CN, 25 °C): δ = 8.73 (d, *J* = 4.7 Hz, 3H, **Py**$_3$CH), 7.83 (td, *J* = 7.7, 1.8 Hz, 3H, **Py**$_3$CH), 7.50 (d, *J* = 7.6 Hz, 3H, **Py**$_3$CH), 7.30 (ddd, *J* = 7.6, 5.3, 1.4 Hz, 3H, **Py**$_3$CH), 7.28-7.24 (m, 1H, C_6H_4), 7.00-6.93 (m, 1H, C_6H_4), 6.78-6.69 (m, 2H, C_6H_4), 5.99 (s, 1H, Py_3**CH**), 0.99 (s, 6H, CMe_2), 0.66 ppm (s, 2H, $NiCH_2$).

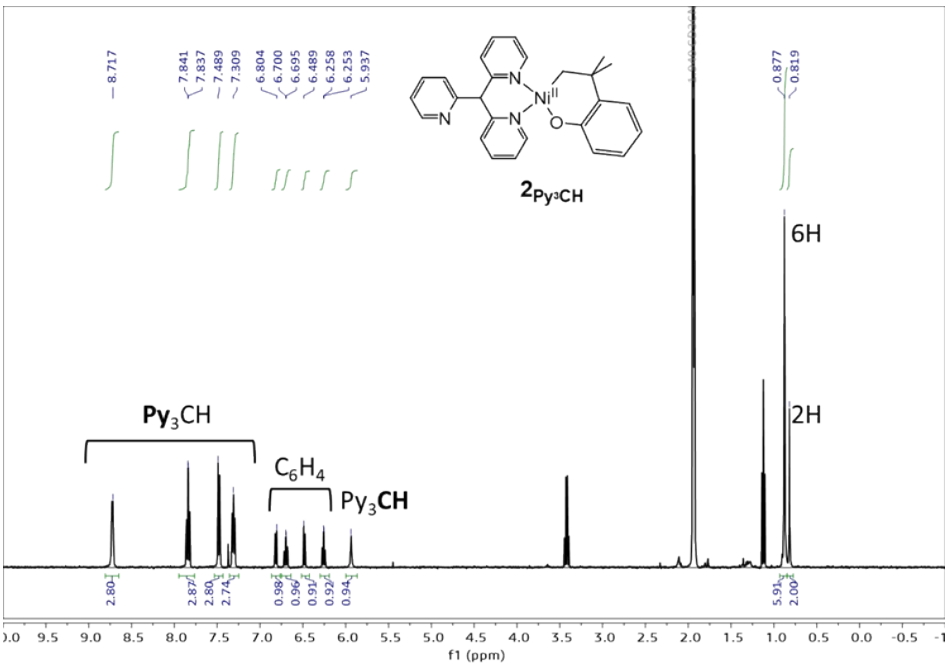

Figure S56. ^1H-NMR spectrum of **2_{Py_3CH}**. ^1H NMR (400 MHz, CD_3CN, 25 °C): δ = 8.72 (d, *J* = 5.0 Hz, 3H, **Py**$_3$CH), 7.84 (td, *J* = 7.6, 1.8 Hz, 3H, **Py**$_3$CH), 7.48 (d, *J* = 8.1 Hz, 3H, **Py**$_3$CH),

7.31 (ddd, *J* = 7.6, 5.5, 1.4 Hz, 3H, **Py**$_3$CH), 6.82 (dd, *J* = 7.5, 1.8 Hz, 1H, C_6H_4), 6.70 (ddd, *J* = 7.9, 7.0, 1.8, Hz, 1H, C_6H_4), 6.48 (dd, *J* = 7.9, 1.4 Hz, 1H, C_6H_4), 6.26 (td, *J* = 7.3, 1.4 Hz, 1H, C_6H_4), 5.94 (s, 1H, Py$_3$**CH**), 0.88 (s, 6H, CMe_2), 0.82 ppm (s, 2H, $NiCH_2$).

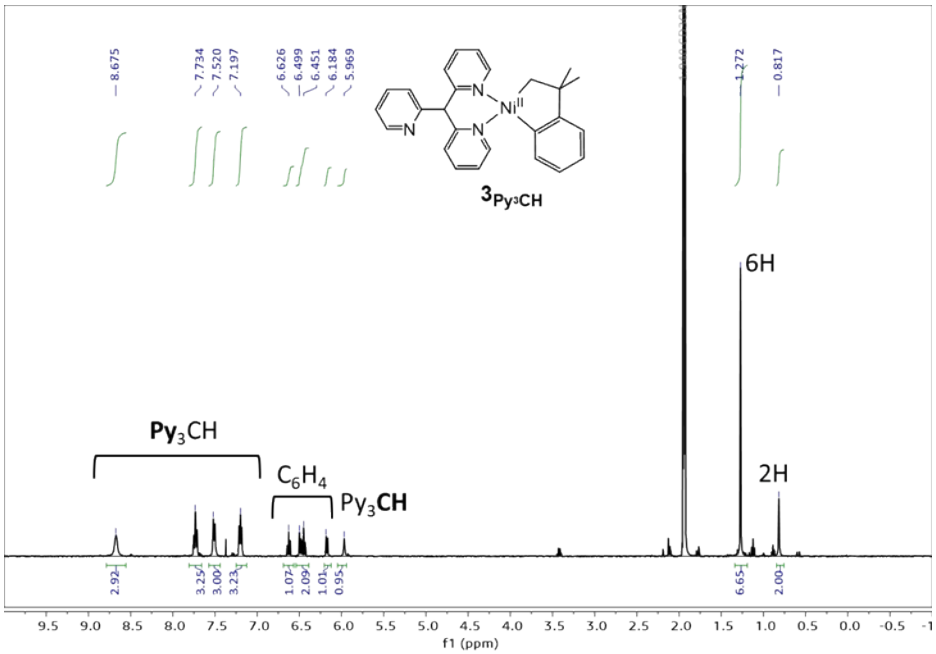

Figure S57. ^{1}H-NMR spectrum of $\mathbf{3_{Py_3CH}}$. ^{1}H NMR (400 MHz, CD_3CN, 25 °C): δ = 8.68 (s, 3H, **Py**$_3$CH), 7.73 (td, *J* = 7.6, 1.7 Hz, 3H, **Py**$_3$CH), 7.51 (d, *J* = 7.6 Hz, 3H, **Py**$_3$CH), 7.20 (ddd, *J* = 7.3, 5.3, 1.3 Hz, 3H, **Py**$_3$CH), 6.63 (td, *J* = 7.3, 1.3 Hz, 1H, C_6H_4), 6.49 (dd, *J* = 7.5, 1.5 Hz, 1H, C_6H_4), 6.45 (td, *J* = 7.3, 1.5 Hz, 1H, C_6H_4), 6.17 (d, *J* = 7.5 Hz, 1H, C_6H_4), 5.97 (s, 1H, Py$_3$**CH**), 1.27 (s, 6H, CMe_2), 0.82 ppm (s, 2H, $NiCH_2$).

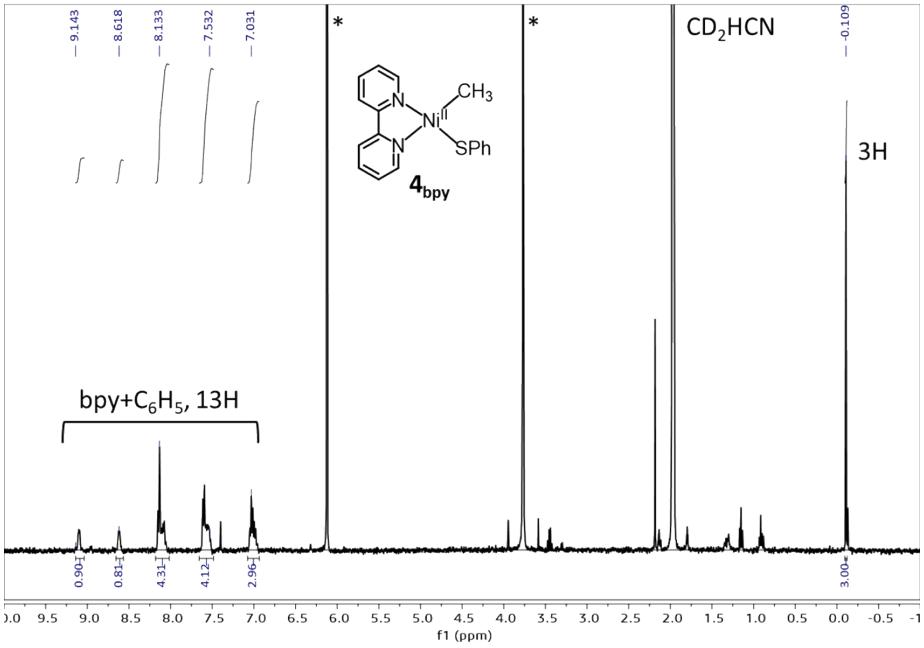

Figure S58. ^{1}H-NMR spectrum of $\mathbf{4_{bpy}}$. Peaks with asterisks are from internal standard, 1,3,5-trimethoxybenzene.^{1}H NMR (400 MHz, CD_3CN, 25 °C): δ = 9.04 (s, 1H), 8.56 (s, 1H, **Py**$_3$CH), 8.13-8.00 (m, 4H), 7.62-7.47 (m, 4H), 7.04-6.92 (m, 3H), –0.14 ppm (s, 3H, $NiCH_3$).

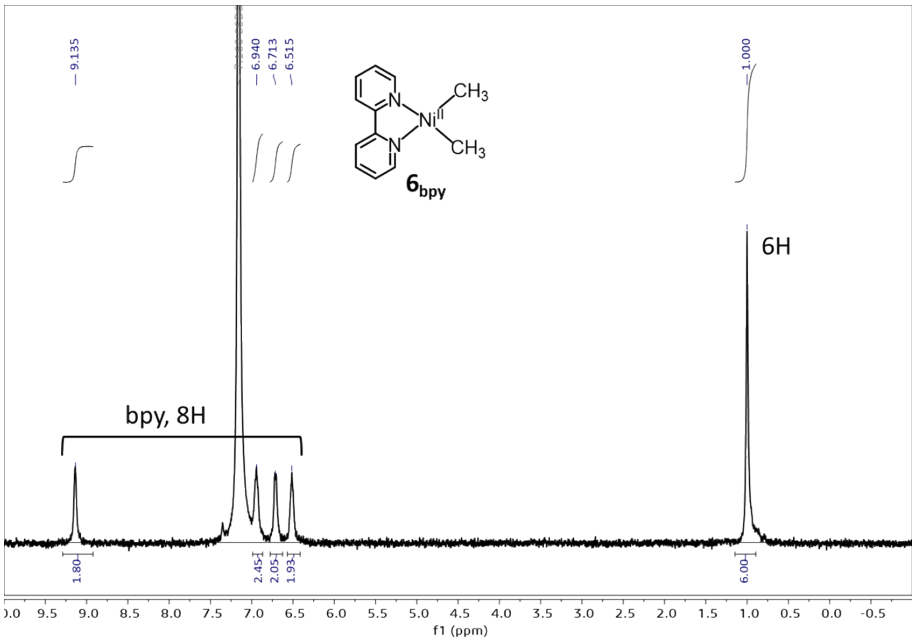

Figure S59. ^{1}H-NMR spectrum of $\mathbf{6_{bpy}}$. ^{1}H NMR (400 MHz, C_6D_6, 25 °C): δ = 9.14 (s, 2H, bpy), 6.94 (s, 2H, bpy), 6.71 (s, 2H, bpy), 6.52 (s, 2H, bpy), 1.00 ppm (s, 6H, $NiCH_3$).

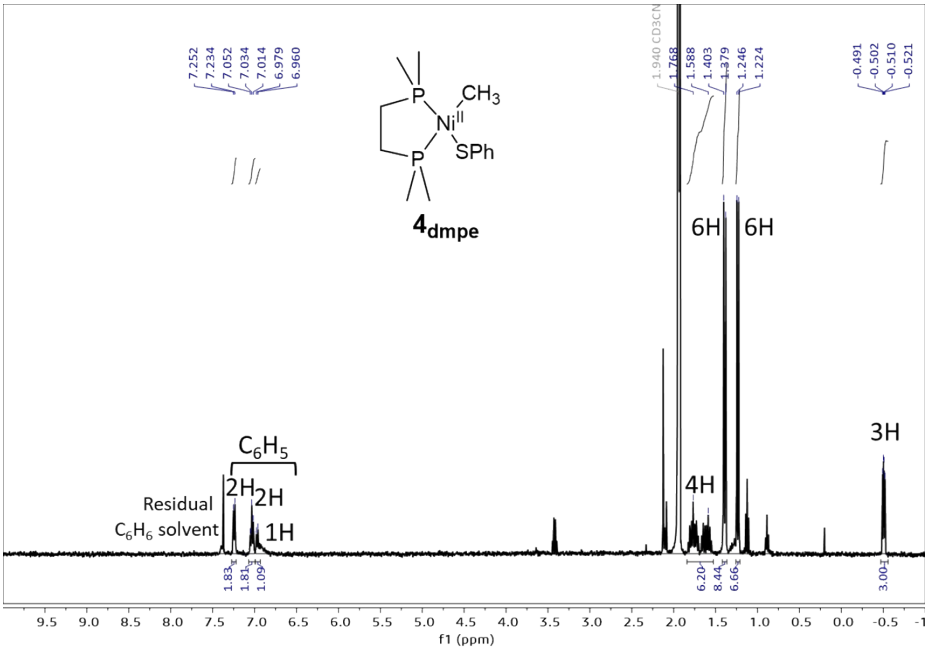

Figure S60. ^{1}H-NMR spectrum of $\mathbf{4}_{\mathbf{dmpe}}$. ^{1}H NMR (400 MHz, CD_3CN, 25 °C): δ = 7.24 (d, *J* = 7.3 Hz, 2H, C_6H_5), 7.03 (t, *J* = 7.5 Hz, 2H, C_6H_5), 6.97 (d, *J* = 7.5 Hz, 1H, C_6H_5), 1.84-1.54 (m, 4H, PCH_2), 1.39 (d, *J* = 9.7 Hz, 6H, PCH_3), 1.23 (d, *J* = 8.7 Hz, 6H, PCH_3), –0.51 ppm (dd, *J* = 7.5, 4.4 Hz, 3H, $NiCH_3$).

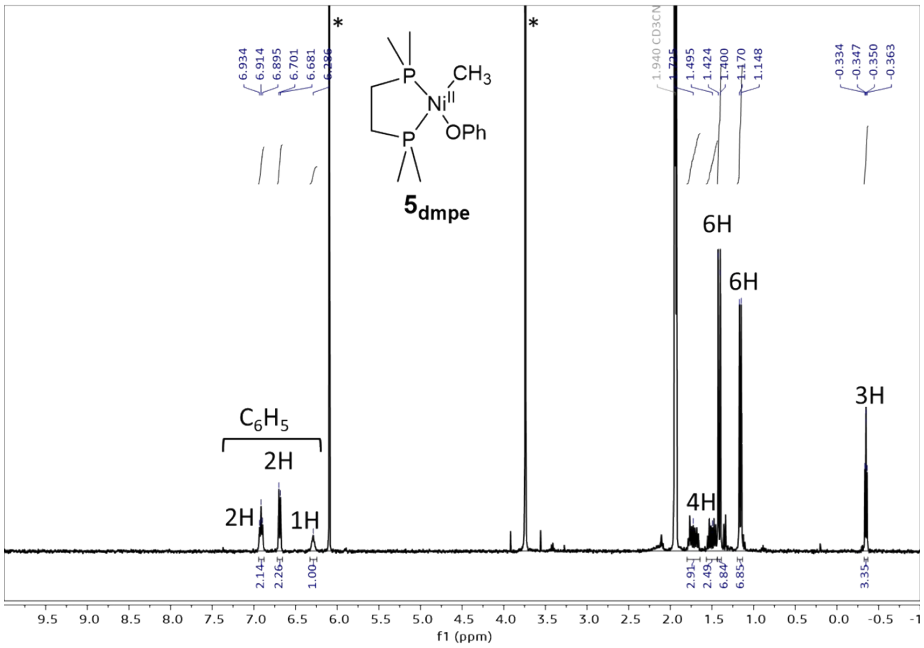

Figure S61. ^{1}H-NMR spectrum of $\mathbf{5}_{\mathbf{dmpe}}$. Peaks with asterisks are from internal standard, 1,3,5-trimethoxybenzene. ^{1}H NMR (400 MHz, CD_3CN, 25 °C): δ = 6.91 (t, *J* = 7.7 Hz, 2H, C_6H_5), 6.69 (d, *J* = 7.9 Hz, 2H, C_6H_5), 6.29 (s, 1H, C_6H_5), 1.79-1.42 (m, 4H, PCH_2), 1.41 (d, *J* = 9.7 Hz, 6H, PCH_3), 1.16 (d, *J* = 8.6 Hz, 6H, PCH_3), –0.35 ppm (dd, *J* = 6.4, 5.2 Hz, 3H, $NiCH_3$).

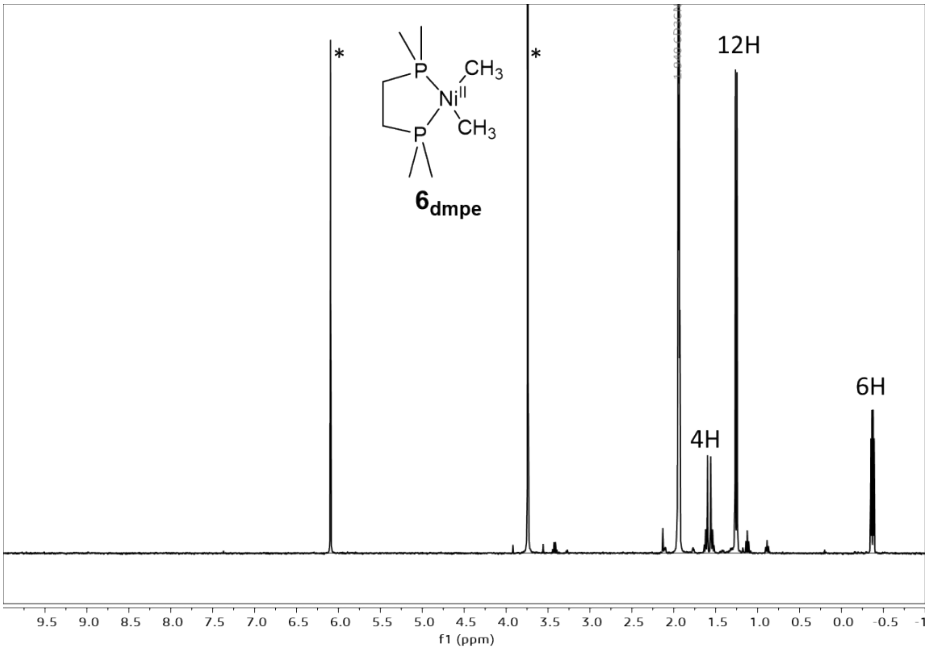

Figure S62. ^{1}H-NMR spectrum of $\mathbf{6}_{\mathbf{dmpe}}$. Peaks with asterisks are from internal standard, 1,3,5-trimethoxybenzene. ^{1}H NMR (400 MHz, CD_3CN, 25 °C): δ = 1.65-1.51 (m, 4H, PCH_2), 1.25 (dd, J = 7.6, 0.4 Hz, 12H, PCH_3), –0.38 ppm (dd, J = 11.2, 4.4 Hz, 6H, $NiCH_3$).

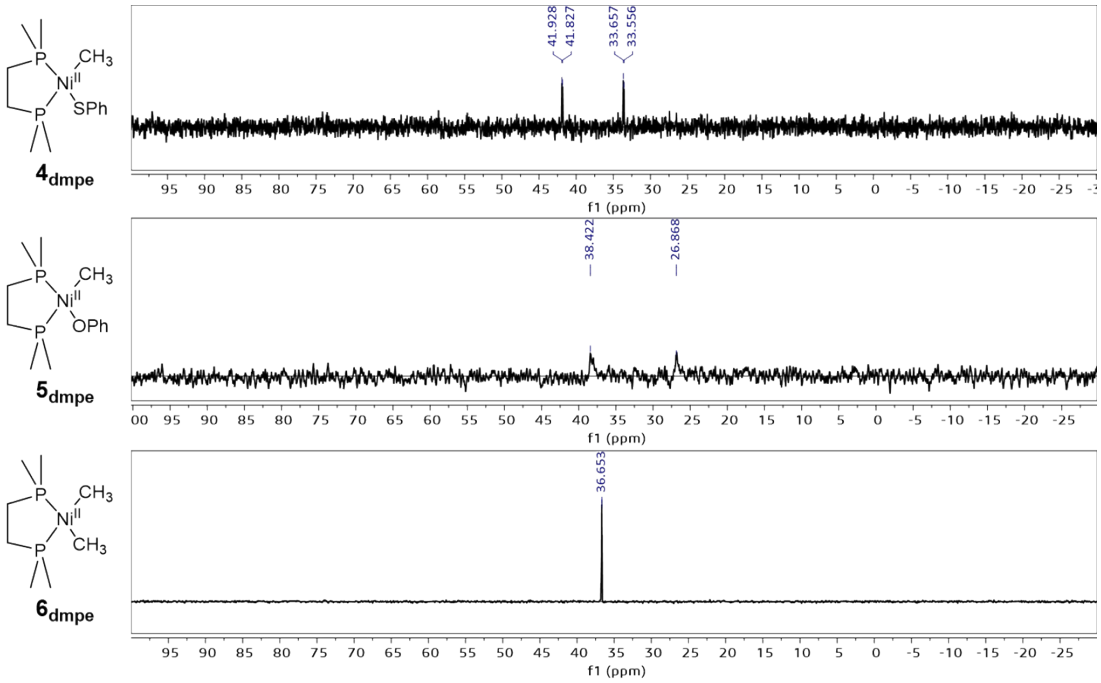

Figure S63. ^{31}P-NMR spectra of $\mathbf{4}_{\mathbf{dmpe}}$ (top), $\mathbf{5}_{\mathbf{dmpe}}$ (middle), and $\mathbf{6}_{\mathbf{dmpe}}$ (bottom). $\mathbf{4}_{\mathbf{dmpe}}$. ^{31}P NMR (162 MHz, CD_3CN, 25 °C): δ = 41.9 (d, J = 16.4 Hz), 33.6 ppm (d, J = 16.3 Hz). $\mathbf{5}_{\mathbf{dmpe}}$. ^{31}P NMR (162 MHz, CD_3CN, 25 °C): δ = 38.4 (br, s), 26.9 ppm (br, s). $\mathbf{6}_{\mathbf{dmpe}}$. ^{31}P NMR (162 MHz, CD_3CN, 25 °C): δ = 36.7 ppm (s).

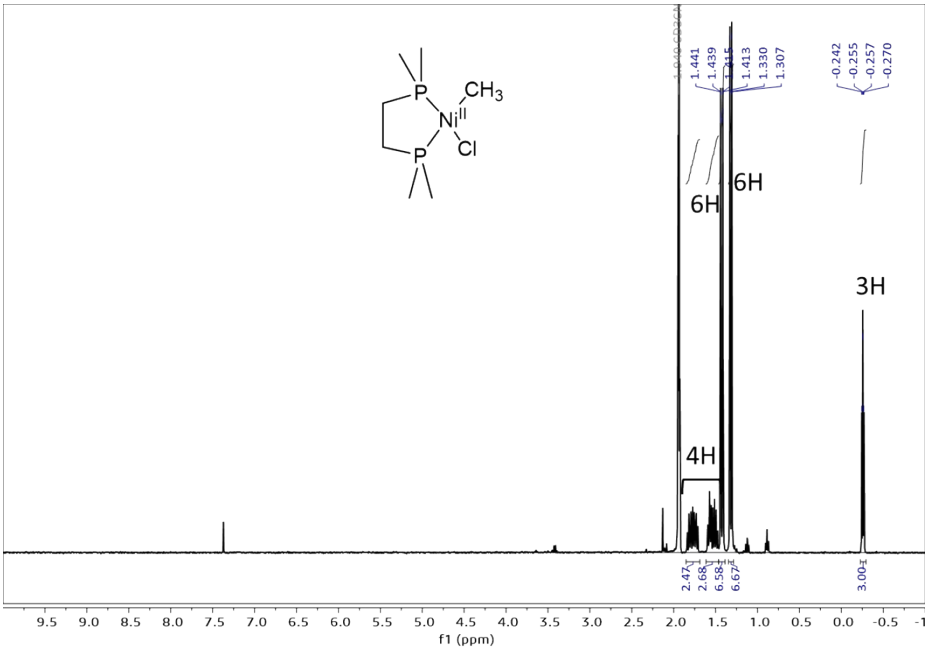

Figure S64. ^{1}H-NMR spectrum of (dmpe)Ni(Me)(Cl). ^{1}H NMR (400 MHz, CD_3CN, 25 °C): δ = 1.84-1.70 (m, 2H, PCH_2), 1.61-1.46 (m, 2H, PCH_2), 1.39 (dd, *J* = 10.5, 0.7 Hz, 6H, PCH_3), 1.32 (d, *J* = 8.9 Hz, 6H, PCH_3), –0.26 ppm (dd, *J* = 6.0, 5.2 Hz, 3H, $NiCH_3$).

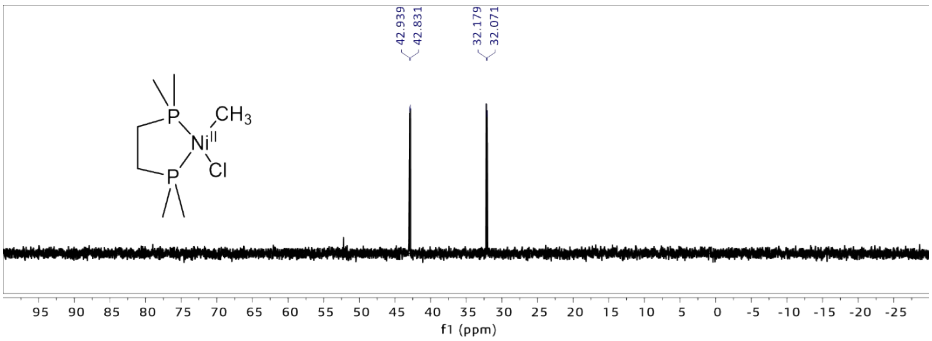

Figure S65. ^{31}P-NMR spectra of (dmpe)Ni(Me)(Cl). ^{31}P NMR (162 MHz, CD_3CN, 25 °C): δ = 42.9 (d, *J* = 17.6 Hz), 32.1 ppm (d, *J* = 17.5 Hz).

Cartesian coordinates of DFT-optimized Ni^{II} complexes

$\mathbf{1}_{bpy}$

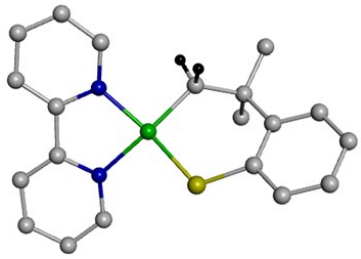

C	-0.968009	1.368924	0.273917	Ni	0.362722	0.01293	-0.013023
C	-2.30285	1.122171	1.009224	N	1.824024	-1.287586	0.074557
C	-3.248491	0.290118	0.142879	C	3.067512	-0.731116	0.035576
C	-2.782991	-0.890738	-0.483226	C	1.731899	-2.60839	0.345097
C	-3.664993	-1.672033	-1.253284	C	4.226611	-1.483482	0.24835
C	-5.00302	-1.312318	-1.40663	C	3.049873	0.709414	-0.245772
C	-5.474636	-0.147983	-0.796236	C	2.841521	-3.415559	0.565205
C	-4.599118	0.633723	-0.037044	H	0.720567	-3.017458	0.373771
C	-2.897713	2.512092	1.325767	C	4.115252	-2.844341	0.516898
C	-2.073606	0.404747	2.358381	H	5.205158	-1.006201	0.218456
H	-2.170989	3.092846	1.91331	N	1.796942	1.260616	-0.210566
H	-3.118579	3.077241	0.40717	C	4.18764	1.463226	-0.544791
H	-3.820673	2.444226	1.922311	H	2.70179	-4.475784	0.774214
H	-1.690805	-0.613175	2.208167	H	5.006684	-3.447515	0.690967
H	-1.336804	0.960938	2.960295	C	1.688573	2.575121	-0.516939
H	-3.012231	0.348227	2.931541	C	4.057524	2.816929	-0.838697
H	-0.416575	2.103105	0.890495	H	5.166822	0.986719	-0.564611
H	-1.186732	1.838493	-0.705756	C	2.778567	3.377053	-0.831084
H	-3.281201	-2.573186	-1.737322	H	0.681861	2.988785	-0.499184
H	-5.668891	-1.935462	-2.007597	H	4.934015	3.418826	-1.079378
H	-6.517097	0.15598	-0.910101	H	2.616952	4.428754	-1.066141
H	-4.985743	1.540238	0.429857	S	-1.118748	-1.492167	-0.335725

2_{bpy}

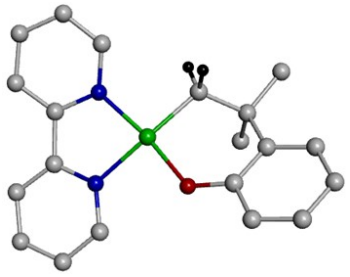

C	-0.991799	1.664071	0.236858	Ni	0.243972	0.239459	-0.078071
C	-2.26876	1.289747	1.011128	N	1.576959	-1.183907	-0.073211
C	-3.086393	0.288091	0.203204	C	2.862473	-0.747322	-0.028137
C	-2.400332	-0.835402	-0.341044	C	1.328515	-2.500321	0.063265
C	-3.142095	-1.814331	-1.042641	C	3.933421	-1.626921	0.152794
C	-4.520908	-1.692076	-1.216358	C	2.967452	0.70615	-0.21665
C	-5.195637	-0.583908	-0.696155	C	2.345568	-3.433124	0.239651
C	-4.469217	0.387361	0.006281	H	0.270606	-2.76519	0.019075
C	-3.05686	2.582714	1.297192	C	3.669861	-2.988691	0.288757
C	-1.886271	0.653204	2.368363	H	4.956621	-1.255395	0.194489
H	-2.415793	3.291506	1.843391	N	1.752191	1.345164	-0.244515
H	-3.385045	3.070435	0.36637	C	4.170135	1.391377	-0.398053
H	-3.946271	2.394868	1.919509	H	2.099457	-4.489981	0.34016
H	-1.323697	-0.276605	2.209219	H	4.488803	-3.694172	0.433037
H	-1.249971	1.343384	2.946384	C	1.753975	2.673455	-0.513057
H	-2.784052	0.42976	2.965677	C	4.152617	2.761136	-0.644922
H	-0.461101	2.427923	0.835054	H	5.113792	0.848296	-0.363227
H	-1.267142	2.117162	-0.737218	C	2.916614	3.406184	-0.716379
H	-2.598501	-2.669986	-1.450988	H	0.778406	3.153668	-0.555253
H	-5.067077	-2.463538	-1.765396	H	5.082825	3.30999	-0.79245
H	-6.273176	-0.47221	-0.832054	H	2.842984	4.472714	-0.927117
H	-5.005165	1.246468	0.41556	O	-1.089966	-1.024259	-0.189224

3_{bpy}

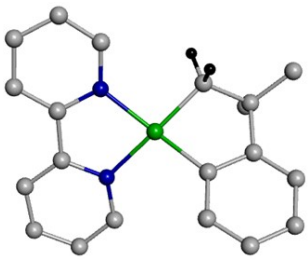

C	-1.403952	3.219559	2.068914	Ni	-3.183858	3.5836	1.440175
C	-1.206229	1.711393	2.353918	N	-4.840168	3.777554	0.45549
C	-2.528023	1.302195	2.976273	C	-4.96428	4.94137	-0.247997
C	-3.604893	2.134327	2.575525	C	-5.746949	2.80207	0.222383
C	-4.855012	1.907108	3.186236	C	-6.015779	5.165403	-1.139481
C	-5.044864	0.86247	4.10528	C	-3.860114	5.882715	-0.007216
C	-3.978996	0.024451	4.44348	C	-6.813438	2.955101	-0.657488
C	-2.714559	0.252655	3.881513	H	-5.597291	1.878034	0.778961
C	0.006891	1.459665	3.264939	C	-6.960934	4.162355	-1.343563
C	-1.000285	0.948933	1.028654	H	-6.081553	6.105552	-1.686044
H	0.918644	1.870791	2.802525	N	-2.809719	5.317371	0.659452
H	-0.126062	1.94579	4.243912	C	-3.848387	7.21654	-0.421981
H	0.18048	0.384922	3.438523	H	-7.515181	2.133331	-0.799019
H	-1.843805	1.130721	0.345626	H	-7.787188	4.314885	-2.038461
H	-0.075784	1.284156	0.530082	C	-1.739964	6.099597	0.924349
H	-0.922363	-0.136342	1.202149	C	-2.733752	8.005737	-0.148397
H	-0.665296	3.562703	1.316805	H	-4.709202	7.637422	-0.94045
H	-1.229046	3.793053	3.00064	C	-1.660379	7.433002	0.537039
H	-5.704928	2.558879	2.959576	H	-0.923515	5.620046	1.463224
H	-6.026503	0.710291	4.56265	H	-2.706444	9.050306	-0.459855
H	-4.124383	-0.791767	5.155465	H	-0.766758	8.009157	0.775983
H	-1.871778	-0.381172	4.173996				

1_{tmeda}

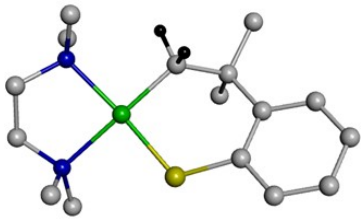

C	-0.408172	1.355816	-0.317204	C	3.638129	0.376361	-0.712122
C	-1.71283	1.452735	0.50893	S	-0.595316	-1.489429	0.215989
C	-2.697881	0.375041	0.057446	C	2.691813	2.187688	0.602681
C	-2.256556	-0.959468	-0.103271	H	3.567091	2.826986	0.384681
C	-3.169227	-1.955212	-0.499397	H	1.809685	2.820728	0.747925
C	-4.511128	-1.656577	-0.726559	H	2.866215	1.63707	1.534283
C	-4.958461	-0.342822	-0.572395	C	2.235916	2.019315	-1.761442
C	-4.053283	0.649796	-0.187627	H	3.12926	2.627028	-1.991825
C	-2.284513	2.869451	0.285552	H	2.040552	1.326743	-2.589483
C	-1.437084	1.302786	2.021868	H	1.370415	2.680271	-1.648903
H	-1.534349	3.617061	0.586029	C	2.196152	-2.18703	1.566049
H	-2.531556	3.043981	-0.77308	H	3.029867	-2.894957	1.72452
H	-3.187499	3.055411	0.887723	H	2.159606	-1.470348	2.396534
H	-1.080064	0.292415	2.260209	H	1.246962	-2.734789	1.54437
H	-0.663823	2.022534	2.338783	C	2.366187	-2.423975	-0.826654
H	-2.350081	1.501421	2.605258	H	3.183652	-3.15908	-0.707922
H	0.121003	2.310699	-0.13852	H	1.39909	-2.938929	-0.847646
H	-0.68099	1.334586	-1.391968	H	2.482796	-1.901422	-1.783786
H	-2.803421	-2.976395	-0.628445	H	4.564023	0.978285	-0.676072
H	-5.200501	-2.447277	-1.031114	H	4.507244	-1.403098	0.16999
H	-6.004517	-0.086863	-0.752884	H	3.564753	-0.05865	-1.718003
H	-4.420407	1.670776	-0.075747	H	3.76542	-0.288881	1.33774
Ni	0.918779	-0.007081	-0.0597	N	2.442161	1.243251	-0.51425
C	3.655434	-0.717728	0.332121	N	2.366623	-1.450809	0.29196

2_{tmeda}

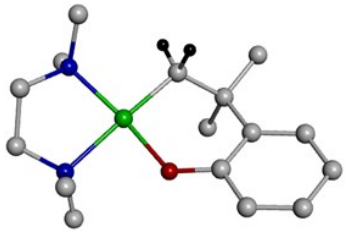

C	-0.368195	1.630439	-0.345074	C	3.549953	0.259387	-0.763142
C	-1.667675	1.581278	0.481694	C	2.797426	2.084959	0.669809
C	-2.502083	0.379391	0.050796	H	3.737293	2.63698	0.48651
C	-1.839652	-0.874812	-0.077391	H	1.985286	2.797393	0.850377
C	-2.604157	-2.015955	-0.415856	H	2.908505	1.465118	1.566666
C	-3.978773	-1.931718	-0.630505	C	2.336223	2.11083	-1.699039
C	-4.629545	-0.70015	-0.519639	H	3.295659	2.620847	-1.896111
C	-3.882033	0.434192	-0.179308	H	2.061789	1.498082	-2.566337
C	-2.422149	2.909747	0.276401	H	1.554384	2.859779	-1.537655
C	-1.336045	1.450089	1.986682	C	1.790062	-2.070772	1.526515
H	-1.772371	3.751611	0.56258	H	2.428351	-2.957401	1.69607
H	-2.714051	3.04843	-0.776015	H	1.937449	-1.354019	2.345296
H	-3.330745	2.970489	0.896262	H	0.733094	-2.35971	1.502152
H	-0.827812	0.496534	2.184566	C	1.908826	-2.385503	-0.858737
H	-0.669157	2.269045	2.305749	H	2.530449	-3.288425	-0.71113
H	-2.252154	1.494925	2.596478	H	0.845888	-2.651197	-0.880902
H	0.143737	2.578269	-0.08497	H	2.166236	-1.923858	-1.82057
H	-0.629492	1.683457	-1.422061	H	4.530827	0.766609	-0.736654
H	-2.080542	-2.971116	-0.504702	H	4.230662	-1.654052	-0.001264
H	-4.541168	-2.831907	-0.892096	H	3.400451	-0.126377	-1.780815
H	-5.704246	-0.61838	-0.693368	H	3.708071	-0.511537	1.252383
H	-4.399512	1.391638	-0.088097	N	2.451277	1.239449	-0.501636
Ni	0.839477	0.17138	-0.110148	N	2.108171	-1.418176	0.241193
C	3.484237	-0.875865	0.240113	O	-0.535061	-1.032006	0.139555

3_{tmeda}

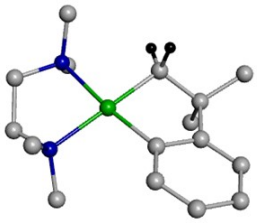

C	-1.490168	3.291496	2.767111	H	-3.912083	6.414564	-0.337118
C	-0.857389	1.886068	2.779812	H	-4.787553	5.981762	1.144326
C	-2.052601	0.984986	3.016919	C	-4.700797	4.392128	-0.314038
C	-3.287786	1.56506	2.612183	H	-5.661841	4.651988	-0.796071
C	-4.438331	0.804258	2.915301	H	-4.025099	4.028567	-1.100524
C	-4.375726	-0.461743	3.517543	C	-1.738552	5.161984	0.074261
C	-3.141496	-1.019902	3.850529	H	-1.58228	6.16729	-0.360205
C	-1.977971	-0.281463	3.604705	H	-0.81726	4.830573	0.564242
C	0.225787	1.766522	3.866215	H	-1.964168	4.452694	-0.731162
C	-0.221296	1.568146	1.410846	C	-2.52824	6.17745	2.11487
H	1.006691	2.52811	3.707353	H	-1.595745	5.895756	2.615333
H	-0.202949	1.922762	4.867905	H	-2.419059	7.18926	1.682365
H	0.719975	0.781145	3.856606	H	-3.334077	6.184403	2.859677
H	-0.969057	1.657818	0.608242	C	-5.100326	2.036045	-0.093065
H	0.604435	2.266939	1.19345	H	-5.243476	1.20244	0.600368
H	0.184085	0.543791	1.389923	H	-5.981797	2.125227	-0.7556
H	-0.758529	4.01881	2.361643	H	-4.209602	1.825242	-0.698525
H	-1.706047	3.596219	3.810682	C	-6.073087	3.57771	1.499069
H	-5.439012	1.18688	2.700411	H	-6.979982	3.673968	0.872088
H	-5.300193	-1.006416	3.729381	H	-6.223095	2.775017	2.225802
H	-3.084284	-2.007469	4.314532	H	-5.92515	4.50615	2.062704
H	-1.006502	-0.693914	3.893652	N	-2.844003	5.185902	1.061764
Ni	-3.153627	3.285897	1.809265	N	-4.883293	3.288765	0.665133
C	-4.099694	5.594895	0.380218				

$\mathbf{1}_{dmpe}$

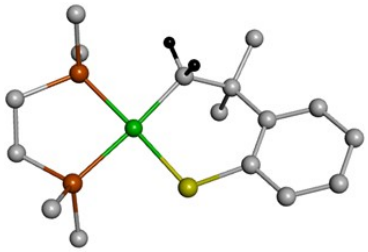

C	-0.54064	1.35176	-0.46141	C	3.96516	0.43025	-0.59593
C	-1.79333	1.478849	0.444862	S	-0.77285	-1.56271	0.270188
C	-2.81123	0.393226	0.082884	C	2.622587	2.56749	0.840017
C	-2.42081	-0.96355	-0.02832	H	3.477813	3.213329	0.594934
C	-3.37631	-1.94203	-0.36091	H	1.723242	3.185457	0.962738
C	-4.71317	-1.6116	-0.56984	H	2.811791	2.049448	1.789654
C	-5.11233	-0.27866	-0.45921	C	2.305902	2.307279	-2.02711
C	-4.16563	0.697475	-0.14037	H	3.199887	2.942743	-2.09956
C	-2.37074	2.892809	0.217622	H	2.275305	1.618833	-2.88205
C	-1.42065	1.376994	1.941331	H	1.409506	2.939565	-2.05779
H	-1.59993	3.640424	0.459703	C	2.226231	-2.6316	1.765777
H	-2.67221	3.045242	-0.83019	H	3.085204	-3.3148	1.825341
H	-3.23811	3.100366	0.86335	H	2.212548	-1.97357	2.644877
H	-1.05457	0.373253	2.192217	H	1.293689	-3.21124	1.755197
H	-0.62347	2.100033	2.181035	C	2.525388	-2.80698	-1.10278
H	-2.29199	1.603398	2.576046	H	3.352635	-3.49895	-0.88985
H	-0.06631	2.349646	-0.44964	H	1.590923	-3.37198	-1.22097
H	-0.863	1.181705	-1.50743	H	2.721607	-2.27464	-2.04313
H	-3.04551	-2.97916	-0.45128	H	4.801663	1.120861	-0.41343
H	-5.4349	-2.39152	-0.82244	H	4.777425	-1.45357	0.199634
H	-6.15383	0.005986	-0.62237	H	4.053462	0.067932	-1.63239
H	-4.50018	1.732365	-0.06446	H	4.045995	-0.38864	1.421472
Ni	0.758063	-0.0646	-0.0939	P	2.327968	1.316564	-0.47932
C	3.954621	-0.74737	0.384077	P	2.300251	-1.58872	0.25772

2_{dmpe}

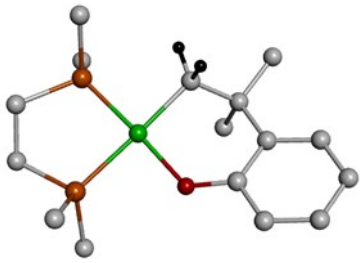

C	-0.51611	1.614462	-0.47993	C	3.882743	0.317264	-0.64194
C	-1.76025	1.592434	0.436853	C	2.734607	2.516216	0.876076
C	-2.64445	0.399572	0.075456	H	3.650383	3.084578	0.659914
C	-2.03765	-0.88398	-0.05514	H	1.895822	3.211259	1.01351
C	-2.85713	-1.99632	-0.35873	H	2.863634	1.949173	1.807633
C	-4.23376	-1.86404	-0.52641	C	2.402787	2.401892	-1.99635
C	-4.83229	-0.60735	-0.40309	H	3.352026	2.953498	-2.04968
C	-4.0306	0.500663	-0.10441	H	2.303204	1.758343	-2.88043
C	-2.50265	2.932169	0.263059	H	1.568518	3.114903	-1.98939
C	-1.32726	1.480296	1.917947	C	1.822668	-2.53201	1.741853
H	-1.82191	3.763311	0.504627	H	2.52693	-3.37221	1.816056
H	-2.85173	3.068866	-0.77199	H	1.945828	-1.8664	2.606551
H	-3.37246	3.014348	0.933786	H	0.790793	-2.90774	1.739159
H	-0.83505	0.515864	2.103049	C	2.163266	-2.82651	-1.11745
H	-0.61577	2.284096	2.171462	H	2.881162	-3.62	-0.8659
H	-2.19671	1.565101	2.588627	H	1.164827	-3.26319	-1.25423
H	-0.04267	2.606796	-0.35992	H	2.458088	-2.34738	-2.06055
H	-0.8291	1.540114	-1.54041	H	4.781291	0.928281	-0.46892
H	-2.36863	-2.96914	-0.45495	H	4.551167	-1.63702	0.113496
H	-4.83881	-2.74446	-0.7584	H	3.918641	-0.03697	-1.68462
H	-5.90899	-0.4854	-0.53657	H	3.930972	-0.53582	1.362728
H	-4.51018	1.476832	-0.00867	P	2.334343	1.350243	-0.49178
Ni	0.669718	0.109326	-0.16336	P	2.063176	-1.55554	0.209288
C	3.789153	-0.87238	0.323537	O	-0.73444	-1.09865	0.123148

3_{dmpe}

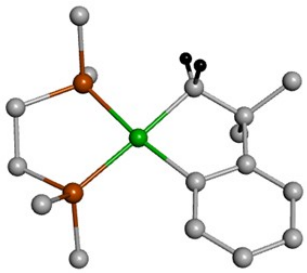

C	-1.39112	3.235388	2.842545	H	-3.96526	6.610433	-0.49166
C	-0.78687	1.815873	2.892427	H	-4.88422	6.261084	0.989197
C	-1.97867	0.903854	3.120913	C	-4.91542	4.625623	-0.44841
C	-3.2144	1.429244	2.660271	H	-5.92706	4.872036	-0.80427
C	-4.35472	0.629568	2.876003	H	-4.33076	4.285357	-1.3182
C	-4.28458	-0.62692	3.494801	C	-1.40701	5.278792	-0.17728
C	-3.05078	-1.12684	3.914708	H	-1.30595	6.304397	-0.56021
C	-1.89811	-0.35537	3.72704	H	-0.44989	4.951563	0.250033
C	0.285784	1.709999	3.990848	H	-1.65906	4.601768	-1.00446
C	-0.14226	1.479614	1.530682	C	-2.29184	6.544431	2.263274
H	1.068795	2.468166	3.828349	H	-1.36635	6.296446	2.799443
H	-0.15196	1.880856	4.986246	H	-2.15711	7.493116	1.724593
H	0.778749	0.724046	3.999478	H	-3.10016	6.652393	2.998678
H	-0.8857	1.577151	0.724822	C	-5.37197	1.782741	-0.34729
H	0.692795	2.167653	1.316497	H	-5.50046	0.871169	0.24967
H	0.249235	0.45002	1.517677	H	-6.28575	1.976774	-0.92709
H	-0.62951	3.943272	2.460645	H	-4.52845	1.625069	-1.03292
H	-1.64655	3.56455	3.869031	C	-6.53914	3.520137	1.659465
H	-5.34499	0.984422	2.57333	H	-7.38866	3.582769	0.964055
H	-5.19545	-1.21196	3.648933	H	-6.7267	2.722213	2.389457
H	-2.98526	-2.10642	4.394539	H	-6.44897	4.465639	2.211335
H	-0.93312	-0.73942	4.070995	P	-2.71852	5.17296	1.114871
Ni	-3.10002	3.196684	1.894719	P	-4.95864	3.196073	0.757491
C	-4.22622	5.817361	0.224847				

1_{Py_3CH}

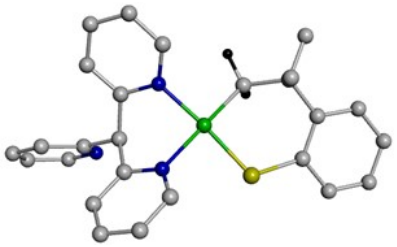

Ni	8.444013	10.886125	7.00523	H	2.361454	11.497103	3.610125
N	9.133797	11.127622	8.765684	C	3.913061	11.86426	5.068591
N	10.259716	10.379136	6.449912	H	3.255696	12.487469	5.675952
C	8.928841	12.265569	9.469135	C	5.237767	11.651784	5.488673
H	8.321171	13.02461	8.978864	C	5.792268	12.298066	6.76114
C	9.444794	12.468978	10.742802	C	6.638573	11.273417	7.552352
H	9.251966	13.408379	11.260116	H	6.090651	10.311865	7.584765
C	10.187038	11.447558	11.332291	H	6.702261	11.631353	8.594775
H	10.586194	11.554649	12.341521	C	4.657757	12.774796	7.694226
C	10.417399	10.278989	10.606129	H	4.043414	13.567301	7.239413
H	10.98958	9.465882	11.047814	H	5.096662	13.191265	8.613381
C	9.902829	10.149009	9.315801	H	3.994597	11.944399	7.982073
C	10.147199	8.946018	8.403165	C	6.621355	13.542177	6.368396
C	10.914746	9.43574	7.171248	H	7.430793	13.271979	5.676791
C	12.176661	8.982101	6.786375	H	7.074941	14.002004	7.261411
H	12.66923	8.190621	7.347352	H	5.982891	14.299744	5.886481
C	12.798825	9.541753	5.669305	C	10.716557	7.713709	9.08506
H	13.785817	9.194689	5.360968	C	11.987482	7.668205	9.678146
C	12.14159	10.546722	4.962391	N	9.890728	6.649668	9.078373
H	12.593631	11.022183	4.092391	C	12.412746	6.484369	10.28278
C	10.871246	10.928196	5.378129	H	12.638309	8.543951	9.669449
H	10.297102	11.682917	4.840725	C	10.313162	5.517684	9.663289
C	6.061784	10.837651	4.673296	C	11.559058	5.381626	10.277769
C	5.533653	10.266219	3.498442	H	13.397115	6.428241	10.749916
H	6.181393	9.629774	2.890451	H	9.613869	4.676888	9.636651
C	4.217442	10.498014	3.104311	H	11.847831	4.436225	10.737786
H	3.835703	10.044434	2.186958	H	9.15356	8.632116	8.038715
C	3.39759	11.305277	3.896223	S	7.774875	10.494373	4.998625

$\mathbf{1}_{dppe}$

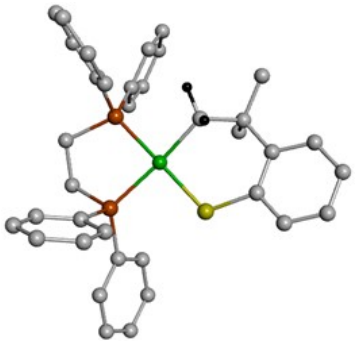

C	-1.657591	3.177182	2.807832	H	-9.410341	4.780044	3.05781
C	-0.560743	2.083244	2.774016	C	-5.299907	2.067694	-1.104584
C	-1.136353	0.777027	3.329997	C	-6.652166	1.7488	-1.289464
C	-2.394236	0.294326	2.893379	C	-4.319982	1.384385	-1.843222
C	-2.908579	-0.901461	3.429034	C	-7.01941	0.760241	-2.206667
C	-2.196914	-1.641944	4.369974	H	-7.418877	2.268227	-0.711962
C	-0.951652	-1.181841	4.801479	C	-4.691558	0.403035	-2.763614
C	-0.443535	0.011979	4.284098	H	-3.26316	1.608066	-1.678512
C	0.615128	2.594631	3.634127	C	-6.04189	0.089563	-2.946083
C	-0.015666	1.857365	1.345283	H	-8.074202	0.513804	-2.342062
H	0.973221	3.55007	3.222062	H	-3.923994	-0.126898	-3.330476
H	0.309633	2.766807	4.677738	H	-6.331389	-0.683784	-3.660042
H	1.468783	1.899213	3.631448	C	-2.769845	6.479977	2.321283
H	-0.784804	1.426105	0.690861	C	-2.30386	7.797282	2.175097
H	0.305821	2.816266	0.908349	C	-3.498055	6.12935	3.467504
H	0.849948	1.176245	1.364808	C	-2.556425	8.745486	3.168227
H	-1.140047	4.148585	2.874317	H	-1.736776	8.081469	1.285954
H	-2.244279	3.076817	3.74073	C	-3.74957	7.081318	4.459389
H	-3.886852	-1.244719	3.084676	H	-3.868366	5.107578	3.577606
H	-2.617125	-2.569328	4.765492	C	-3.277828	8.387858	4.311998
H	-0.376719	-1.743106	5.540966	H	-2.188581	9.766319	3.049042
H	0.527259	0.356683	4.641474	H	-4.313932	6.798783	5.349836
Ni	-3.016955	3.187152	1.39832	H	-3.472122	9.129957	5.088675
C	-4.373052	4.793462	-1.12301	C	-0.880673	5.501918	0.31752
C	-3.71173	5.929276	-0.338816	C	-0.619078	5.171459	-1.022471
S	-3.395317	1.06343	1.638693	C	0.181969	5.913047	1.137243
P	-2.57347	5.229916	0.985101	C	0.67529	5.265965	-1.536523
P	-4.730485	3.389341	0.038489	H	-1.426404	4.827603	-1.672299
C	-6.243979	3.882298	0.965665	C	1.47784	6.002835	0.620819
C	-7.03404	4.988164	0.618978	H	-0.000573	6.171761	2.18162

C	-6.60797	3.099978	2.076041	C	1.727706	5.681163	-0.715226
C	-8.166616	5.311338	1.372344	H	0.862802	5.008764	-2.580606
H	-6.776878	5.608243	-0.241441	H	2.294613	6.326039	1.268877
C	-7.746869	3.418328	2.817912	H	2.740433	5.751526	-1.116004
H	-5.992845	2.238934	2.3518	H	-3.160602	6.622131	-0.989855
C	-8.525264	4.527051	2.471045	H	-5.271019	5.121982	-1.665907
H	-8.7702	6.17804	1.096369	H	-4.469591	6.512603	0.203966
H	-8.022754	2.801022	3.674844	H	-3.686744	4.365593	-1.869698

4_{dmpe}

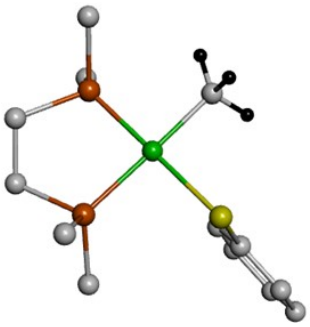

C	-1.58531	3.277777	2.886524	H	-4.63275	1.932263	-1.2425
H	-0.77541	3.992942	2.660413	C	-6.56523	3.758367	1.545945
H	-1.88402	3.440085	3.937059	H	-7.42834	3.857793	0.872617
Ni	-3.21754	3.340945	1.816565	H	-6.72697	2.912737	2.227675
C	-4.13053	6.03998	0.225773	H	-6.46076	4.671948	2.146353
H	-3.79455	6.851441	-0.43686	P	-2.68827	5.262895	1.119593
H	-4.77281	6.486368	1.001658	P	-5.01602	3.458948	0.60026
C	-4.88737	4.939606	-0.52476	H	-1.16638	2.262119	2.818391
H	-5.87646	5.273638	-0.87048	C	-3.07123	0.184322	1.548707
H	-4.31599	4.611192	-1.40746	C	-3.28714	-1.19938	1.725372
C	-1.34083	5.282823	-0.13274	C	-2.21567	0.587286	0.501617
H	-1.13962	6.30561	-0.48163	C	-2.67661	-2.13396	0.890185
H	-0.42971	4.861524	0.312084	H	-3.94245	-1.53395	2.532508
H	-1.62849	4.654157	-0.98594	C	-1.60812	-0.35466	-0.33285
C	-2.19994	6.565123	2.317013	H	-2.02348	1.653438	0.355233
H	-1.30003	6.252546	2.861167	C	-1.83223	-1.72118	-0.14791
H	-2.00328	7.51518	1.800407	H	-2.86197	-3.19835	1.053054
H	-3.01449	6.70396	3.040062	H	-0.9488	-0.01226	-1.13434
C	-5.46019	2.093076	-0.53951	H	-1.35548	-2.45523	-0.7999
H	-5.60168	1.176374	0.047509	S	-3.8676	1.329324	2.635712
H	-6.3799	2.325721	-1.09464				

5_{dmpe}

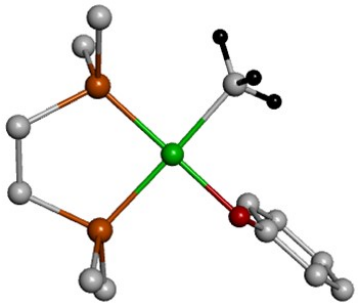

C	-1.5224	3.1908	2.6982	H	-4.4649	2.1195	-1.5611
H	-0.6838	3.8722	2.4769	C	-6.5187	3.5269	1.3814
H	-1.8295	3.3712	3.7437	H	-7.392	3.6305	0.7219
Ni	-3.1438	3.27	1.6252	H	-6.617	2.6109	1.9793
C	-4.1889	6.0711	0.3522	H	-6.4734	4.3814	2.0694
H	-3.8889	6.9659	-0.2133	P	-2.7108	5.2676	1.1633
H	-4.851	6.4006	1.1687	P	-4.9553	3.4288	0.4165
C	-4.8979	5.0324	-0.5256	H	-1.1534	2.1572	2.6202
H	-5.9011	5.3628	-0.8316	O	-3.5859	1.4801	2.0991
H	-4.3156	4.8394	-1.4405	C	-3.0483	0.4371	1.4914
C	-1.3712	5.4931	-0.0774	C	-3.392	-0.8753	1.9157
H	-1.2378	6.5564	-0.3217	C	-2.1359	0.5443	0.4069
H	-0.4333	5.0877	0.324	C	-2.8594	-1.9996	1.2895
H	-1.6232	4.9352	-0.989	H	-4.0876	-0.9753	2.7522
C	-2.2802	6.4496	2.4988	C	-1.6091	-0.5917	-0.2107
H	-1.366	6.1163	3.0057	H	-1.8493	1.5446	0.0687
H	-2.1275	7.46	2.0941	C	-1.9623	-1.875	0.219
H	-3.0976	6.469	3.2318	H	-3.1473	-2.9932	1.6439
C	-5.3074	2.159	-0.8587	H	-0.9086	-0.4697	-1.0416
H	-5.3914	1.18	-0.3689	H	-1.5473	-2.7599	-0.2666
H	-6.2366	2.3805	-1.4027				

6_{dmpe}

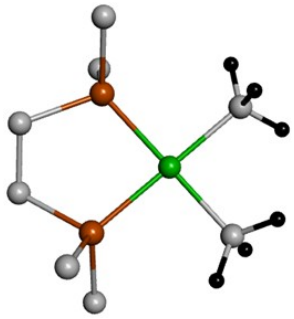

C	-1.54572	3.1093	2.743753	H	-3.0894	6.528463	3.19184
H	-0.71288	3.795238	2.500609	C	-5.33716	2.177408	-0.80876
H	-1.83904	3.323585	3.788995	H	-5.44521	1.19733	-0.32566
Ni	-3.15913	3.260382	1.642664	H	-6.26015	2.418171	-1.35531
C	-4.19048	6.096353	0.322702	H	-4.49621	2.124168	-1.51327
H	-3.89978	6.97287	-0.27564	C	-6.53107	3.573606	1.412882
H	-4.84138	6.450832	1.138199	H	-7.39222	3.700884	0.741219
C	-4.91204	5.031927	-0.51266	H	-6.66727	2.663221	2.012223
H	-5.92276	5.348035	-0.8112	H	-6.47298	4.427946	2.100562
H	-4.34485	4.817799	-1.43283	P	-2.7086	5.298975	1.137109
C	-1.36862	5.547443	-0.1073	P	-4.95045	3.441979	0.469811
H	-1.23276	6.612124	-0.34606	H	-1.13923	2.085088	2.727309
H	-0.42929	5.139904	0.290356	C	-3.5506	1.3864	2.0621
H	-1.61769	4.995139	-1.02343	H	-4.61409	1.083802	2.032068
C	-2.27058	6.499644	2.460339	H	-3.02241	0.764133	1.31487
H	-1.3622	6.156251	2.972768	H	-3.15939	1.102059	3.052348
H	-2.10229	7.508485	2.057158				

4_{bpy}

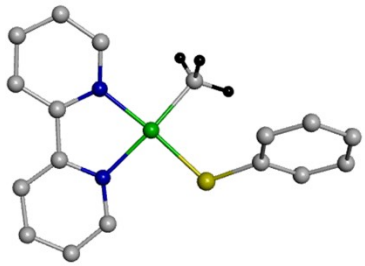

C	-0.98574	-1.63323	-0.9618	C	1.679583	-2.63938	-0.1238
C	-3.33631	-0.54287	1.033283	C	4.031655	-1.28872	0.229321
C	-3.17195	0.403783	0.005974	C	2.669019	0.840928	0.106121
C	-4.30619	0.811775	-0.71826	C	2.851023	-3.36357	0.059389
C	-5.57004	0.29617	-0.41597	H	0.72968	-3.14818	-0.27156
C	-5.72335	-0.64603	0.60552	C	4.055878	-2.67994	0.229202
C	-4.59832	-1.0642	1.325395	H	4.949873	-0.72319	0.380478
H	-0.41228	-2.16173	-1.74367	N	1.37	1.254397	0.07157
H	-1.2046	-2.33956	-0.14113	C	3.734024	1.739505	0.217552
H	-4.19059	1.539397	-1.52435	H	2.808661	-4.45239	0.065219
H	-6.43806	0.629067	-0.98938	H	4.993662	-3.21798	0.368802
H	-6.70946	-1.05179	0.838626	C	1.130964	2.58066	0.163341
H	-4.70407	-1.79875	2.126978	C	3.470046	3.103642	0.300405
Ni	0.098868	-0.18617	-0.31536	H	4.760765	1.376849	0.234323
S	-1.59948	1.170903	-0.33762	C	2.140899	3.529208	0.27717
H	-2.46277	-0.86392	1.603367	H	0.07889	2.872027	0.1504
H	-1.94757	-1.33693	-1.40065	H	4.287456	3.820328	0.384317
N	1.63959	-1.28611	-0.14465	H	1.88003	4.584958	0.345639
C	2.818215	-0.61904	0.053153				

$Ni^{I}(SC^{\bullet-})$ intermediate of $\mathbf{1}_{\mathbf{tmeda}}$

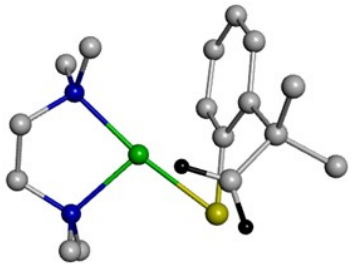

C	0.7856	2.2049	0.7875	C	-4.0093	5.4367	0.3589
C	0.532	0.8755	1.4372	C	-1.6099	5.7782	0.6093
C	-0.9461	0.7531	1.8483	H	-1.6745	6.8495	0.3391
C	-1.584	1.8211	2.5825	H	-0.7633	5.6112	1.285
C	-2.926	1.6226	3.0667	H	-1.431	5.1885	-0.2985
C	-3.6026	0.4079	2.8224	C	-3.0602	6.1351	2.4952
C	-2.9951	-0.5925	2.0785	H	-3.1516	7.2116	2.2563
C	-1.6764	-0.4086	1.6102	H	-3.9707	5.7974	3.007
C	1.4036	0.7206	2.7058	H	-2.2103	5.9797	3.1707
C	0.9502	-0.2338	0.4372	C	-3.6394	1.819	-0.557
H	2.4684	0.8367	2.4485	H	-4.3549	1.6395	-1.3824
H	1.1412	1.4846	3.4499	H	-2.6419	2.0034	-0.9756
H	1.2625	-0.2754	3.1519	H	-3.5848	0.9312	0.0837
H	0.3303	-0.2128	-0.4718	C	-5.3836	2.7163	0.8371
H	1.9959	-0.0711	0.1391	H	-6.1383	2.593	0.0368
H	0.8837	-1.239	0.8842	H	-5.3402	1.8036	1.4414
H	0.1513	2.5356	-0.0373	H	-5.6869	3.5419	1.4928
H	1.7	2.7613	0.9926	H	-3.9619	6.3633	-0.2425
H	-3.2923	2.2658	3.872	H	-4.9442	4.2501	-1.207
H	-4.5945	0.2506	3.2546	H	-4.9203	5.491	0.9714
H	-3.5109	-1.5358	1.8871	H	-3.167	4.1898	-1.1937
H	-1.2104	-1.2271	1.0597	N	-2.851	5.3285	1.2763
Ni	-2.6452	3.3119	1.7467	N	-4.0451	2.9746	0.2677
C	-4.0563	4.2131	-0.548	S	-0.7781	3.3386	3.053

$Ni^{I}(SC^{\bullet-})$ intermediate of $\mathbf{2}_{\mathbf{tmeda}}$

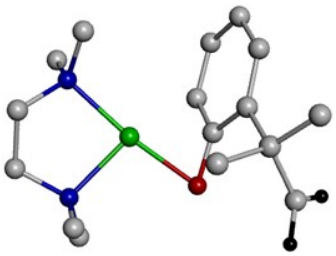

C	3.5122	-0.5496	1.6272	C	-1.486	2.6115	-1.8436
C	2.8177	-1.4492	0.6432	C	0.9519	2.5248	-1.6422
C	1.3377	-1.5857	1.0263	H	1.1204	3.4911	-2.1567
C	0.5965	-0.3767	1.3278	H	1.7561	2.3429	-0.9197
C	-0.7829	-0.5129	1.763	H	0.9725	1.7157	-2.383
C	-1.3839	-1.7871	1.8475	C	-0.3301	3.6045	0.0831
C	-0.678	-2.9257	1.4784	H	-0.1666	4.5954	-0.3825
C	0.6763	-2.8075	1.0946	H	-1.2876	3.609	0.6198
C	3.5462	-2.8176	0.6454	H	0.4657	3.3974	0.8091
C	2.9194	-0.854	-0.7799	C	-1.8734	-1.1259	-1.6902
H	4.6097	-2.6644	0.4103	H	-2.6734	-1.4053	-2.4025
H	3.4811	-3.3064	1.6286	H	-0.8961	-1.2558	-2.1721
H	3.1297	-3.5011	-0.1127	H	-1.9102	-1.785	-0.8134
H	2.3995	0.1112	-0.8125	C	-3.3273	0.4471	-0.59
H	3.974	-0.7012	-1.0613	H	-4.1523	0.2206	-1.2928
H	2.4605	-1.5328	-1.5153	H	-3.387	-0.2264	0.2732
H	4.271	0.161	1.2972	H	-3.439	1.4751	-0.2239
H	3.3049	-0.6359	2.6943	H	-1.2805	3.2956	-2.6879
H	-1.2238	0.3203	2.3221	H	-2.738	1.2583	-3.0037
H	-2.4025	-1.8757	2.2371	H	-2.3346	3.0306	-1.2848
H	-1.142	-3.9124	1.5353	H	-1.0095	0.8362	-2.9832
H	1.2245	-3.7229	0.8614	O	1.1098	0.8412	1.2347
Ni	-0.5112	0.7155	0.0497	N	-0.3336	2.5222	-0.919
C	-1.8348	1.2182	-2.3657	N	-2.0113	0.2722	-1.2357

$Ni^{I}(SC^{\bullet-})$ intermediate of $\mathbf{3}_{\mathbf{tmeda}}$

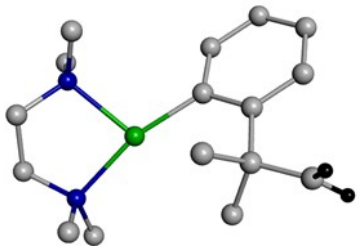

C	-0.0655	0.3418	4.4124	H	-3.138	5.5253	-0.7556
C	-1.0579	1.0962	3.5842	H	-4.3877	5.5364	0.5048
C	-2.5413	0.7811	3.9484	C	-4.184	3.6353	-0.5056
C	-3.599	1.5255	3.3456	H	-4.9523	3.8595	-1.2711
C	-4.8986	1.1626	3.7787	H	-3.3963	3.0407	-0.9899
C	-5.1634	0.1408	4.6996	C	-1.2874	4.3117	0.5006
C	-4.1029	-0.5854	5.2408	H	-0.8972	5.1924	-0.0452
C	-2.7992	-0.2535	4.8585	H	-0.5754	4.0291	1.2847
C	-0.8292	0.7816	2.0916	H	-1.3732	3.4672	-0.1939
C	-0.8038	2.6012	3.8258	C	-2.4575	5.7511	2.0356
H	0.1998	1.0315	1.7861	H	-1.7309	5.4937	2.8166
H	-1.0109	-0.2836	1.8834	H	-2.1097	6.6585	1.5058
H	-1.5414	1.3776	1.4933	H	-3.4211	5.9559	2.5184
H	-0.9374	2.8663	4.8849	C	-4.9336	1.4246	0.1683
H	0.207	2.8976	3.5045	H	-5.2675	0.8328	1.0287
H	-1.5537	3.1814	3.243	H	-5.6757	1.3493	-0.6502
H	0.4951	-0.5014	4.0051	H	-3.9741	1.014	-0.172
H	0.0816	0.5944	5.4647	C	-6.0249	3.3792	1.0605
H	-5.7641	1.7087	3.388	H	-6.7619	3.4264	0.2348
H	-6.1939	-0.0844	4.9902	H	-6.4255	2.7448	1.8576
H	-4.2811	-1.3954	5.9523	H	-5.883	4.3844	1.4751
H	-1.9556	-0.8124	5.2772	N	-2.6034	4.6069	1.1103
Ni	-3.2943	2.9467	2.095	N	-4.7405	2.8214	0.598
C	-3.5963	4.9241	0.0511				

$Ni^{I}(SC^{\bullet-})$ intermediate of $\mathbf{1}_{\mathbf{dmpe}}$

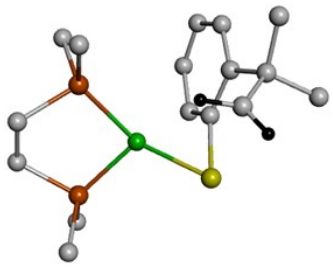

C	0.996415	1.344869	0.398838	C	-4.39517	5.510131	0.37064
C	0.522952	0.306087	1.371051	C	-1.86149	6.835451	0.864703
C	-0.86054	0.655749	1.952027	H	-2.38719	7.798236	0.783244
C	-1.11353	1.956944	2.52135	H	-0.98559	6.950564	1.517599
C	-2.29921	2.150523	3.317223	H	-1.5051	6.527119	-0.12736
C	-3.26205	1.127238	3.422545	C	-3.66035	6.330084	3.046531
C	-3.06884	-0.07474	2.761108	H	-4.12175	7.297566	2.79951
C	-1.86476	-0.30294	2.06212	H	-4.41462	5.664063	3.486253
C	1.515194	0.199622	2.554812	H	-2.86132	6.487739	3.783399
C	0.517208	-1.06031	0.636887	C	-2.9607	1.954316	-1.47276
H	2.524589	-0.0323	2.179908	H	-3.74906	1.894625	-2.2377
H	1.563353	1.145777	3.110997	H	-2.07881	2.454929	-1.89445
H	1.209841	-0.60104	3.244611	H	-2.67227	0.939608	-1.16753
H	-0.20544	-1.07049	-0.19262	C	-5.09689	2.029668	0.442254
H	1.516912	-1.24602	0.219167	H	-5.77114	1.959681	-0.42426
H	0.281195	-1.89184	1.320277	H	-4.86023	1.022512	0.808588
H	0.33299	1.705392	-0.38815	H	-5.59791	2.574181	1.253729
H	2.046953	1.633903	0.364671	H	-4.58102	6.517517	-0.03157
H	-2.33343	2.98498	4.02142	H	-5.02628	4.312752	-1.36223
H	-4.14604	1.285846	4.044635	H	-5.27953	5.21679	0.958976
H	-3.81214	-0.87192	2.828229	H	-3.32878	4.841384	-1.40603
H	-1.70935	-1.28944	1.623745	P	-2.95206	5.517477	1.552911
Ni	-2.15305	3.493711	1.608522	P	-3.52496	2.889687	0.010633
C	-4.13348	4.48591	-0.742	S	-0.0406	3.367686	2.356596

$Ni^{I}(SC^{\bullet-})$ intermediate of $\mathbf{2}_{\mathbf{dmpe}}$

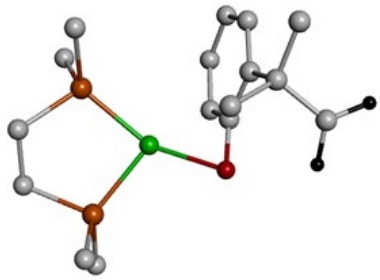

C	1.2997	1.0701	2.8842	C	-4.2896	5.4664	-0.0538
C	0.3641	0.6561	1.7816	C	-1.5107	6.2807	0.1641
C	-1.058	0.7338	2.3737	H	-1.8288	7.276	-0.18
C	-1.5533	1.9986	2.8845	H	-0.6216	6.3828	0.801
C	-2.8508	2.0236	3.5121	H	-1.2376	5.665	-0.7034
C	-3.6428	0.8676	3.5863	C	-3.3084	6.7254	2.3559
C	-3.1787	-0.3257	3.0435	H	-3.5472	7.6835	1.8712
C	-1.8918	-0.379	2.4701	H	-4.1799	6.3727	2.9233
C	0.7281	-0.7655	1.3196	H	-2.4743	6.8714	3.0554
C	0.4872	1.6082	0.5674	C	-3.6107	1.3928	-1.0751
H	1.7569	-0.7649	0.9306	H	-4.4181	1.3127	-1.8181
H	0.6829	-1.4892	2.1475	H	-2.666	1.6238	-1.5852
H	0.0627	-1.1151	0.5154	H	-3.4985	0.4331	-0.5529
H	0.2897	2.6425	0.8721	C	-5.6419	2.2603	0.7584
H	1.5006	1.5446	0.1413	H	-6.3398	2.1031	-0.0772
H	-0.2371	1.3234	-0.2125	H	-5.5679	1.341	1.3547
H	1.3119	2.1109	3.2072	H	-6.0253	3.0566	1.4102
H	1.7582	0.3101	3.5204	H	-4.2832	6.3816	-0.6652
H	-3.1127	2.9126	4.0925	H	-5.2122	4.0771	-1.4858
H	-4.6131	0.9073	4.0879	H	-5.1956	5.4896	0.573
H	-3.7861	-1.2317	3.0915	H	-3.4483	4.2361	-1.6416
H	-1.5424	-1.3394	2.0868	O	-0.8938	3.1453	2.7851
Ni	-2.5273	3.3459	1.6595	P	-2.8423	5.4358	1.1245
C	-4.2777	4.1971	-0.9168	P	-3.956	2.7112	0.1657

$Ni^{I}(SC^{\bullet-})$ intermediate of $\mathbf{3}_{\mathbf{dmpe}}$

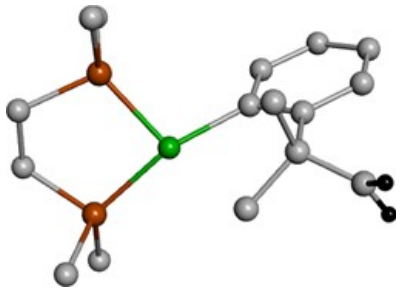

C	-0.1495	0.1179	4.4982	H	-3.5574	6.078	-0.5994
C	-1.151	0.5955	3.4901	H	-4.846	5.609	0.5317
C	-2.5703	0.7192	4.0974	C	-4.1165	3.9505	-0.6725
C	-3.5169	1.6551	3.6014	H	-4.9643	3.9994	-1.3728
C	-4.7936	1.6331	4.2148	H	-3.216	3.6896	-1.2521
C	-5.1327	0.7578	5.2518	C	-1.0623	5.3109	0.6706
C	-4.1863	-0.163	5.7077	H	-1.0233	6.2929	0.1767
C	-2.9176	-0.1748	5.1242	H	-0.2731	5.2576	1.433
C	-1.2109	-0.3869	2.3002	H	-0.872	4.5239	-0.0717
C	-0.6467	1.9647	2.9772	C	-2.9307	6.5523	2.4655
H	-0.2205	-0.4917	1.8277	H	-2.1727	6.5899	3.2593
H	-1.5429	-1.381	2.6339	H	-2.8482	7.455	1.842
H	-1.9221	-0.0229	1.5444	H	-3.9229	6.5216	2.9355
H	-0.6317	2.7112	3.7833	C	-4.1024	1.0758	-0.4484
H	0.3664	1.8745	2.5556	H	-4.3201	0.186	0.1574
H	-1.3124	2.3347	2.1548	H	-4.764	1.0861	-1.3274
H	0.5822	-0.6522	4.248	H	-3.0556	1.0289	-0.7767
H	-0.0465	0.6379	5.4528	C	-6.1711	2.571	0.8328
H	-5.5627	2.3336	3.87	H	-6.6989	2.4311	-0.1223
H	-6.1311	0.7903	5.6975	H	-6.4335	1.7537	1.5179
H	-4.4314	-0.867	6.5067	H	-6.4914	3.5163	1.2914
H	-2.1671	-0.8924	5.4738	P	-2.6983	5.0134	1.4758
Ni	-3.1276	3.0375	2.3082	P	-4.3405	2.584	0.585
C	-3.9027	5.2751	0.0697				

$Ni^{I}(SC^{\bullet-})$ intermediate of $\mathbf{1}_{\mathbf{bpy}}$

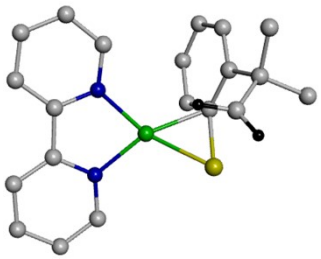

C	0.715106	1.865189	0.341222	Ni	-2.30045	3.466973	1.886276
C	0.434919	0.598148	1.094737	S	-0.19037	3.346997	2.638851
C	-0.91413	0.705787	1.822107	N	-3.04003	5.259027	1.781761
C	-1.23426	1.898041	2.565485	C	-4.01107	5.43299	0.840575
C	-2.43416	1.928566	3.365777	C	-2.62569	6.331207	2.491717
C	-3.30924	0.821555	3.368323	C	-4.56754	6.691279	0.585594
C	-3.0211	-0.29688	2.603056	C	-4.39707	4.184216	0.158781
C	-1.82088	-0.3496	1.85859	C	-3.1509	7.602861	2.302341
C	1.536067	0.35137	2.152965	H	-1.84419	6.136133	3.227678
C	0.461497	-0.58301	0.090668	C	-4.13598	7.788478	1.325626
H	2.523199	0.303818	1.666744	H	-5.32951	6.811606	-0.18385
H	1.553265	1.165744	2.89044	N	-3.65502	3.103654	0.540383
H	1.363309	-0.60006	2.677794	C	-5.41843	4.077044	-0.79023
H	-0.33913	-0.49112	-0.65824	H	-2.7892	8.433946	2.907368
H	1.425531	-0.58432	-0.43799	H	-4.55995	8.776378	1.143141
H	0.358266	-1.55666	0.596311	C	-3.91644	1.907921	-0.03202
H	-0.04624	2.278065	-0.32277	C	-5.68079	2.838945	-1.37157
H	1.73914	2.226615	0.238479	H	-6.00423	4.951995	-1.07056
H	-2.51801	2.660521	4.173831	C	-4.91262	1.73573	-0.98627
H	-4.20284	0.847756	3.996262	H	-3.29514	1.077851	0.305761
H	-3.69411	-1.15659	2.601546	H	-6.47258	2.73601	-2.1142
H	-1.60049	-1.2619	1.302548	H	-5.08034	0.749802	-1.41964

T_1 excited state of $\mathbf{1}_{\mathbf{tmeda}}$

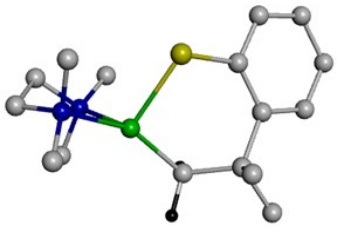

C	-1.07191	2.827447	1.457953	C	-4.33045	5.771447	0.842667
C	-0.87925	1.444034	2.121928	S	-4.08285	2.199323	2.450272
C	-1.54049	1.434083	3.51532	C	-1.90285	6.071824	0.724468
C	-2.91232	1.759368	3.722207	H	-1.96567	7.159373	0.913916
C	-3.44562	1.711747	5.025821	H	-0.95443	5.686846	1.117954
C	-2.67585	1.351377	6.129129	H	-1.91103	5.898501	-0.35895
C	-1.33122	1.034519	5.940573	C	-2.94973	5.56112	2.835592
C	-0.79134	1.080732	4.652829	H	-3.04304	6.63328	3.089125
C	0.637738	1.16316	2.204033	H	-3.74942	4.987444	3.319226
C	-1.48389	0.315529	1.253567	H	-1.99008	5.182079	3.207841
H	1.055255	1.1939	1.186178	C	-4.04249	3.168272	-1.81528
H	1.162144	1.925373	2.80099	H	-4.77881	3.410124	-2.60482
H	0.868376	0.170362	2.624127	H	-3.06468	3.581615	-2.09618
H	-2.57725	0.392474	1.193145	H	-3.94683	2.077259	-1.74127
H	-1.0737	0.373775	0.231476	C	-5.75612	3.112773	-0.1311
H	-1.22981	-0.67375	1.666151	H	-6.51839	3.325174	-0.90386
H	-0.43939	2.845532	0.54283	H	-5.64393	2.027795	-0.01604
H	-0.6403	3.588657	2.137991	H	-6.0947	3.51336	0.832063
H	-4.49951	1.968364	5.153789	H	-4.41605	6.874113	0.81363
H	-3.12512	1.323769	7.124392	H	-5.53877	5.50406	-0.93971
H	-0.69923	0.752706	6.785477	H	-5.0939	5.393645	1.537558
H	0.261973	0.827846	4.533769	H	-3.79381	5.558764	-1.24391
Ni	-2.88464	3.317588	0.912291	N	-3.01356	5.351505	1.375725
C	-4.55658	5.185502	-0.54605	N	-4.45425	3.705088	-0.5021

T_1 excited state of $\mathbf{1}_{\mathbf{dmpe}}$

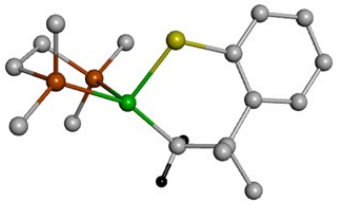

C	-1.00232	2.587121	1.514529	C	-4.3911	6.054297	0.637542
C	-0.86514	1.223659	2.224321	S	-3.94348	2.305244	2.688195
C	-1.43899	1.321368	3.651033	C	-1.50028	6.332636	0.496705
C	-2.75647	1.793354	3.919028	H	-1.64838	7.411952	0.644151
C	-3.2178	1.836406	5.251007	H	-0.52412	6.039146	0.905891
C	-2.42785	1.42433	6.32264	H	-1.50402	6.107292	-0.57804
C	-1.13555	0.962899	6.072595	C	-2.78153	5.989225	3.063665
C	-0.66647	0.920449	4.756636	H	-2.89155	7.082453	3.093556
C	0.632148	0.841566	2.231905	H	-3.59763	5.514121	3.622924
C	-1.60139	0.108481	1.44517	H	-1.82734	5.707022	3.528578
H	0.990403	0.810228	1.191983	C	-4.43127	2.982071	-2.30873
H	1.239344	1.585094	2.771039	H	-5.27111	3.382611	-2.89465
H	0.820741	-0.15047	2.67413	H	-3.48265	3.322744	-2.74429
H	-2.68593	0.278878	1.431484	H	-4.45632	1.884691	-2.34107
H	-1.24514	0.087819	0.40228	C	-6.20028	3.007182	-0.03594
H	-1.40583	-0.87922	1.892569	H	-6.96062	3.350029	-0.75205
H	-0.44021	2.537415	0.556105	H	-6.23148	1.91154	0.032934
H	-0.5025	3.354757	2.133997	H	-6.42207	3.416897	0.958474
H	-4.22938	2.207231	5.432024	H	-4.33688	7.149432	0.545241
H	-2.82009	1.470916	7.340946	H	-5.67422	5.6459	-1.09572
H	-0.48957	0.639061	6.89133	H	-5.18489	5.816161	1.363484
H	0.347176	0.556958	4.588756	H	-3.93952	5.702493	-1.46508
Ni	-2.79948	3.156686	0.941882	P	-2.81552	5.364769	1.340941
C	-4.67736	5.381937	-0.71261	P	-4.51387	3.532051	-0.55476

T_1 excited state of $\mathbf{1_{bpy}}$

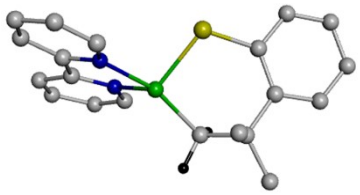

C	-0.99439	1.459099	0.896405	Ni	0.354202	0.126406	0.446525
C	-2.36845	0.917569	1.34525	N	1.90843	-1.12751	0.670474
C	-3.15214	0.384856	0.13053	C	3.083234	-0.68394	0.146823
C	-2.59712	-0.54032	-0.7984	C	1.87343	-2.33856	1.262773
C	-3.38291	-0.99866	-1.87502	C	4.25155	-1.45279	0.217488
C	-4.70085	-0.58526	-2.05728	C	2.990399	0.640435	-0.4954
C	-5.25731	0.319471	-1.15299	C	2.995896	-3.14936	1.374253
C	-4.48346	0.785816	-0.08708	H	0.903076	-2.64787	1.655134
C	-3.12079	2.064798	2.055776	C	4.208402	-2.69563	0.842226
C	-2.20668	-0.21818	2.38469	H	5.181015	-1.08975	-0.21958
H	-2.50383	2.422713	2.893603	N	1.718517	1.12066	-0.60388
H	-3.294	2.916499	1.379963	C	4.086081	1.363817	-0.98174
H	-4.08981	1.74883	2.474873	H	2.921134	-4.11685	1.869845
H	-1.7409	-1.10909	1.941828	H	5.108052	-3.30828	0.90809
H	-1.56682	0.124527	3.213928	C	1.518268	2.29763	-1.23151
H	-3.18304	-0.50992	2.803035	C	3.869347	2.579745	-1.62272
H	-0.55345	2.032526	1.738933	H	5.098198	0.980388	-0.85803
H	-1.15339	2.17742	0.070492	C	2.558496	3.04952	-1.7623
H	-2.93004	-1.70004	-2.57953	H	0.48217	2.631922	-1.29413
H	-5.28057	-0.96366	-2.90199	H	4.711014	3.154969	-2.00955
H	-6.28542	0.667488	-1.2721	H	2.343647	3.989034	-2.27073
H	-4.94154	1.494481	0.602571	S	-0.95564	-1.23803	-0.71827

References

1. (a) A. J. Canty, N. Chaichit, B. M. Gatehouse, E. E. George and G. Hayhurst, *Inorg. Chem.*, 1981, **20**, 2414-2422; (b) A. Maleckis, J. W. Kampf and M. S. Sanford, *J. Am. Chem. Soc.*, 2013, **135**, 6618-6625.
2. D. G. Yakhvarov, E. Hey-Hawkins, R. M. Kagirov, Y. H. Budnikova, Y. S. Ganushevich and O. G. Sinyashina, *Russ. Chem. Bull.*, 2007, **56**, 935-942.
3. G. Booth and J. Chatt, *J. Chem. Soc.*, 1965, 3238-3241.
4. R. Han and G. L. Hillhouse, *J. Am. Chem. Soc.*, 1998, **120**, 7657-7658.
5. K. M. Koo, G. L. Hillhouse and A. L. Rheingold, *Organometallics*, 1995, **14**, 456-460.
6. J. Cámpora, M. D. Conejo, K. Mereiter, P. Palma, C. Pérez, M. L. Reyes and C. Ruiz, *J. Organomet. Chem.*, 2003, **683**, 220-239.
7. E. Carmona, E. Gutiérrez-Puebla, J. M. Marín, A. Monge, M. Paneque, M. L. Poveda and C. Ruiz, *J. Am. Chem. Soc.*, 1989, **111**, 2883-2891.
8. J. Cámpora, E. Gutiérrez, A. Monge, P. Palma, M. L. Poveda, C. Ruiz and E. Carmona, *Organometallics*, 1994, **13**, 1728-1745.
9. N. M. Camasso and M. S. Sanford, *Science*, 2015, **347**, 1218-1220.
10. E. Carmona, M. Paneque, M. L. Poveda, E. Gutiérrez-Puebla and A. Monge, *Polyhedron*, 1989, **8**, 1069-1075.
11. P. D. Binger, M. J.; Krüger, C.; Tsay, Y.-H., *Z. Naturforsch*, 1979, **34B**, 1289-1292.
12. P. T. Matsunaga, G. L. Hillhouse and A. L. Rheingold, *J. Am. Chem. Soc.*, 1993, **115**, 2075-2077.
13. A. Enachi, M. Freytag, J. Raeder, P. G. Jones and M. D. Walter, *Organometallics*, 2020, **39**, 2470-2478.
14. W. Kaschube, K. R. Porschke and G. Wilke, *J. Organomet. Chem.*, 1988, **355**, 525-532.
15. C. G. Hatchard and C. A. Parker, *Proc. R. Soc. London Ser. A*, 1956, **235**, 518-536.
16. J. N. Demas, W. D. Bowman, E. F. Zalewski and R. A. Velapoldi, *J. Phys. Chem.*, 1981, **85**, 2766-2771.
17. M. J. Frisch, G. W. Trucks, H. B. Schlegel, G. E. Scuseria, M. A. Robb, J. R. Cheeseman, G. Scalmani, V. Barone, G. A. Petersson, H. Nakatsuji, X. Li, M. Caricato, A. V. Marenich, J. Bloino, B. G. Janesko, R. Gomperts, B. Mennucci, H. P. Hratchian, J. V. Ortiz, A. F. Izmaylov, J. L. Sonnenberg, Williams, F. Ding, F. Lipparini, F. Egidi, J. Goings, B. Peng, A. Petrone, T. Henderson, D. Ranasinghe, V. G. Zakrzewski, J. Gao, N. Rega, G. Zheng, W. Liang, M. Hada, M. Ehara, K. Toyota, R. Fukuda, J. Hasegawa, M. Ishida, T. Nakajima, Y. Honda, O. Kitao, H. Nakai, T. Vreven, K. Throssell, J. A. Montgomery Jr., J. E. Peralta, F. Ogliaro, M. J. Bearpark, J. J. Heyd, E. N. Brothers, K. N. Kudin, V. N. Staroverov, T. A. Keith, R. Kobayashi, J. Normand, K. Raghavachari, A. P. Rendell, J. C. Burant, S. S. Iyengar, J. Tomasi, M. Cossi, J. M. Millam, M. Klene, C. Adamo, R. Cammi, J. W. Ochterski, R. L. Martin, K. Morokuma, O. Farkas, J. B. Foresman and D. J. Fox, *Gaussian 09*, 2013.
18. (a) O. A. Vydrov and G. E. Scuseria, *J. Chem. Phys.*, 2006, **125**, 234109; (b) O. A. Vydrov, J. Heyd, A. V. Krukau and G. E. Scuseria, *J. Chem. Phys.*, 2006, **125**, 074106; (c) S. Ragot and P. J. Becker, *J. Chem. Phys.*, 2006, **125**, 154109.
19. (a) M. M. Francl, W. J. Pietro, W. J. Hehre, J. S. Binkley, M. S. Gordon, D. J. Defrees and J. A. Pople, *J. Chem. Phys.*, 1982, **77**, 3654-3665; (b) R. Krishnan, J. S. Binkley, R. Seeger and J. A. Pople, *J. Chem. Phys.*, 1980, **72**, 650-654; (c) A. D. McLean and G. S. Chandler, *J. Chem. Phys.*, 1980, **72**, 5639-5648.
20. V. Barone and M. Cossi, *J. Phys. Chem. A*, 1998, **102**, 1995-2001.
21. E. Runge and E. K. U. Gross, *Phys. Rev. Lett.*, 1984, **52**, 997-1000.
22. A. L. Tenderholt, *QMForge 2.4*, 2018.